Control Analysis of Adrenal Steroidogenesis

by

Tyrone Genade

Thesis presented in partial fulfillment of the requirements for the degree of Masters of Science (Biochemistry) at the University of Stellenbosch

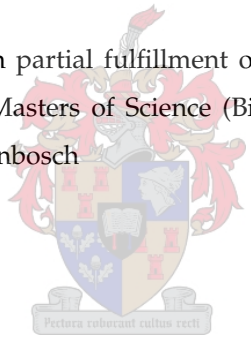

Study leader: **Prof. P. Swart**

Co-study leader: **Prof. J-H.S. Hofmeyr**

Department of Biochemistry

June 2004

Declaration

I, the undersigned, hereby declare that the work contained in this thesis is my own original work and has not previously in its entirety or in part been submitted to any university for a degree.

_____ _____

Signature Date

Summary

This study describes:

1. Investigation of product inhibition regarding the metabolism of progesterone in ovine adrenal micosomes.
2. The employment of novel cell culture techniques to study the effect of CYP17 and CYP21 concentration on adrenal progesterone metabolism.
3. The formulation of a mathematical model describing the behaviour of the observed results in point 2.

Opsomming

Hierdie studie beskryf:

1. ’n Ondersoek van produk inhibisie met betrekking tot die metabolisme van progesteroon in skaapbyniermikrosome.

2. Die aanwending van nuwe sel-kultuur metodes om die impak van CYP17 en CYP21 konsentrasie op adrenale progesteroon metabolisme te ondersoek.

3. Die formulering van ’n wiskundige model wat die waargenome resultate in punt 2 beskryf.

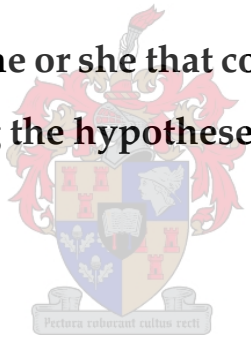

Dedicated to he or she that comes after me, confirming or refuting the hypotheses expressed in this thesis.

This thesis and the associated model can be downloaded at
http://tgenade.freeshell.org/thesis

Acknowledgements

Without the help of the following people this project would never have come to fruition. The people whom I wish to thank are:

Prof. P. Swart whose insight, guidance, support and tolerance made this work possible.

Prof. J-H.S. Hofmeyr for sharing his modeling brilliance and introducing me to LaTeX.

Dr. A. Swart for helping with the molecular biology work and other helpful advice.

Ms R. Louw for her help and for maintaining a functional laboratory environment in spite of the tremendous entropy generated by the students.

Prof. D. Bellstedt for the use of his heat sealer, and his assistant **Coral de Villiers** for help with the centrifuges.

Mr Tiedt, Mr Rehder and Ms Immelman for technical assistance. **Mr K. Botha** for his help in collecting ovine adrenals and countless other smaller tasks. **Mr Burns** and the Physics workshop for the speedy preparation of the tissue culture dish slices.

Norbert Kolar and **Christie Malherbe** for their positive work ethic and the example they set. **Nic Lombard, Hannes Slabbert, Natasja Brown, Zyno Allie, David Richfield, Selvan Govender** and **Wesley Williams** for all the help. **Michael Vismer** for helping me puzzle out problems with LaTeX.

The University of Stellenbosch for assorted mercies.

Cornelia Malherbe and **Uni-Ed** for the work that kept my bank account out of the red.

My parents, family and friends for their encouragement and support.

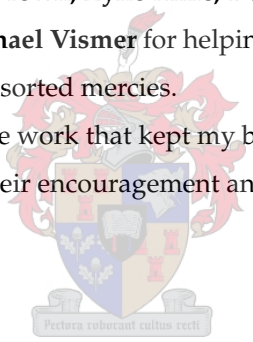

Abbreviations

ACTH	Adrenocorticotrophic hormone
3βHSD	3β-hydroxysteroid dehydrogenase/$\triangle$5-$\triangle$4 isomerase
BCA	Bicinchoninic acid
BSA	Bovine serum albumin
CPM	Counts per minute
CPR	Cytochrome P450 reductase
CYP11A1	Cytochrome P450 side-chain cleavage
CYP11B1	Cytochrome P450 11β-hydroxylase
CYP11B2	Cytochrome P450 aldosterone synthase
CYP17	Cytochrome P450 17α-hydroxylase/17-20 lyase
CYP19	P450 aromatase
CYP21	Cytochrome P450 21-hydroxylase
DTT	Dithiothreitol
DHEA	Dehydroepiandrosterone
DMEM	Dulbecco's modified Eagles medium
DMSO	Dimethyl sulfoxide
DOC	Deoxycorticosterone
EDTA	Ethylenediaminetetraacetic acid
EtAct	Ethyl acetate
FCS	Fetal Calf Serum
HEPES	*N*-2-Hydroxyethylpiperazine-*N'*-2-ethanesulphonic acid
HPLC	High-performance liquid chromatography
LB	Luria-Bertani
MeOH	Methanol
OD	Optical density
17OHP4	17-hydroxy-progesterone
P4	Progesterone
PBS	Phosphate buffered saline
PenStrep	Penicillin-streptomycin
rpm	Revolutions per minute
S	Deoxycortisol
TLC	Thin layer chromatography
TRIS	Tris(hydroxymethyl)aminomethane

Contents

List of Figures

List of Tables

Chapter 1

Introduction

Steroid hormones, present in the correct concentrations and ratios to one another, are vital to the survival of vertebrates [1, 2]. These hormones have wide ranging activities involving the biological development and the maintenance of homeostasis of the animal.

The sex steroids orchestrate the differentiation of the sexes from embryological development; and later regulate sexual maturation and reproductive functions. The glucocorticoids regulate the energy metabolism of the organism as well as enabling the animal to cope with stressful stimuli. The mineralocorticoids regulate the mineral and water balance of the organism.

1.1 Steroid metabolism

The adrenal gland and gonads are the two major sources of steroid hormones [1]—with the brain emerging as a third important source [3]. Our understanding of the stress response, and the associated side effects observed with prolonged stress (hypertension) as well as inborn errors (congenital adrenal hyperplasia, CAH), is limited by our lack of understanding of the intricate regulation and control mechanisms of steroidogensis [1].

The adrenal gland lies just above the kidney and occurs in fish, reptiles, birds and mammals [2]. It consists of two main parts: the outer cortex and the inner medulla [4]. The medulla secretes epinephrine and norepinephrine that are of great importance in the sympathetic and parasympathetic nervous system function [1]. The cortex supplies the organism with the steroid hormones involved in osmoregulation (mineralocorticoids) and regulation of metabolism (glucocorticoids); and maintenance of neurochemical balance and anatomical features (dehydroepiandrosterone, DHEA) [1].

All steroids are derived from cholesterol [1]. Very little of the body's cholesterol is synthesized *de novo* [5]. Most of the cholesterol is obtained from the diet [5]. Cholesterol is converted to pregnenolone (P5) by cytochrome P450 cholesterol side chain cleavage (CYP11A1). P5 is the precursor of all the other steroids and stands at the first branch point in the adrenal steroidogenic network

(Figure 1.1).

From P5 mineralocorticoids are synthesized in the adrenal cortex *zona glomerulosa* (Figure 1.1). Glucocorticoids are produced in the *zona fasciculata* from P5 via progesterone (P4) and 17α-hydroxy progesterone (17OHP4) [1, 4, 6, 7]. The DHEA branch begins at P5, which is converted to 17α-hydroxy-pregnenolone (17OHP5) that is in turn converted to DHEA.

Defects in the steroidogenic network can have serious consequences. Hypoandrenocorticism results from a shortage of cortisol. The animal cannot respond to stressful stimuli and may perish. Angora goats display this steroidogenic aberration [8] and are unable to respond to challenges of low temperature or other stress. In humans steroidogenic defects can cause congenital adrenal hyperplasia (CAH) [1, 7]. This condition may cause symptoms ranging from mild acne and salt wasting to virilization, depending on the nature of the genetic mutation.

In hypoandrenocorticism and CAH the error involves the two enzymes cytochrome P450 17α-hydroxylase/17-20 lyase (CYP17) and cytochrome P450 21-hydroxylase (CYP21) respectively. In the case of hypoandrenocorticism in the angora goat a DNA point mutation has been found in the *CYP17* gene that is hypothesized to result in less cortisol being produced when needed [8, 9]

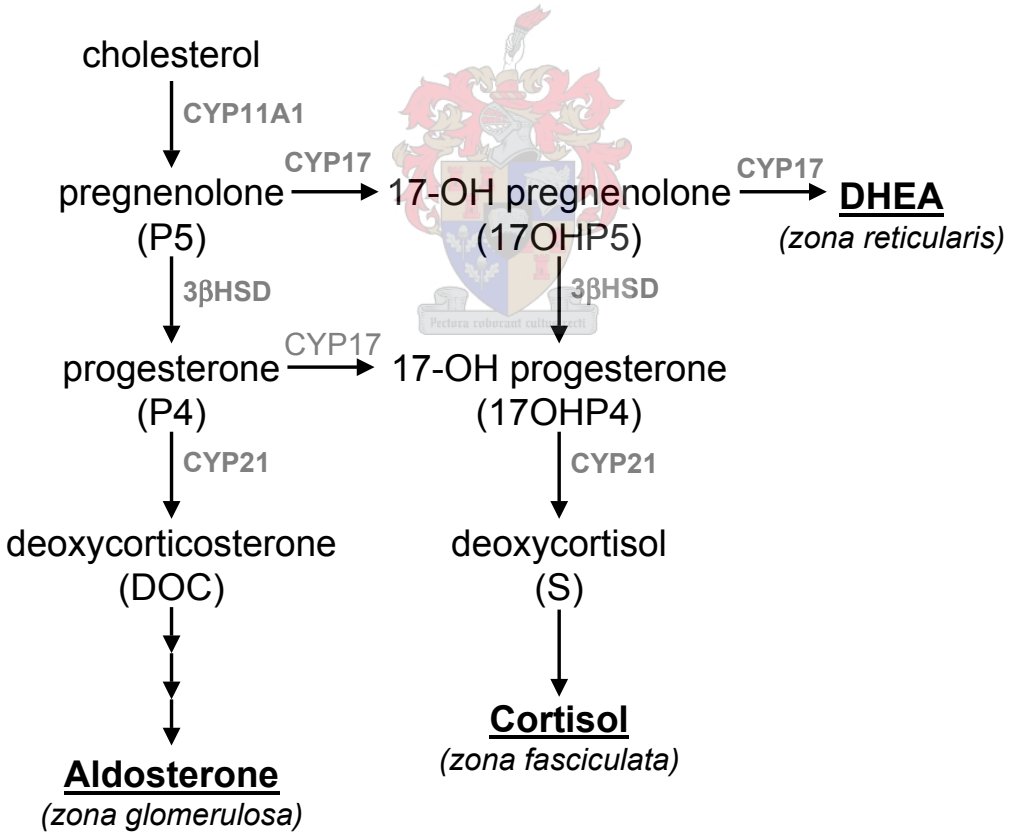

Figure 1.1: Major branches of adrenal steroidogenesis in *Homo sapiens*. In the first branch cholesterol is metabolized to aldosterone in the *zona glomerulosa*. In the second branch cholesterol is metabolized to cortisol and a small amount of corticosterone in the *zona fasciculata*. In the *zona reticularis* cholesterol is converted primarily to DHEA and androstenedione (not shown in above figure) with minuscule amounts of cortisol and deoxycorticosterone [1]. The enzymes active at the branch points are CYP17, CYP21 and 3βHSD.

but leaving mineralocorticoid supply unaffected. In CAH there is an error in CYP21 [7] that results in inefficient glucocorticoid and/or mineralocorticoid production. Because of a lack of glucocorticoids and mineralocorticoids the brain signals the adrenal gland with adrenocorticotrophic hormone (ACTH) to produce more of the deficient steroids [1, 7]. Consequently, there is an over production of P5 that in turn leads to an over production of DHEA. The excess DHEA in circulation is metabolized in extra-adrenal tissues to androgens and estrogrens [1].

These defects in adrenal steroidogenesis lie in the kinetic characters of the respective enzymes. Many *CYP21* mutations have been identified in patients with CAH [7]. These mutations either increase the K_m or decrease the V_{max}. Defects in 3β-hydroxysteroid dehydrogenase cause 5 to 10% of the CAH cases, 90 to 95% of the cases are caused by *CYP21* mutations [1, 7]. Mutations have been identified in *CYP17* that reduce both androgen and glucocorticoid production; as well as mutations that only affect androgen production [10, 11].

1.2 Analysis of control

A change in the activity of CYP17 and/or CYP21 causes a change in the ratio of the adrenal steroids. This raises the question of the degree of control CYP17 and CYP21 possess over the steroidogenic network.

Control is distinct from regulation [12]. Metabolic regulation is homeostasis (the maintenance of constant conditions in response to external perturbations) and is defined in terms of the performance of the system as a unit. The measure of regulation performance—co-response—is obtained by measuring the change of one variable against another in response to a change in a parameter value [13]. Co-response is mathematically defined as $\Omega_p^{y_1,y_2}$ where p is the perturbed parameter and y_1 and y_2 the steady-state variables that change in accordance with the perturbation of p.

Parameters are those characters of the system that do not ordinarily change such as enzyme concentration, temperature or (under special circumstances defined in a model) a metabolite concentration that is held at fixed concentration. Variables are those characters such as flux or metabolite concentration that change in response to changes in parameter values.

Control (C_v^y) is defined as the degree of influence a particular reaction step or group (v) has on the state (y) of a metabolic system [14]. It is measured as the fractional change in a variable from its previous steady-state value after a parameter perturbation.

For example, adrenocorticotrophic hormone (ACTH) regulates adrenal steroidogenesis by perturbing one or many parameters in the system but does not exercise any direct control over the flux or metabolite concentrations in the steroidogenic network. It is the various enzymes and transport proteins in the steroidogenic system that exert control over flux and metabolite concentrations.

To summate, parameters are regulated and steady-state variables are controlled.

This thesis is about control, not regulation. The question is thus: what degree of control does CYP17 and CYP21 have over the steroidogenic system?

It was previously held that the flux through a metabolic pathway can only be controlled by one enzyme—the rate-limiting enzyme [12]. In steroidogenesis all the control is hypothesized to lie with the activity of steroidogenic acute regulatory (StAR) protein or CYP11A1 [15] depending whether you regard steroidogenesis to begin at the transport of cholesterol into the cell/mitochondria or synthesis of P5 by CYP11A1.

Control analysis [12] has shown that the control over a pathway can be distributed among all the members of the pathway. As a consequence even large changes in K_m or V_{max} of certain enzymes may have only a small effect on the flux through a pathway. The degree to which a particular enzyme exercises control over the flux through a pathway or network is referred to as the flux control coefficient, C_v^J. Concentration control coefficients, C_v^s, relate the control an enzyme's activity has over the metabolite concentrations in the pathway. Such coefficients can be calculated through experimentation. Where experimentation is not possible (due to an inability to isolate the relevant enzymes and their activities, the inability to manipulate the enzymes or the inability of the experimental system to reach steady-state) mathematical models and computer simulations based on kinetic parameters can be used to calculate the control coefficients. (The application of such an approach is presented by Teusink et al (2000) [16]; and Rohwer & Botha (2001) [17] who present supporting data in the article by Schäfer *et al* (2004) [18].)

The simplest way of expressing the control properties, structure and local kinetic properties of a reaction network is by using matrix algebra [19]. Using such methods it is possible to determine which enzymes or sections of a pathway, network or system will have control and which will not without knowing detailed information about the components of the pathway [12, 20]. Insight into the system can be obtained from this methodology. If detailed information and experimental data is available this methodology can be used to calculate the control and regulatory coefficients.

The construction of numerical models can also be used to derive the control and response coefficients. For such a model, reliable and accurate kinetic data is required. One needs to have studied the pathway and accounted for all the interactions between the enzymes and substrates. In order for a model—a hypothesis—to be scientifically valid one also needs an experimental setup capable of testing the model's predictions [21].

1.3 Methods to study steroidogenesis

In cytochrome P450 research two methods of experimentation have been primarily used. These are microsomal and tissue culture studies.

Microsomal suspensions and specific enzyme inhibitors can be used to perform experiments to profile adrenal steroidogenesis. As a tool, this method has shortcomings. Both CYP17 and CYP21 as well as 3βHSD are present in the microsomal preparations at unknown concentrations. It is therefore not possible to ascertain the relative importance of each individual enzyme species on adrenal steroidogenesis.

Another problem is the suspension no longer represents the natural state of the adrenal gland and loses the anatomical features of the steroidogenic network. As was briefly explained above (and will be further explained in Chapter 2) the adrenal gland is composed of two distinct tissue types, the cortex and medulla [1, 4]. The cortex is then further subdivided into three zones: the *zona glomerulosa*, the *zona fasciculata* and the *zona reticularis*. Each of these zones performs a different steroidogenic function. In the preparation of the microsomal suspension, not only is the structure lost and the different tissue enzyme concentrations pooled, but a host of undefined enzymes unrelated to mineralo- and glucocorticoid synthesis are also isolated making controlled study difficult.

Tissue culture using nonsteroidogenic cell lines has been extensively used in the study of steroidogenesis, but the transfection techniques allow for only one steroidogenic enzyme to be expressed with any control. P. Swart (*pers comm.*) has observed that during co-transfections the cells can only assimilate a finite quantity of plasmid and no control exists as to how much of each plasmid is assimilated. For this reason it is not possible to perform controlled experiments using traditional co-transfection and tissue culture techniques.

The parallel transfection method [6] allows for the separate transfection of cell lines with relevant steroidogenic enzymes (see Figure 1.2 and A.4.6) and recombination for experimental purposes according to desired ratios. It has been shown [6] that there is a linear increase in steroid turnover in respect to increasing CYP concentration (i.e. the number of tissue culture dish slices); and that this linear increase is constant over the enzyme concentration range employed in experimentation. This technique allows the experimenter to manipulate the amount of enzyme in a defined environment in a controlled manner eliminating the effects of random plasmid assimilation.

In the case of the bovine pCMVc17 and pCMVc21y401 plasmids it is known how each plasmid behaves in the COS1 cell line and that this behaviour is repeatable over many experiments. Controlled changes can be made to the activity of each enzyme as there is a direct correlation between the number of transfected cells and enzyme activity [6].

1.4 Outline of thesis objectives and content

With a reliable experimental system and mathematical framework meaningful questions can now be asked. These questions are:

1. To what degree will a change in CYP17 and/or CYP21 activity perturb the flux and metabolite concentrations in the steroidogenic network.

2. Which enzyme(s) possess the most control over the steroidogenic system under study.

A model of the CYP17/CYP21 steroidogenic branch point was simultaneously constructed and tested using Parallel transfection techniques. COS1 cells and the well characterized bovine

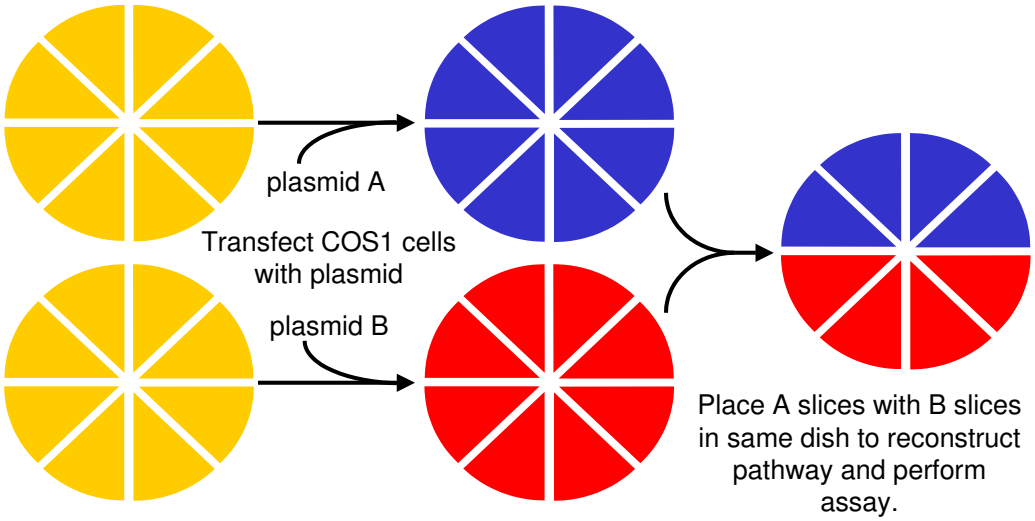

Figure 1.2: Parallel transfection and slice recombination. In the Parallel Transfection method one plate is transfected with one steroidogenic enzyme and another plate transfected with a different enzyme. The tissue culture plate slices on which the cells are growing are then recombined to represent a segment of the steroidogenic network so experiments can be performed to test the importance of the relative enzyme activities.

pCMVc17 and pCMVc21y401 plasmids were used for the transfections.

Chapter 2 reviews the role and metabolism of the adrenal steroids and discusses the regulation of steroidogenesis in relation to the anatomy of the gland. In Chapter 3 the biochemistry of the P450s is discussed and the enzymes CYP17 and CYP21 are briefly reviewed. Chapters 4 and 5 discuss the construction of the computer model, testing, application and analysis thereof. In Chapter 6 the insights from the model are tentatively applied to the physiological state and further research prospects proposed. Appendix A details the methods employed in the experiments reported in this thesis.

Chapter 2

The role of steroids and steroid metabolism in homeostasis

In this chapter the physiological role of steroids will be discussed with emphasis on the glucocorticoids and mineralocorticoids. A brief mention will be given to the role of the sex steroids (androgens and estrogens) along with information regarding their metabolism.

2.1 The role of steroids

Steroids are hormones that can be classed into three groups: glucocorticoids, mineralocorticoids and androgens [1]. The glucocorticoids are concerned with stress response and metabolic homeostasis with regard to energy supply and demand [1]. The mineralocorticoids are responsible for salt balance and proper kidney function [1]. Androgens and estrogens are implicated in the maintenance of secondary sex characteristics, regulation of the reproduction cycle and health and healing [22].

Evidence indicates that DHEA and its derivatives are involved in brain chemistry [23, 24, 25]. Androstenedione, testosterone and estradiol are implicated in the regulation of anabolism [1]. The main sources of androgens are the gonads [1, 26] with small amounts of precursor (DHEA and androstenedione) synthesized by the adrenal gland [1, 22, 27] and brain [24, 25]. The type of androgen synthesized in the adrenal is dependent on the species. Rodents do not synthesize any androgens nor cortisol in the adrenal gland [22, 28, 29, 30]. Estrogens can be synthesized in the plascenta, adipose tissue, fibroblasts, brain, osteoblasts, macrophages and fetal tissues [31].

The glucocorticoids and mineralocorticoids are produced in the adrenal cortex [1, 32] with trace amounts in the skin [33].

2.1.1 Glucocorticoids

The steroids classed as glucocorticoids are: deoxycortisol (S), cortisol and corticosterone. The main roles of the glucocorticoids are maintenance of metabolic homeostasis; and eliciting the body's stress response [1, 22, 32]. They serve to regulate carbohydrate, protein and fat metabolism and osmotic balance, mediating the excretion of water from the body. A lack of glucocorticoids can result in collapse and death from exposure to even minor noxious stimuli or water intoxication [1]. It is interesting to note that a small amount of steroid can correct for such a shortage.

Steroids are amphipathic and easily diffuse through the plasma membranes of cells [1, 32]. In target cells they bind to the glucocorticoid receptor (GR) (see Figure 2.1), that then dimerizes and recruits transcription factors. The GR binds to specific DNA sequences and initiates the expression of diverse homeostatically strategic genes [1, 32, 34, 35]. The products of these genes correct the homeostatic imbalances that then signals the brain to cease the stimulation of glucocorticoid production.

The normal response to stress is an increase in glycogenesis and gluconeogenesis through the upregulation of phosphoenol pyruvate carboxylase, fructose-1,6-bisphosphatase, glucose-6-phosphatase and glycogen synthase [1, 32]. In peripheral tissues glucocorticoids have an anti-insulin effect that can aggravate diabetes. Here they inhibit protein synthesis and increase protein catabolism [32] and have a permissive action: allowing glucagon and catecholamines to exert their calorigenic effects [1]. In addition they increase ketone body formation and plasma lipid levels. Glucocorticoids serve to regulate the osmotic balance and prevent water intoxication by stimulating the excretion of sodium ions.

Glucocorticoids and ACTH regulate their own production via a negative feedback loop preventing the secretion of ACTH [1] (Figure 2.1).

Glucocorticoids are critical for vascular reactivity and are implicated in nervous disorders [1]. A lack of glucocorticoids can cause irritability, apprehension and an inability to concentrate, reminiscent of alcohol intoxication.

Cortisol specifically inhibits lymphocytes, eosinophils and basophils by inhibiting mitosis, DNA replication, antibody production and interleukin-2 (IL-2) secretion [1, 32]. Glucocorticoids have been observed to stimulate the apoptosis of T-lymphocytes stunting the immune system. They also reduce the severity of allergic and inflammatory responses. Fibroblast growth is inhibited slowing wound and broken bone healing [1, 32]. Excess use of glucocorticoids as a medication can cause bone degradation.

Stress causes an increase in ACTH and glucocorticoid levels. The increase in plasma glucocorticoid concentration reachs pharmacologic levels (from a basal 3.8 nM to 14 nM) that are life-saving in the short term but are harmful and disruptive in the long term. This increase relative to the concentration of mineralocorticoid is not well understood [1] and is one of the issues the work reported in this thesis attempts to clarify.

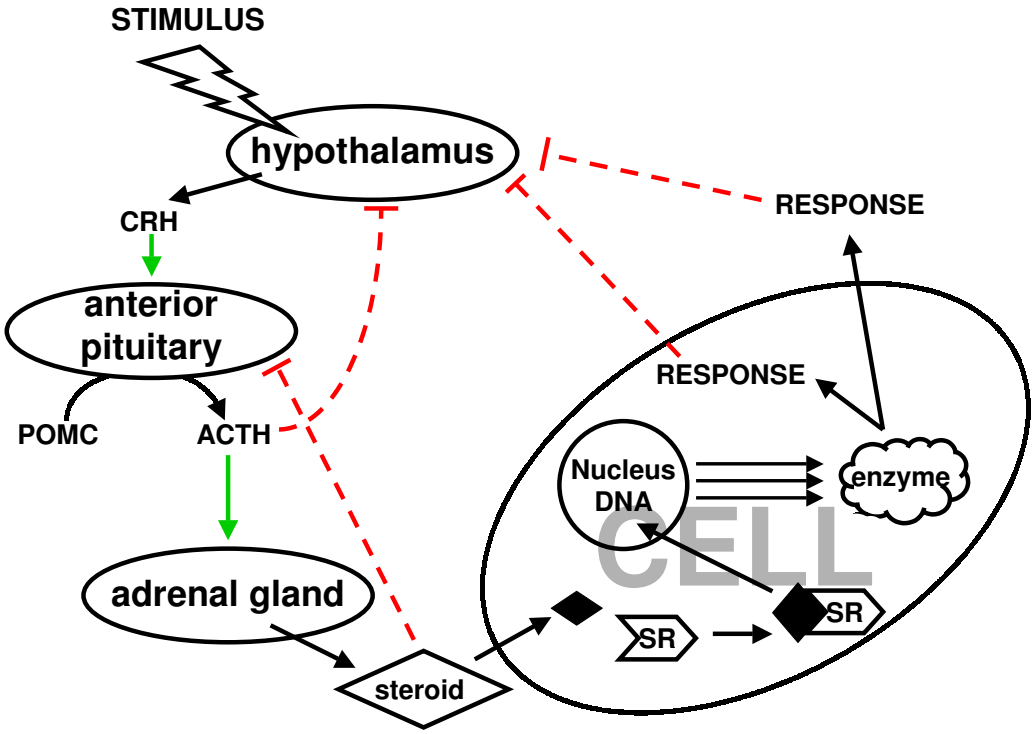

Figure 2.1: The regulation of glucocorticoid release and action. In response to a stimulus the hypothalamus secretes corticotrophin releasing hormone (CRH) that triggers the anterior pituitary to convert pro-opiomelanocortin (POMC) to ACTH. The ACTH stimulates the adrenal gland to synthesize and secrete steroid hormones. This chain of events is referred to as the hypothalamic-pituitary-adrenal-axis, HPA-axis. The steroids diffuse into target cells and initiate gene transcription via steroid receptors (SR) and transcription factors. This results in a physiological response that is perceived by the brain and the release of CRH is stopped. The secretion of ACTH inhibits CRH release and an increase in steroid inhibits ACTH release [1].

2.1.2 Mineralocorticoids

There are three steroids that exert a mineralocorticoid effect. These are, in order of decreasing efficacy: aldosterone, corticosterone and deoxycorticosterone (DOC) [1, 32]. These hormones are involved in the retention and absorption of sodium from the extracellular fluid (urine, sweat, saliva and gastric juices). They affect the epithelial cells of the cortical collecting ducts in the kidney where it acts to increase sodium absorption and potassium and proton excretion. The opposite is caused in the brain and muscle tissues where they promote sodium excretion and potassium retention.

The method of action of the mineralocorticoids is similar to that of the glucocorticoids mentioned above [1]. Their affect can occur within 10 to 30 minutes; but they also have a faster nongenomic effect. Mineralocorticoids directly inhibit the amiloride-inhibitable sodium channels in the apical membrane, presumably via the inositol-triphosphate signaling pathway [1]. They increase the activity of the sodium-potassium exchange via increased expression of the sodium-potassium ATPase. A loss of mineralocorticoids can result in hypotension and circulatory problems that can lead to fatal shock.

Table 2.1: Relative potencies of corticosteroids compared with cortisol. The last three steroids are synthetic and do not occur naturally. The values are approximates based on liver glycogen deposition, of anti-inflammatory assays for glucocorticoid activity, and effect on urinary Na^+/K^+ or maintenance of adrenalectomized animals for mineralocorticoid activity. Data taken from [1]

Steroid	Glucocorticoid activity	Mineralocorticoid activity
Cortisol	1.0	1.0
Corticosterone	0.3	15.
Aldosterone	0.3	3000.
DOC	0.2	100.
Cortisone	0.7	1.0
Prednisolone	4.	0.8
9α-Fluorocortisol	10.	125.
Dexamethasone	25.	~ 0.

The mineralocorticoid response element (MR) is more sensitive to glucocorticoids than mineralocorticoids (see Table 2.1). This problem is solved by the MR sensitive tissues expressing type 2 11β-hydroxysteroid dehydrogenase that converts cortisol to cortisone and corticosterone to 11-oxy-corticosterone [1].

2.2 Steroid metabolism: an overview

Steroid metabolism in the adrenal gland is composed of a complicated network of reactions. An understanding of the topology of the steroidogenic network is crucial to the comprehension of the information presented in this and later chapters.

Using cholesterol metabolism (Figure 2.2) as a starting point for discussion.

Steroids are synthesized in the gonads, brain, adrenal cortex, skin and placenta [26, 28, 31, 33, 36]. They are metabolized by cytochrome P450 enzymes in the endoplasmic reticulum and mitochondria. The endoplasmic reticulum (ER) P450s are linked to cytochrome P450 reductase (CPR) that supplies the electrons for the oxidation of the steroids. The two electrons are used for the activation of oxygen as described in section 3.1.2. In the mitochondria the electrons are derived from the mitochondrial membrane electron transport system.

Steroid metabolism is highly compartmentalized [5]. This feature will be dealt with in Section 2.3.

2.2.1 Cholesterol metabolism

Cholesterol is the precursor of all steroids [1]. Cholesterol is synthesized *de novo* from acetate but is primarily imported into the adrenal cells as low density lipoprotein (LDL) [1, 5].

LDL receptors are especially abundant in the adrenocortical cells of the adrenal cortex [5]. The

LDL that is taken up (reaction 2, Figure 2.2) is ferried across the membrane of the lysosome by cholesterol ester transfer protein (CETP), the cholesterol is then esterfied by acetyl-CoA:cholesterol acyltransferase (ACAT) (reaction 6, Figure 2.2) and stored in lipid droplets in the cell [26, 37]. Cholesterol ester hydrolase (CEH) catalyzes the release of cholesterol (reaction 7, Figure 2.2) in lipid droplets. The free cholesterol is transported to the mitochondria by the sterol carrier protein 2 (SCP2) and across the mitochondrial membranes by steroidogenic acute regulatory protein (StAR), a protein of 32 to 37 kDa [15, 38].

StAR is hypothesized to facilitate the contact points between the outer and inner mitochondrial membrane that allows cholesterol to diffuse to cytochrome P450 side chain cleavage (CYP11A1) that metabolizes it to P5 [1, 5, 15, 38].

2.2.2 The fate of pregnenolone

P5 stands at the first branch in the adrenal steroidogenic pathway. If metabolized by 17α-steroid hydroxylase (CYP17) it can be committed to androgen biosynthesis (see Figure 2.3) [1]. If it is metabolized by 3β-hydroxysteroid dehydrogenase isomerase (3βHSD) to yield progesterone (P4) and one molecule of NADH it is committed to corticoid biosynthesis. It is at P4 that the next branch in the steroidogenic pathway occurs [1]. This branching leads to either mineralocorticoid or glucocorticoid biosynthesis.

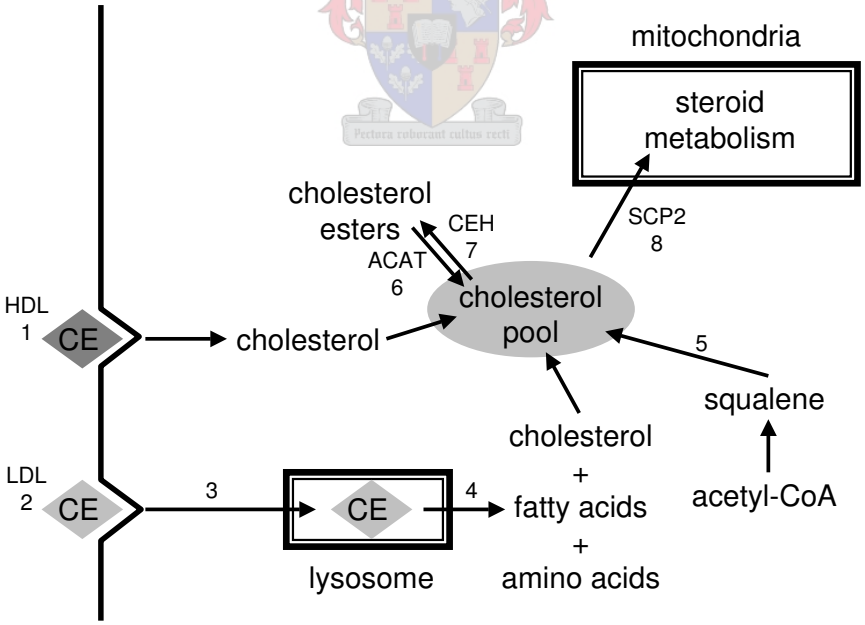

Figure 2.2: Pathways of cholesterol metabolism in steroidogenic tissue. (1) LDL binding and receptor-mediated internalization. (2) HDL binding and cholesterol ester uptake. (3) Sorting of LDL to lysosomes. (4) Lysosomal hydrolysis of CE and other LDL components. (5) *De novo* cholesterol biosynthesis. (6) Esterfication of cholesterol for storage in lipid droplets. (7) Hydrolysis of stored esters. (8) Cholesterol transport to the outer mitochondrial membrane by SCP2 and translocation across the membrane mediated by StAR. (9) CYP11A1 mediated reaction of cholesterol to yield pregnenolone and isocarproaldehyde. Figure redrawn and modified from [5].

2.2.3 The biosynthesis of aldosterone

Aldosterone is the end product of the mineralocorticoid branch of steroidogenesis. The steroid 21-hydroxylase (CYP21) converts P4 to DOC in the ER. The DOC then diffuses back into the mitochondria where it is metabolized to corticosterone via 11β-hydroxylase (CYP11B1). Corticosterone is converted to aldosterone in a two step process whereby it is oxidized at position 18 in a process carried out by the same enzyme: aldosterone synthase (CYP11B2) [1, 3]. The bovine CYP11B1 isoform is capable of the same activities as the human CYP11B2 isoform which is not present in *Bos taurus* (the cow or bull).[6].

Aldosterone diffuses freely out of the mitochondria and the cell into the blood stream where it, and other steroids, are bound and transported by steroid hormone binding globulins (SHBG) [1].

2.2.4 The biosynthesis of cortisol

For cortisol biosynthesis, P4 is converted to 17-hydroxy-progesterone (17OHP4) by CYP17. The 17OHP4 is converted to S by CYP21. The S diffuses into the mitochondria where it is metabolized to cortisol by CYP11B1

Cortisol is further metabolized to cortisone by type 2 11β-hydroxysteroid dehydrogenase (11βHSD) in the liver. In the liver it is reduced and conjugated to form tetrahydrocortisone glucuronide and excreted into the urine in the kidneys [1]. While type 1 11βHSD can convert cortisol to cortisone and *vice versa* using NADH as electron carrier, type 2 11βHSD can only metabolize in the direction of cortisol to cortisone. About 10% of the cortisol is converted to 17-keto-steroid in the liver. The 17-keto-cortisol is conjugated to sulphate and excreted. 20-hydroxy derivatives are also formed.

Corticosterone is metabolized similarly to cortisol except that no 17-keto derivatives are formed [1].

2.2.5 DHEA to β-estradiol

Sex steroid synthesis begins with the conversion of pregnenolone to 17-hydroxy-pregnenolone (17OHP5) via CYP17. 17OHP5 is converted to DHEA via the 17,20-lyase activity of CYP17; or 17OHP5 can be converted to 17OHP4 via 3βHSD and proceed to S or androstenedione. DHEA can be converted to androstenedione by 3βHSD or sulphonated by adrenal sulfokinase to form DHEA-sulphate—the primary form of DHEA secreted from the adrenal. In the adrenal gland of many animals androgen synthesis stops at DHEA or androstenedione. In small mammals it does not occur at all [22, 28, 29, 30].

DHEA and androstenedione can be converted to testosterone and estrogens in the circulation by diffusing into other steroidogenic tissues; and are an important source of sex steroids in men and postmenopausal women [1].

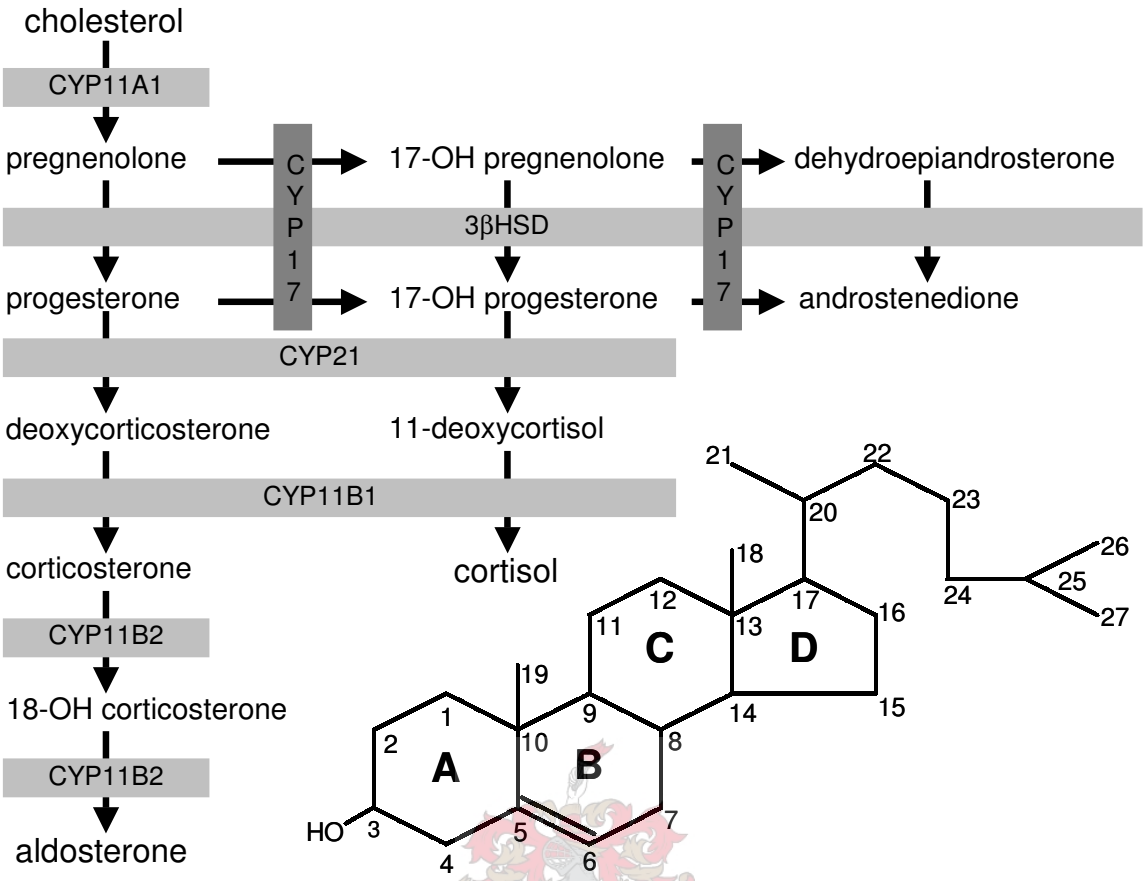

Figure 2.3: Schematic representation of adrenal steroid metabolism terminating at androstenedione. The reactions catalyzed by CYP11A1, CYP11B1 CYP11B2 occur in the mitochondria. All other reactions occur in the ER. The inset is the numbered structure of cholesterol. The CYP11A1 reaction cleaves off carbons 22 to 27.

Androstenedione can be metabolized reversibly to testosterone in a reaction catalyzed by 17β-hydroxysteroid dehydrogenase [1, 26]. Testosterone can be metabolized to dihydrotestosterone by 5α-reductase in the gonads, brain and placenta. Aromatase (CYP19) can metabolize testosterone to 17β-estradiol or form estrone directly from androstenedione. Estrone can be converted to 17β-estradiol in a reversible reaction catalyzed by 17β-hydroxysteroid dehydrogenase.

In the human adrenal gland, DHEA is the major androgen synthesized [1, 3, 10, 27, 30].

2.3 Regulation of steroidogenesis

The anatomy of the adrenal gland is a governing feature of adrenal steroidogenesis. From tissue organization and enzyme expression patterns it is evident that the adrenal gland is a complicated and intricately regulated organ composed of dynamic tissue types. The anatomy and regulation of steroidogenesis in the adrenal gland will be discussed in the following sections.

2.3.1 The adrenal zones of steroidogenesis

The adrenal cortex is divided into three distinct zones from capsule to medulla: the *zona glomerulosa*, *fasciculata* and *reticularis* (Figure 2.4) [4].

In man the *zona glomerulosa* constitutes 15% of the adrenal cortex volume while the *zona fasciculata* occupies 80%. The *zona reticularis* comprises 5 to 7%, but has a wider radius than the *zona glomerulosa* and *zona fasciculata* and thus appears to be larger. The *zona glomerulosa* is a tightly packed collection of ovoid clusters and curved columns that are continuous with the *zona fasciculata*. These cells are surrounded by a rich network of fenestrated sinusoidal capillaries. The large polyhedral cells of the *zona fasciculata* are supplied by the same fenestrated sinusoidal capillary network. The cells of the *zona reticularis* are smaller than those of the *zona fasciculata*. These cells are arranged in anastomising cords separated by fenestrated capillaries. All the cells exhibit a well-developed smooth endoplasmic reticulum and numerous mitochondria.

The determination of the steroid products of the adrenal cortex begins with its anatomy. The fenestrated sinusoidal capillaries flow from the capsule into the medulla. The capillaries flow through the *zona glomerulosa* into the *zona fasciculata* and then into the *zona reticularis*, forming a dense network. It is hypothesized that by this mechanism, excess steroidogenic intermediates are metabolized and so do not exit the adrenal gland and upset the steroid mediated homeostasis of the animal [28].

The anatomical compartmentalization allows for the biosynthesis of a range of steroids from a complicated interconnected pathway (see Figure 2.5). Aldosterone is the major product of the *zona glomerulosa*. The *zona fasciculata* produces cortisol and the *zona reticularis* yields androgens and small amounts of cortisol [4, 28].

The size and output of the adrenals zones has been observed to change with age in the guinea pig [28] and primate fetus [40].

At the onset of andrenarche in great apes there is an increase in androgen/estrogen produc-

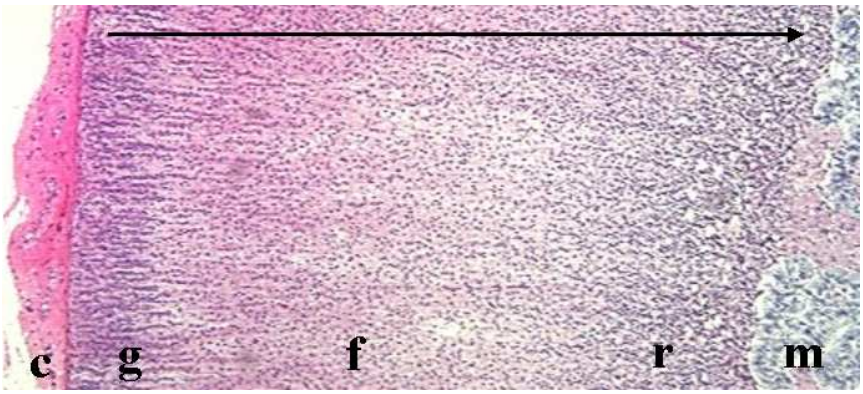

Figure 2.4: Steroidogenic zones in the cat adrenal gland. The picture above displays: (c) the capsule; (g) *zona glomerulosa*; (f) *zona fasciculata*; (r) *zona reticularis*; (m) medulla. The arrow (→) indicates the direction of blood flow. Modified from [39] .

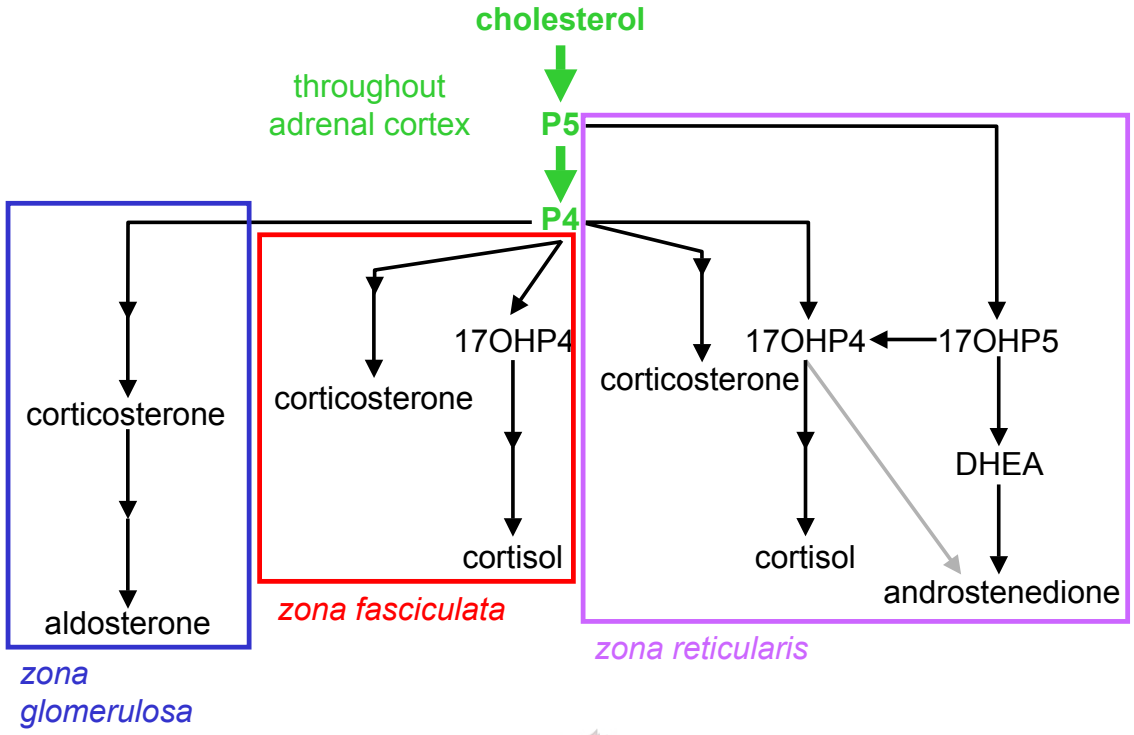

Figure 2.5: Steroid products from the three tissue zones of the adrenal cortex. Each box represents a primary steroid product associated with a particular adrenal cortex zone. The reactions outside the boxes occur in all three tissues. Each arrow head denotes a reaction step. Only beginning, end and branch point metabolites are shown for brevity.

tion independent of the testes [41]. The adrenal gland increases in size resulting in a higher flux from P5 to DHEA. During menopause the adrenal shrinks but the ratio of $[(\mathrm{P5})/(\mathrm{P4})]$: $[(\mathrm{17OHP5})/(\mathrm{17OHP4})]$ remains constant while the concentration of DHEA decreases [41].

In the guinea pig the *zona reticularis* is observed to increase with age with a resulting increase in activity of this region. This is associated with a decrease in the size of *zona fasciculata* and a concomitant decrease in cortisol output. The increase in the size of this zone is accompanied by an increase in the activity of CYP2D16 (an enzyme associated with xenobiotic metabolism) in the guinea pig [28]. This enzyme can degrade cortisol. On account of the blood flow from *zona glomerulosa* to *zona reticularis*, it is put forward that this enzyme activity may serve to modulate the adrenal hormone secretion [28].

CYP11A1 is more active in the *zona fasciculata* than the *zona reticularis* of the guinea pig. This conforms with the observation that in small mammals androgen synthesis is restricted to the gonads [1, 28].

During maturation there is a decline in the activity of CYP2D16 in female guinea pigs. It has been speculated that this is linked to the increase in free estrogens. The *zona reticularis* only reaches a size of 40% adrenal volume in the female compared to the male volume exceeding 50%. This indicates that the difference in male and female steroid hormone ratios are mediated as much by differential enzyme expression as by anatomical modulation and enzyme activity.

2.3.2 Regulation of P450 expression

Different steroidogenic P450 expression patterns exist in the three adrenal steroidogenic tissues as shown in Table 2.2.

Table 2.2: Steroidogenic enzymes expressed in adrenal tissues. Contents of table obtained from information in [1, 3, 4, 28].

zona glomerulosa	*zona fasciculata*	*zona reticularis*
CYP11A1	CYP11A1	CYP11A1
CYP11B1	CYP11B1	CYP11B1
CYP11B2	—	—
CYP21	CYP21	CYP21
—	CYP17	CYP17
3βHSD	3βHSD	3βHSD
CPR	CPR	CPR
—	(CYTB5?)	CYTB5

Steroidogenic P450 expression is regulated in a tissue specific manner [31]. All steroidogenic P450s have a steroidogenic factor 1 (SF1) binding motif upstream of the promoter. SF1 is implicated in the regulation of P450 steroid hydroxylase expression [34]. A Nur77 binding motif (which is implicated in apoptosis signalling pathways in the immune and nervous system [42]) is also associated with P450 expression [35]. Neither DNA binding motifs explain how expression can be regulated independently between tissue types.

The *CYP21A* and *CYP21B* alleles have an intricate promoter structure with various sites for expression regulation [35]. The *CYP21A* gene lies adjacent to the *C4A* gene that codes for the major histocompatibility complex in man and mouse, and the *CYP21B* gene lies adjacent to the *C4B* gene. The order is 5' *C4A*, *CYP21A*, *C4B*, *CYP21B* 3', from telomere to centromere. The Z promoter, of the *CYP21* gene lies in intron 35 of the *C4* gene. This Z promoter is composed of three sub-promoters: ZA, ZB and XA. They are adrenal specific and under the control of SF1 but their regulator is not yet known.

2.3.3 Regulation of adrenal steroidogenic output

Adrenal steroidogenesis is strictly regulated by hormonal means. The two primary effectors of adrenal steroidogenesis are angiotensin II and ACTH [1]. Gonadotrophins are not involved in the regulation of adrenal steroidogenesis but rather the development of the various steroidogenic tissues. The adrenal androgen-stimulating hormone (AASH) secreted by the pituitary during adrenarche is theorized to regulate the androgen/estrogen output of the adrenal [1].

The peptide hormone, ACTH, is secreted by the anterior pituitary in response to physiological stress (e.g. having starved oneself while sleeping during the night) [1] and is the major stimulant

of the adrenal cortex [28]. ACTH is a 39 amino acid polypeptide derived from a 134 amino acid precursor pro-opiomelanocortin (POMC) (see Figure 2.1). POMC is cleaved into ACTH, lipotropin (γ-LPH) and β-endorphin in response to the stimulation of CRH released from the hypothalamus. Some γ-melanotropin (γ-MSH) is also released. The first 23 amino acids of ACTH form the active core of the molecule. ACTH serves to increase the amount of circulating glucocorticoids and androgens. ACTH binds to ACTH receptors on the cell surface of the adrenal cortical cells with high affinity where it activates an adenylate cyclase via a G_s-coupled protein. This initiates an increase in cAMP with a resultant activation of protein kinase A (PKA). PKA activates CEH by phosphorylating it. This results in an increase in free cholesterol that is converted to pregnenolone, feeding the steroid biosynthesis pathways.

PKA upregulates the expression of P450 enzymes CYP11B1 and CYP11A1 [1], and 3βHSD. Protein kinase C (PKC) has been shown to down-regulate the expression of these enzymes [43] and appears to be a tonic negative regulator of steroidogenesis. These effects by PKA in response to ACTH are only observed under chronic stimulation. With acute stimulation, only an increase in StAR mRNA is observed [44]. This increase in StAR mRNA cannot explain the early effects resulting from ACTH stimulation. Under acute stimulation the activity of CYP11A and CYP21 remain unchanged. The acute effects appear to be the result of the increase in free cholesterol [43]. ACTH also increases the levels of c-jun, c-fos, jun-B and fos-B [43] that play a role in the cell cycle [45]. These polypeptides form part of the AP-1 transcription factor that has been shown to work synergisticly with the glucocorticoid receptors and is associated with the expression of a wide range of target genes, many of which are not associated with the cell cycle [43]. Increases in cAMP also causes the up regulation of a 30 amino acid peptide, steroidogenesis activator polypeptide (SAP, a 3.2 kDa 30 amino acid polypeptide) [1, 15]. SAP stimulates CYP11A1 activity *in vitro* and may facilitate cholesterol transportation into the mitochondria but no mechanism has been satisfactorily demonstrated [15, 46]. SAP is present in all steroidogenic tissues that have to date been investigated [15, 26, 46, 47].

ACTH has only major effects on the *zona fasciculata* and *zona reticularis* with acute stimulation. The *zona glomerulosa* is under the control of the peptide angiotensin II (Figure 2.6) that binds to a specific receptor on the surface of the *zona glomerulosa* cells [1]. The *zona glomerulosa* is mildly responsive to ACTH. Angiotensin II serves to increase the amount of mineralocorticoids in circulation [33]. It is linked to a G-protein that activates PKC. In the *zona glomerulosa* PKC triggers an increase in the conversion of cholesterol to pregnenolone as well as DOC to 18-hydroxycorticosterone. Angiotensin II is produced in the liver as Angiotensin (see Fig. 2.6).

Tumor necrosis factor α (TNF-α) stimulates steroidogenesis by triggering a release of ACTH [48]. TNF-α decreases the synthesis of cortisol, shifting metabolism to androgen synthesis. Glucocorticoids reciprocate by suppressing the effect of TNF-α by inhibiting the monocytes that secrete it. This feedback loop functions over a time frame dependent on the duration of the stimulus. At the onset of illness (e.g. a viral infection) there is a release of TNF-α that results in a decrease in

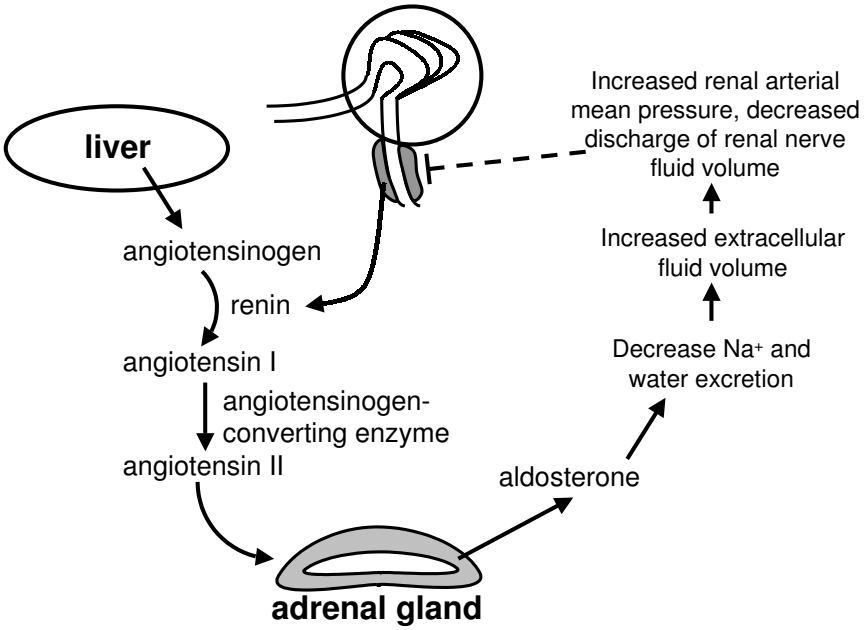

Figure 2.6: Schematic representation of the regulation of the *zona glomerulosa* by angiotensin. The juxtaglomerular apparatus in the kidney perceives low blood pressure and synthesizes renin that initiates a signal cascade leading to the negative feedback regulation of renin release via the adrenal synthesis and release of aldosterone. Figure modified from [1].

cortisol and increase in androgens that promote healing and stimulate the immune system. The released TNF-α causes an increase in ACTH that increases cortisol levels that then in turn decreases the levels of TNF-α returning the physiology back to its original state.

Cortisol mediates a direct effect on the pituitary as well as on the hypothalamus where it inhibits corticotropin-releasing hormone that would stimulate the release of ACTH in response to stress [1].

2.3.4 Allosteric and covalent effectors of steroidogenesis

The main allosteric effector of the steroidogenic pathway is cytochrome b5 (CYTB5) and the covalent modifier ATP, which is used to phosphorylate certain enzymes as explained for CEH in section 2.2.1.

CYP17 has been identified as a target of allosteric regulation in the adrenal [10, 30, 36, 49]. As the reactions catalyzed by CYP17 (see Figure 2.3) stand at critical branch points, it must be strictly regulated to avoid developmental and metabolic abnormalities. No definitive information is currently available as to the factors that limit its expression to the *zona fasciculata* and *zona reticularis*.

The switch between 17-hydroxylase to 17,20-lyase activity is mediated by CYTB5, phosphorylation and the concentration of NADPH-CPR [22, 30, 36, 41, 50, 51, 52]. The lyase activity is regulated independently of the 17-hydroxylase activity in an age-dependent pattern to regulate the onset of andrenarche [41, 52]. This developmental regulation is only seen in man and the great apes.

While CYTB5 and CPR have been implicated experimentally in the activity of the 17,20-lyase reaction, these show no increase relative to the activities of CYP17 *in situ* [11, 41]. The ability of CYTB5 to increase the catalysis of Δ4- as well as Δ5-steroids brings into question its role as a selective allosteric activator CYP17 [41].

Using ovine microsomes it has been found that CYTB5 exists as a tetramer [53] and in addition to increasing the reaction rate of CYP17 it also increases the reaction rate of CYP21 [54].

CYTB5 is found as two types: 1 and 2. Type 2 bears 45.8% homology to Type 1. These two isoforms are products of transcriptional modification [55]. Both have been shown to stimulate lyase activity [30, 50, 56]. Type 1 is mainly expressed in the liver, testes and *zona reticularis* of the adrenal with trace expression in the *zona glomerulosa* and *zona fasciculata*.

The phosphorylation of CYP17 seems to be the most reasonable explanation for the switch between 17-hydroxylase and 17,20-lyase activity [41, 52].

2.4 Summary

The synthesis of steroid hormones occurs in an intricate network of reactions that are regulated at many different levels. From the data it is clear that it is the anatomy of the gland more than any other one factor that determines the end products of the steroidogenic network. Effectors such as ACTH, angiotensin, CYTB5 and the phosphorylation of certain enzymes only serve as tonic regulators of the various enzymes involved. This is not to claim that the kinetic properties of the enzymes are irrelevant, to the contrary, the kinetics of each enzyme is important. The flux through any pathway can only be as fast as the slowest reaction in the pathway. The maximal pace at which the enzymes can work is determined by their kinetic properties. These properties will be discussed in the next chapter.

Chapter 3

Cytochromes P450: structure, stoichiometry and kinetics

3.1 What are P450s and how to they work?

P450s are cytochromes belonging to the CYP gene superfamily [57]. These hemeoproteins are mixed-function oxidases and exhibit a peak at 450 nm upon reduction and saturation with CO (Figure 3.1) [32, 58, 59].

There are no less than 3703 unique named CYP genes and pseudogenes as of July 2004 [60] in 368 families and 814 subfamilies [60]. P450s occur in a wide range of organisms, from simple bacteria to all animals and plants [58, 61].

The P450 family is responsible for the metabolism of endogenous compounds such as fatty acids, sterols, prostaglandins and ketones [57, 58, 59, 62, 63]. They play an important role in the metabolism of xenobiotics and are hypothesized to play a role in redox cycling to generate reactive oxygen species in the cell [63].

3.1.1 The CYP family: discovery, nomenclature and structure

Klingenberg published the discovery of a CO binding pigment in liver microsomes in 1958 [59]. Omura and Sato established that this CO binding pigment was a hemoprotein in 1961 [64, 65] when they observed the characteristic absorbance spectrum in the Soret region with an absorbance maximum of 450 nm after saturation with CO and reduction (Figure 3.1).

Cytochromes P450 constitute a large gene superfamily classified by amino acid sequence homology, i.e. structure rather than function [61, 66]. The nomenclature of P450s can be described with reference to an example: CYP3A1. CYP is the class of protein, the three designates the family and the letter A denotes the subfamily. The last number, in this case one, identifies the type [59, 66].

The structures of four bacterial P450s have been resolved. These are P450cam, P450BM3,

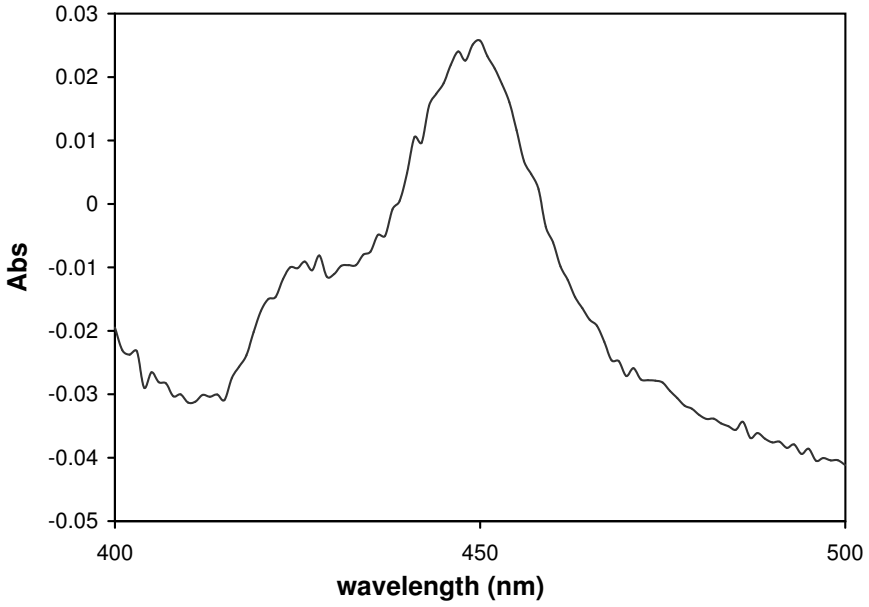

Figure 3.1: CO-induced difference spectrum of reduced ovine microsome P450s. Microsomes diluted 10× in 100 mM Phosphate buffer at pH 7.2 and gassed with CO. Sodium dithionite was added to reduce the P450 and generate the difference spectrum. Graph plotted from the author's data.

P450terp and P450eryF [10, 67]. P450cam has been solved to a resolution of 2.0 Å [10], and has been used to develop structural computer models for mammalian P450s. Animal and plant P450s are membrane-bound, and present special challenges for X-ray crystallographic analysis. The first X-ray crystallographic structures of animal and plant P450s were only published after 2000 [68, 69]. In addition to the structure of CYP2C5 [68, 69], the structure of CYP2B4 has been resolved to 1.6 Å resolution [70]. Comparison of CYP2C5 and CYP2B4 reveals that there can be large differences in binding site conformation without perturbing the general P450 structure [70, 71]. It is hypothesized that this flexibility of conformation in xenobiotic metabolizing P450s facilitates substrate access, metabolic versatility and product dissociation. The adrenal steroidogenic P450s, which are regarded as being more selective in substrate choice, should have a more restrictive catalytic site [72]. These structures were obtained by truncation of the hydrophobic N-terminal domain through mutagenesis rendering the protein more hydrophilic and easier to crystallize [68, 69, 70]. Without the N-terminal leader sequence anchoring the protein to the membrane, the protein still associates with the membrane suggesting that the catalytic site also interacts with the membrane [72].

At the core of the P450 is an iron protoporphyrin IX moiety. A cysteine residue in the protein forms a thiolate bond with the moiety serving as one of the two non-heme ligands for the heme iron (Fe^{3+}) [73]. Computer models of CYP17 based on P450BM3 confirm the role of positively charged residues around the active site in holding the heme-group in position [10].

For proper P450 activity endoplasmic and mitochondrial P450s must be in contact with the membrane [10]. They are held in contact with the membrane by a hydrophobic N-terminal do-

main. The catalytic domain is found on the membrane surface, and enzymatic activity is associated with the C-terminal. Protein-protein interaction between the P450 and a specific redox partner is required for catalysis to proceed. In the microsomes the redox partner is cytochome P450 reducatase, CPR. CPR supplies the electrons from NADPH needed for oxygen activation. The lipid environment has been shown to play an important role in the function of P450s [74]. The extent and nature of this interaction is not understood.

P450s interact with N-acetyltransferases in xenobiotic metabolism [75]. The extent of the enzymatic collaboration is uncertain. In some circumstances the N-acetyltransferases metabolize P450 products, while in other circumstances, the P450s metabolize the products of the N-acetyltransferases.

3.1.2 The P450 reaction cycle

All P450s are the terminal electron acceptors in a short electron transport chain (Figure 3.2). Microsomal P450s use a single redox partner: CPR, NADPH-ferrihemoprotein reductase, E.C. 1.6.2.4 [63, 76, 77]. CPR is a 78 kDa membrane-bound flavoprotein. It contains one molecule each of flavin mononucleotide (FMN) and flavin adenine dinucleotide (FAD). It has a hydrophobic N-terminal of 6 kDa, an FMN and FAD binding domain constituting the 72 kDa hydrophilic domain [77]. It only accepts electrons from NADPH. CPR supplies both the first and second electron in the form of a hydride ion [77, 78].

Mitochondrial P450s use adrenodoxin and adrenodoxin reductase as redox partners [58]. CYTB5 can also transfer electrons from NADH to select P450s [78] but this role is not fully understood.

P450s are classified according to the above electron sources. Class I P450s are bacterial (and mitochondrial) and obtain electrons from FAD-ferredoxin reductase and Fe_2S_2 ferredoxin. Class

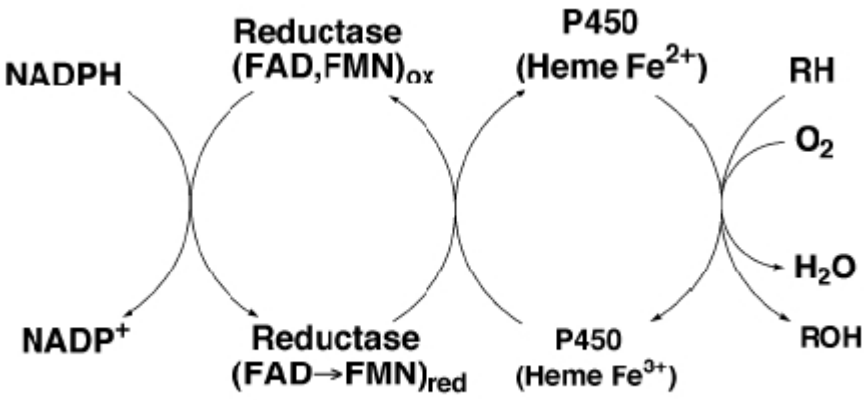

Figure 3.2: Electron transfer from NADPH to P450 substrate. This scheme of electrons transfer occurs between all studied Class II P450s and CPR [79].

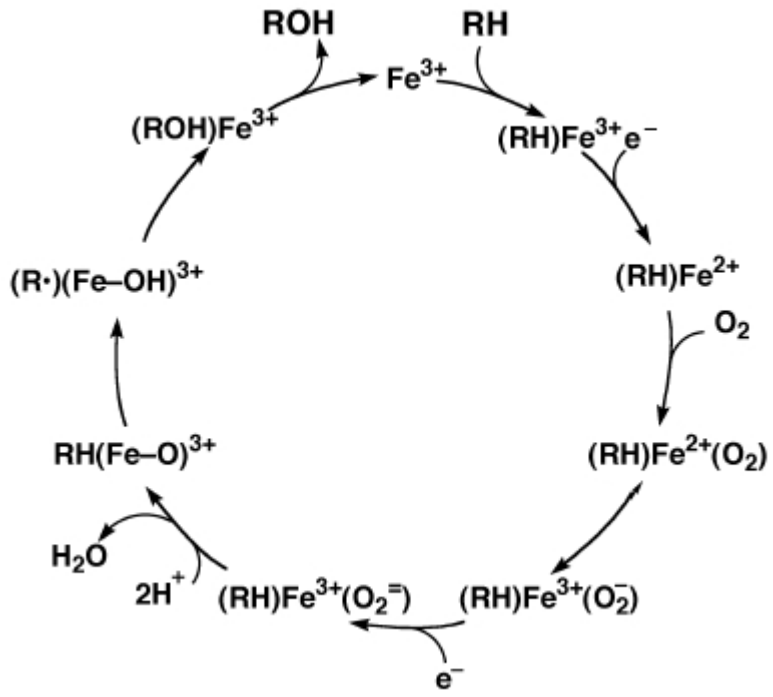

Figure 3.3: Reaction mechanism of P450s.[79]

II P450s receive electrons from CPR. Class III P450s catalyze reactions different to monooxygenations, such as the reduction of nitric oxide to nitrous oxide [74].

Figure 3.3 shows the proposed catalytic cycle of P450s. The reaction begins with the substrate binding to the active site of the enzyme [79, 80]. This results in a shift in absorbance from 417 to 394 nm as the outer electrons of the Fe atom in the heme group changes from low to high spin yielding a type I spectrum (Figure 3.4) [81].

Next, CPR donates the first electron reducing Fe^{3+} to Fe^{2+}. In this state the heme is ready to bind oxygen. Oxygen binds to the heme group and proceeds to abstract an electron from the Fe^{2+}. With the oxygen negatively charged, CPR donates the next electron generating an iron-oxene, $Fe^{3+}(O2^{=})$ [76].

Two protons then attack the iron-oxene complex yielding water and a highly reactive $(Fe=O)^{3+}$ (step 3). This $(Fe=O)^{3+}$ abstracts a proton from the substrate (RH) to produce a reactive intermediate, $R^{\bullet}$ (step 4). The $(Fe=O)^{3+}$ then decomposes into the oxidized product (ROH) and Fe^{3+}. The oxidized substrate then dissociates from the P450 and the cycle can then repeat itself.

There is considerable debate regarding the validity of this model. Some models involve a peroxy oxygen donor while others, such as the model proposed by Auchus and Miller [10], do not. The possibility exists that both reaction schemes are valid depending on the type of P450 involved.

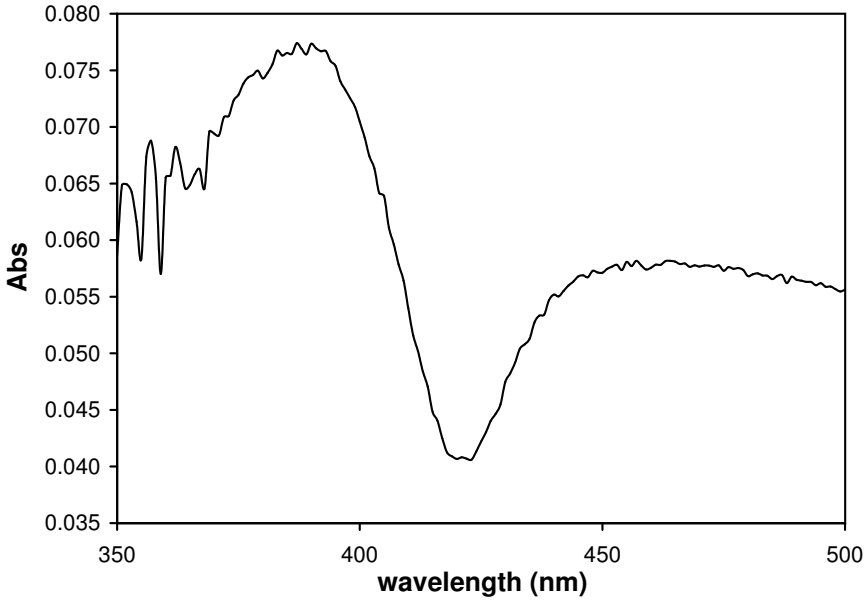

Figure 3.4: Progesterone induced type I difference spectrum. The spectrum was obtained using ovine adrenal microsomes and P4 dissolved in ethanol. Graph plotted from the author's data.

3.2 Kinetics of the steroidogenic P450s: CYP17 and CYP21

3.2.1 CYP17

CYP17 is important in the biosynthesis of glucocorticoids and sex steroids [1, 30, 36, 49, 56]. This role and its hypothesized means of regulation have been discussed in Sections 2.2 and 2.3 respectively.

Only one isoform has been isolated in the adrenals and gonads. In the human there is only one known gene (located 10q24.3) while three bovine genes are proposed to exist [82]. Sequence alignment with the porcine gene shows 85% homology to that of *Bos taurus*, 78% to the human and 71% to the rat. CYP17 is also expressed in the skin [33] and brain [25]. This enzyme is characterized by two activities: a 17α-hydroxylase and 17,20-lyase activity [10, 22, 83] that catalyze the following four reactions with NADPH supplying 2 electrons per reaction:

$$\mathrm{P5} \xrightarrow{a} \mathrm{17OHP5} \xrightarrow{b} \mathrm{DHEA} \tag{3.1}$$

$$\mathrm{P4} \xrightarrow{a} \mathrm{17OHP4} \xrightarrow{b} \mathrm{A4} \tag{3.2}$$

In reference to Eqn. 3.1 and 3.2, reactions a are the hydroxylase reactions and b the lyase reactions. In smaller animals the P4 pathway is favoured over the P5 pathway [10, 22, 28, 29, 30]. In larger animals the P5 pathway is preferred 100-fold over the P4 pathway for the 17,20-lyase reaction [10]. The conversion of P4 to androstenedione is reported to be one reaction where there is an adequate concentration of CPR and CYTB5 present [29, 30, 84, 85, 86]. No androstenedione is formed by human nor bovine CYP17 via 17OHP4. In yeast transformed with CYP17 it is found

that the catalytic efficiency ($^{V_{max}}/_{K_m}$) for the P5 17,20-lyase reaction is 100-fold greater than that of the P4 17,20-lyase reaction [51]. The K_m values with CPR expressed in the yeast along with CYP17 are 0.40 μM for reactions 3.1a and b; 1.1 μM for reaction 3.2a; and 6.5 μM for reaction 3.2b. How applicable these findings are to the physiological situation in the adrenal gland remains to be determined. No k_{cat} values are available for these and related experiments.

Swart *et al.* [85] gives K_m values of 2.0 μM for the conversion of P4 to 17OHP4; and 1.6 μM for P5 to 17OHP5 for bovine CYP17 expressed in COS1 cells. The K_m for the P4 17-hydroxylase reaction is higher than that for the P5 17-hydroxylase reaction suggesting that bovine CYP17 has a higher affinity for P5 than P4.

The lyase reaction increases with an increase in the CPR concentration while the hydoxylation reaction rate is unaffected [10, 84, 87]. The testes have a four times greater CPR activity than the adrenal [41, 51]. Both CPR and CYTB5 are required for optimum activity of the lyase activity in a complex age dependent pattern [52].

The ratio of CYP17 to 17OHP5 concentration has been shown to alter the observations concerning the 17OHP5 to DHEA reaction [30]. The more CYP17 there is the less 17OHP5 is observed to be produced creating the impression of a single reaction. In the presence of high enough concentrations of CPR the reaction from pregnenolone to DHEA is alleged to occur in one step [30] with very little 17OHP5 being released. Other reports clearly show 17OHP5 [30, 85, 86].

In the testes the 17,20-lyase activity of CYP17 is equal to that of the hydroxylase activity; i.e. all the precursor steroids are converted to sex steroids [52]. Kominami *et al.* [78, 84] have shown that the rate of 17-hydroxy-steroid dissociation from the catalytic site determines the 17,20-lyase rate at steady-state. These two activities are regulated independently [10, 41]. Research has shown that CYP17 needs to be phosphorylated at serine and threonine residues by cAMP dependent protein kinase before proper interaction with CYTB5 and CPR can occur and the lyase reactions proceed [10, 36, 41, 51, 52].

The human *CYP17* gene product shows a third activity whereby P4 is converted to 16α-hydroxy-progesterone (16OHP4) [86]. This activity is not observed with P5 as substrate. The role of the 16OHP4 is not known. 17OHP4 and 16OHP4 exist at a ratio of ≈4:1 in the adrenal microsome suspension and COS1 expression system [86].

3.2.2 CYP21

CYP21 plays an important role in the production of glucocorticoids and mineralocorticoids as it catalyzes the conversion of P4 and 17OHP4 to DOC and S respectively (see Figure 2.3) [36, 88, 89, 90]. These roles have been in Chapter 2 along with its regulation. The reactions catalyzed by CYP21 are shown in Eqn. 3.3 and 3.4 with NADPH as electron source.

$$\text{P4} \longrightarrow \text{DOC} \tag{3.3}$$

$$17\text{OHP4} \longrightarrow \quad \text{S} \tag{3.4}$$

The conversion rates for reactions 3.3 and 3.4 are significantly different [78, 91, 92]. These rates are dependent on the concentration of CPR. CYP21's K_d for CPR is ≈16 nM. The major difference in the two reactions' kinetics lies in the vastly different K_m values. The enzyme's K_m for 17OHP4 (0.7 μM) is half that for P4 (1.3 μM) in the case of the bovine enzyme [91]. For the ovine [89] and bovine [91] CYP21 expressed in COS1 cells, the rate of 17OHP4 21-hydroxylation occurs 2-fold faster than P4 21-hydroxylation. The 17OHP4 ⟶ S reaction reaches steady-state faster than the P4 ⟶ DOC reaction [78]. This is because the conversion rate of P4 ⟶ DOC is faster than its rate of enzyme-product dissociation. This is not the case when 17OHP4 is the substrate because S dissociates from the binding site faster than 17OHP4 is converted to S.

CYP21 has a 20β-oxidase activity whereby it can convert 20β-hydroxy P4 to P4 in the adrenal [93]. This reaction proceeds at a rate nearly equal to that for the 17OHP4 conversion. 20β-hydroxy-steroids are produced as products of P4 and 17OHP4 metabolism in the ovaries, adrenal gland, placenta and testes by 20β-HSD. These products inhibit CYP17 activity and may serve to divert androgen synthesis in immature animals. CYP21 may regulate against over production of 20β-hydroxy-steroids. CYP21's K_d for 17α,20β-hydroxyP4 is 2.3 μM, which is higher than the K_m values for the normal substrates P4 and 17OHP4.

A lack of normal active CYP21 results in congenital adrenal hyperplasia (CAH) [92]. The classical form has an incidence of 1 in 15 000 births (compared to 1 in 250 000 for cystic fibrosis, a relatively common genetic disorder) [92, 94, 95]. This disorder is characterized by an increase in androgen synthesis as the conversion of steroid precursor to mineralocorticoids and glucocorticoids are blocked [1]. The physiological result is virilization and severe salt loss in classical cases while the mild form results in acne. The mild form has an incidence of 1 in 100 births. 90 to 95% of the CAH cases are due to a reduction in CYP21 activity. The V218L mutation is present in the majority of mild cases and the resulting enzyme retains as much as 64% of its activity whereas in the classical form (caused by various mutations) only 7 to 10% of the enzyme activity may be retained [92]. The P30L, I172N and V281L mutations result in a decreased V_{max} but unchanged K_m. The P453S mutation lies in the heme binding domain of the protein.

There are two isoenzymes in the ovine adrenal that differ in their 3′ region [89]. The first isoform is similar to the bovine, murine and human protein while the other is truncated approximately 500 bp from the C terminus resulting in a -18 residue protein that is inactive. There is, however, only one transcribed gene, the two forms being the product of differential mRNA splicing.

The human, murine, bovine and ovine genomes have a CYP21 pseudogene. The structure of CYP21 locus has been discussed in Section 2.3.2. The first hydrophobic domain of CYP21 is the membrane targeting and anchoring domain and is important in *in vivo* protein stability. CYP21 is degraded physiologically in a monophasic pattern and has a half life of approximately 24 hours. The truncated forms have a much shorter half life [89].

3.3 Kinetic synopsis

As CYP17 and CYP21 are at the central branch points of steroid biosynthesis many complicated features have evolved to maintain homeostasis. It is speculated that the ratio of substrate to enzyme concentration could play an important role in the modulation of the 17α-hydroxylation and 17,20-lyase activities, and likewise the activities of CYP21 [30].

Many questions remain to be answered regarding P450 kinetics and structure.

There is evidence that the lipid environments of the CYP17 affect its kinetics [74]. As consequence, even if the CYP17 and CYP21 could be isolated from the membrane and k_{cat} values could be determined for the enzymes and the K_d values worked out for all the interactions, the accuracy and worth of these values could still be questioned. Table 3.1 lists V_{max} and K_m values for CYP17 and CYP21 derived in various experimental systems. While the trends of a higher CYP17 affinity for P5 and CYP21 affinity for 17OHP4 can be seen the determined V_{max} values vary significantly from expression system to expression system. Because of these reasons it is impossible to define each enzyme's effect on the system it forms a part of using traditional techniques.

In the next chapters two techniques will be employed to escape the problem of varying results from one expression system to another. These techniques are metabolic modeling and simulation; and control analysis.

Table 3.1: Summary of CYP17 and CYP21 kinetic parameters. V_{max} and K_m values are given with reference to the species and the experimental system employed. K_m values are in μM.

Enzyme	Substrate	K_m	V_{max}		System	Reference
bovine CYP17	17OHP4		0.17	nmol/min/nmol P450	*E. coli* membranes	[29]
bovine CYP17	P4	2	0.03	nmol/min/60 mm dish	COS1 cells	[85]
bovine CYP17	P4		1.6	nmol/min/nmol P450	*E. coli* membranes	[29]
bovine CYP17	P5	1.6	0.02	nmol/min/60 mm dish	COS1 cells	[85]
bovine CYP21	17OHP4	0.8	0.07	nmol/min/60 mm dish	COS1 cells, pCMVc21H401	[91]
bovine CYP21	17OHP4	0.7	0.07	nmol/min/60 mm dish	COS1 cells, pCMVc21Y401	[91]
bovine CYP21	17OHP4	1			purified	[91]
bovine CYP21	17OHP4	0.29	28	nmol/min/nmol P450	yeast microsomes	[96]
bovine CYP21	P4	1.4	0.03	nmol/min/60 mm dish	COS1 cells, pCMVc21H401	[91]
bovine CYP21	P4	1.3	0.03	nmol/min/60 mm dish	COS1 cells, pCMVc21Y401	[91]
bovine CYP21	P4	7.9			purified	[91]
human CYP17	17OHP4	ND			yeast	[51]
human CYP17	17OHP5	0.83	0.02	nmol/min/nmol P450	yeast	[51]
human CYP17	P4	0.62	0.0083	nmol/min/60 mm dish	COS1 cells	[85]
human CYP17	P4	0.73	0.66	nmol/min/nmol P450	yeast	[51]
human CYP17	P4⟶ 16OHP4	0.7	0.002	nmol/min/mg prot	COS1 cells	[86]
human CYP17	P5	0.97	0.0073	nmol/min/60 mm dish	COS1 cells	[85]
human CYP17	P5	0.8	0.7	nmol/min/nmol P450	purified	[36]
human CYP17	P5	0.79	0.66	nmol/min/nmol P450	yeast	[51]
human CYP17 + b5	17OHP4	0.59	0.13	nmol/min/nmol P450	yeast	[51]
human CYP17 + b5	17OHP5	1	0.29	nmol/min/nmol P450	yeast	[51]
human CYP17 + b5	P4	0.78	0.59	nmol/min/nmol P450	yeast	[51]
human CYP17 + b5	P5	0.6	0.76	nmol/min/nmol P450	yeast	[51]
human CYP17 + CPR	17OHP4	6.5	0.03	nmol/min/nmol P450	yeast	[51]
human CYP17 + CPR	17OHP5	0.4	0.1	nmol/min/nmol P450	yeast	[51]
human CYP17 + CPR	P4	1.1	6.6	nmol/min/nmol P450	yeast	[51]
human CYP17 + CPR	P5	0.4	3	nmol/min/nmol P450	purified	[36]

continued on next page

continued from previous page

Enzyme	Substrate	K_m	V_{max}		System	Reference
human CYP17 + CPR	P5	0.4	3	nmol/min/nmol P450	yeast	[51]
human CYP21	17OHP4	1.3	0.0885	nmol/min/mg prot	COS1 cells	[92]
human CYP21	17OHP4	0.56			COS1 cells	[97]
human CYP21	17OHP4	1.11	0.01	nmol/min/10^6 cells	yeast *in vivo*	[97]
human CYP21	17OHP4	0.23	7.5	nmol/min/nmol P450	yeast microsomes	[97]
human CYP21	17OHP4	0.15	10.75	nmol/min/nmol P450	yeast microsomes	[90]
human CYP21	P4	6.5	0.0858	nmol/min/mg prot	COS1 cells	[92]
human CYP21	P4	0.27	0.67	nmol/min/nmol P450	yeast	[98]
human CYP21	P4	0.18			yeast*in vivo*	[97]
human CYP21	P4	0.33	4.67	nmol/min/nmol P450	yeast microsomes	[97]
porcine CYP17	17OHP4	1.7	6.3	nmol/min/nmol P450	microsomes	[87]
porcine CYP17	17OHP4	2.4	2.6	nmol/min/nmol P450	microsomes	[83]
porcine CYP17	17OHP4	0.7	3.64	nmol/min/nmol P450	purified	[27]
porcine CYP17	17OHP4	ND	0	nmol/min/nmol P450	purified	[27]
porcine CYP17	17OHP5	0.32	2.29	nmol/min/nmol P450	purified	[27]
porcine CYP17	17OHP5	ND	0	nmol/min/nmol P450	purified	[27]
porcine CYP17	P4	0.4	6.3	nmol/min/nmol P450	microsomes	[87]
porcine CYP17	P4	1.5	4.6	nmol/min/nmol P450	microsomes	[83]
porcine CYP17	P4	0.44	3.1	nmol/min/nmol P450	purified	[27]
porcine CYP17	P4	1	3.33	nmol/min/nmol P450	purified	[27]
porcine CYP17	P5	0.33	1	nmol/min/nmol P450	purified	[27]
porcine CYP17	P5	0.65	2.2	nmol/min/nmol P450	purified	[27]
porcine CYP17 + b5	17OHP4	1.4	10	nmol/min/nmol P450	purified	[27]
porcine CYP17 + b5	17OHP4	5	1.8	nmol/min/nmol P450	purified	[27]
porcine CYP17 + b5	17OHP5	0.32	5.52	nmol/min/nmol P450	purified	[27]
porcine CYP17 + b5	17OHP5	1.18	2.45	nmol/min/nmol P450	purified	[27]
porcine CYP17 + b5	P4	0.44	3.33	nmol/min/nmol P450	purified	[27]
porcine CYP17 + b5	P4	1	4.66	nmol/min/nmol P450	purified	[27]
porcine CYP17 + b5	P5	0.33	1.75	nmol/min/nmol P450	purified	[27]
porcine CYP17 + b5	P5	0.65	3.9	nmol/min/nmol P450	purified	[27]

Chapter 4

Building a model of adrenal steroidogenesis

It is important that the concepts of regulation and control be separated for the purpose of this and the next chapter; and the understanding of the questions being asked in this thesis. This was already done in the introductory Chapter on page 3. To recap: an enzyme's activity is *regulated*; and steady-state reaction rate (flux) or metabolite concentration is *controlled*.

While the regulatory mechanisms are important for a complete understanding of steroidogenesis the explicit topic of this thesis is the control over steroidogenic flux. The questions are: what degree of control does CYP17 and CYP21 have over the CYP17/CYP21 branch point of mineralocorticoid and glucocorticoid synthesis; and which enzymes have the most control? We therefore need to calculate concentration (C_i^s) and flux control coefficients (C_i^J) for the relevant enzymes and metabolites to answer these questions.

In Chapter 1 the question of rate-limiting steps in steroidogenesis was addressed. This chapter does not focus on these questions any more than to say that there need not be a single rate-limiting step. The analytical framework of control analysis, while not ruling out the possibility of one rate-limiting step per pathway, suggests that each reaction in a pathway can posses some degree of control over the flux and metabolite concentrations in the pathway [12]. With the model and experiments described below we cannot elucidate the degree of control CYP17 and CYP21 have over the whole steroidogenic network but we can determine if they have any control over the branch point under investigation.

As explained in Section 2.3, the steroidogenic network shown in Figure 2.3 is an oversimplification. In reality the three branches of adrenal steroidogenesis (Figure 2.5) are separated anatomically. While in theory the enzymatic reaction of P5→17OHP5→DHEA may have control over mineralocorticoid and glucocorticoid synthesis in reality this reaction to DHEA does not occur in the adrenal zones where mineralocorticoid and glucocorticoid synthesis occur. For these reasons the model proposed below should not be taken out of context. *Conclusions drawn from the model can*

only strictly apply to the model, but may offer insights into the real system.

4.1 Defining the model pathway

The model pathway is displayed in Figure 4.1. CYP17 converts P4 to 17OHP4 (reaction 1). CYP21 converts 17OHP4 to S (reaction 2) and P4 to DOC (reaction 3). There is competitive inhibition between P4 and 17OHP4 for the steroid binding site on CYP21 and competition between CYP17 and CYP21 for P4.

The balanced reactions are given in equations 4.2 to 4.4.

$$\mathrm{P4} + \mathrm{NADPH} + \mathrm{O_2} + \mathrm{H^+} \overset{\mathrm{CYP17}}{\longrightarrow} \mathrm{17OHP4} + \mathrm{NADP^+} + \mathrm{H_2O} \tag{4.1}$$

$$\mathrm{17OHP4} + \mathrm{NADPH} + \mathrm{O_2} + \mathrm{H^+} \overset{\mathrm{CYP21}}{\longrightarrow} \mathrm{S} + \mathrm{NADP^+} + \mathrm{H_2O} \tag{4.2}$$

$$\mathrm{P4} + \mathrm{NADPH} + \mathrm{O_2} + \mathrm{H^+} \overset{\mathrm{CYP21}}{\longrightarrow} \mathrm{DOC} + \mathrm{NADP^+} + \mathrm{H_2O} \tag{4.3}$$

4.1.1 Kinetic constants

K_m and V_{max} values have been determined by means of the Michaelis-Menten equation (Eqn. 4.4) in the experiments by Swart *et al* [85] and Lorence *et al* [91].

$$v = \frac{V_{max} s}{s + K_m} \tag{4.4}$$

The V_{max} values are composites of the effects of the lipid environment [74], the relative concentrations CPR and NADPH, and additional effectors discussed in Chapter 3. Consequently the V_{max} values vary considerably from experimental setup to experimental setup (see Table 3.1). The literature V_{max} values cannot be relied upon for the model construction as they are poorly defined and

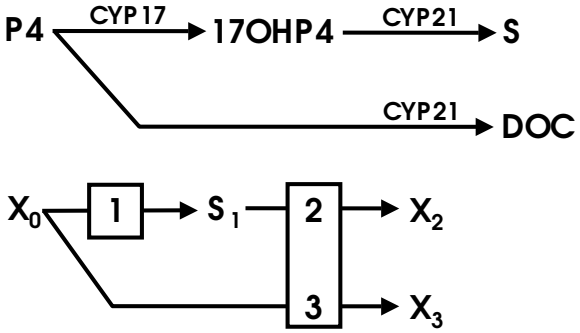

Figure 4.1: Segment of the steroidogenic pathway under study. The CYP17 enzyme catalyzes one reaction: P4→17OHP4. The CYP21 enzyme catalyzes both the P4→DOC (reaction 3) and the 17OHP4→S reaction (reaction 2). There is competition for substrate between the CYP17 and CYP21 enzymes; and competition for enzyme binding site between 17OHP4 and P4. The bottom scheme is a skeleton representation of the scheme above it.

not reproducible across experimental systems. In addition, neither k_{cat} values nor the relations describing the interaction between P450 enzymes and CPR are available. As consequence the V_{max} values used in the model had to be determined by fitting the model to the experimental data sets (to be presented in section 4.3).

The K_m values vary littel from experimental system to experimental system. As seen in Table 3.1 the K_m values for CYP17 and CYP21 are constant within the COS1 expression system.

The K_m values chosen for the model are presented in Table 4.1.

Table 4.1: K_m values used in the model.

	K_m	Reference
reaction 1:	2 μM	[54]
reaction 2:	0.7 μM	[91]
reaction 3:	1.3 μM	[91]

4.1.2 Rate Equations

Michaelis-Menten kinetics (Eqn. 4.4) was used, where aV replaces V_{max} and represents the relationship between enzyme concentration (a) and the rate per unit enzyme, V (μmol/hr/% tissue culture dish slice). V is in essence a k_{cat} value describing the turn over per tissue culture dish slice. The Michaelis-Menten equation was modified to allow for competitive inhibition. For the K_i values, the respective K_m values were used.

The general equation is:

$$v = \frac{aV[S]}{[S] + K_m(1 + \frac{I}{K_i})} \tag{4.5}$$

The equations for each reaction are:

Reaction 1: for the conversion of P4→17OHP4:

$$v_1 = \frac{a_{[\mathrm{CYP17}]}V_1 \cdot [\mathrm{P4}]}{[\mathrm{P4}] + K_{m_1}} \tag{4.6}$$

Reaction 2: for the conversion of 17OHP4→S:

$$v_2 = \frac{a_{[\mathrm{CYP21}]}V_2 \cdot [\mathrm{17OHP4}]}{[\mathrm{17OHP4}] + K_{m_2}\left(1 + \frac{[\mathrm{P4}]}{K_{m_3}}\right)} \tag{4.7}$$

Reaction 3: for the conversion of P4→DOC:

$$v_3 = \frac{a_{[\mathrm{CYP21}]}V_3 \cdot [\mathrm{P4}]}{[\mathrm{P4}] + K_{m_3}\left(1 + \frac{[\mathrm{17OHP4}]}{K_{m_2}}\right)} \tag{4.8}$$

The change in metabolite concentration were expressed in the form of the following differential equations:

$$\frac{d[\mathrm{P4}]}{dt} = -v_1 - v_3 \tag{4.9}$$

$$\frac{d[\mathrm{17OHP4}]}{dt} = v_1 - v_2 \tag{4.10}$$

$$\frac{d\mathrm{S}}{dt} = v_2 \tag{4.11}$$

$$\frac{d[\mathrm{DOC}]}{dt} = v_3 \tag{4.12}$$

4.1.3 Requirements for model validation

To complete and validate the above model the following was needed:

- Ascertain if there is product inhibition between the enzymes and their products.
- Perform experiments whereby the V values could be calculated.

The next sections present the data used in meeting these criteria.

4.2 Is there product inhibition?

All enzymes have some affinity for their products. The experiments by Kominami *et al.* [78] show that CYP21 has more affinity for its product DOC relative to S. It was also shown that CYP17 retains little affinity for 17OHP4 [29]. Microsome P4 conversion assays and steroid binding assays were performed to test the extent of product inhibition.

4.2.1 Microsome P4 conversion assays

Experiments were carried out using ovine microsomes in the presence of 10 μM P4 and 10 μM DOC or 10 μM S and the metabolite concentrations traced over 10 minutes. If the products DOC and/or S had any measurable effect on the final product concentrations it was expected to be visible at high inhibitor concentrations.

The materials were obtained and the experiments performed as described in Appendix A. All experiments were performed in triplicate. The P450 and protein concentration was determined as described in Section A.2.4, page 72. Figure 3.1 shows the CO-difference spectrum obtained from which the concentration was determined. The P450 concentration was determined to be 11.6 $\pm$1.3 μM; and the protein concentration to be 18.2 $\pm$1.4 mg/mL (specific activity of 0.637 μM P450/mg protein).

Figure 4.2 represents a 'normal' P4 conversion profile over 10 minutes using ovine adrenal microsomes. Of note is the pseudo-steady-state characteristic of adrenal microsome P4 conversion. The 17OHP4 concentration increases slowly to a point where its rate of synthesis is matched by its rate of conversion to S giving rise to a pseudo-steady-state. In the microsome system eventually

the P4 concentration falls to a level where the synthesis of 17OHP4 is slower than its conversion to S. This creates a false impression of steady-state, the so called pseudo-steady-state.

The pseudo-steady-state is the result of fluctuating metabolite concentrations. The reaction rate of an enzyme is dependent on the availability of substrate. As P4 is not held constant the rates of the P4⟶17OHP4 and P4⟶DOC reactions decline; while the 17OHP4⟶S reaction rate initially increases. At a true steady-state these reaction rates nor the metabolite concentrations would change unless by alteration of the parameter values such as enzyme activity. Where the concentration of P4 held constant a true steady-state would evolve in respect to the rate of 17OHP4⟶S.

It is the metabolite concentrations at pseudo-steady-state that are of interest. To draw conclusions regarding the effect of DOC and S concentrations on steady-state flux and concentration we must compare steady-state flux and concentration values. The microsomal system allows this to be done at the pseudo-steady-state.

In Figure 4.3 the time course of all three experiments is shown. The P4 declines at nearly the same rate in all the experiments. The variation between the points falls within the range of the experimental error. If either product had an affect on the metabolite profile it does not appear to be in the conversion of P4 to DOC or 17OHP4.

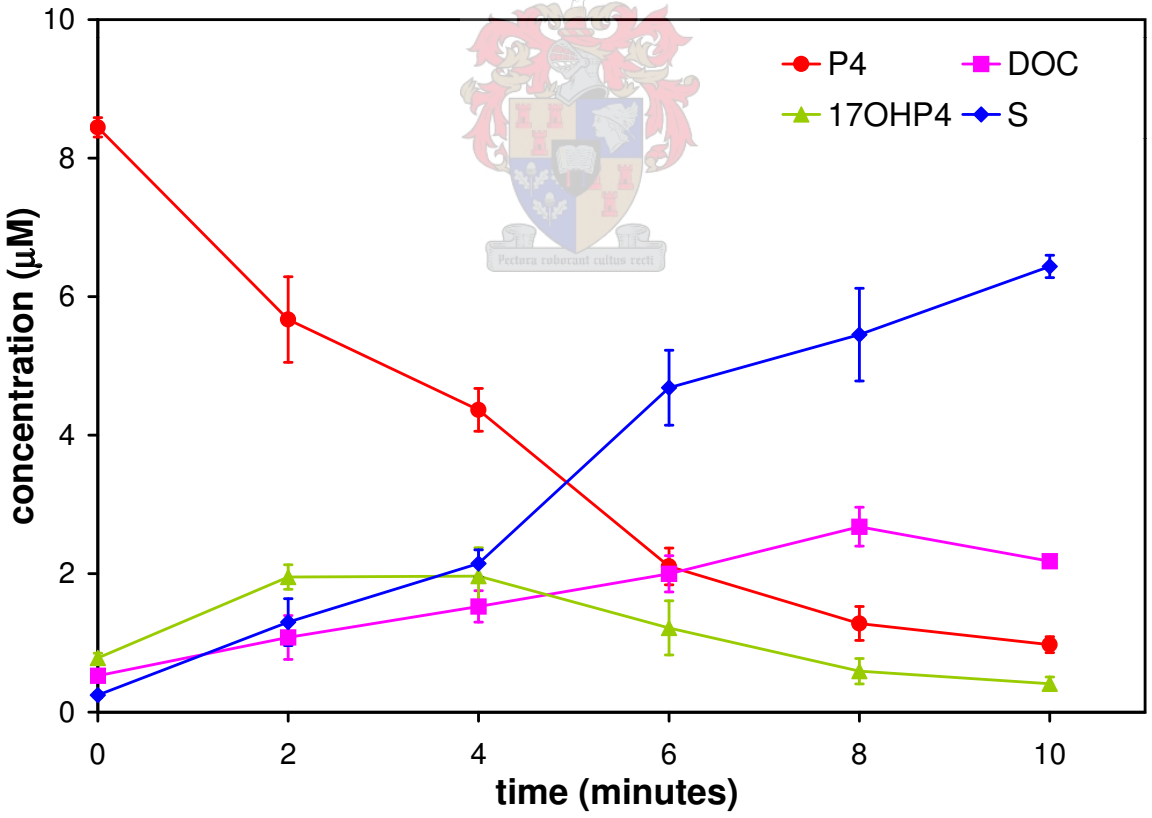

Figure 4.2: Conversion of P4 to products via microsomal CYP17 and CYP21. Time course spans 10 minutes and 6 data points. Note 17OHP4 pseudo-steady-state at 2 to 4 minutes. The initial P4 concentration was 10 μM. Standard errors were worked out as described in [99] from triplicate data sets.

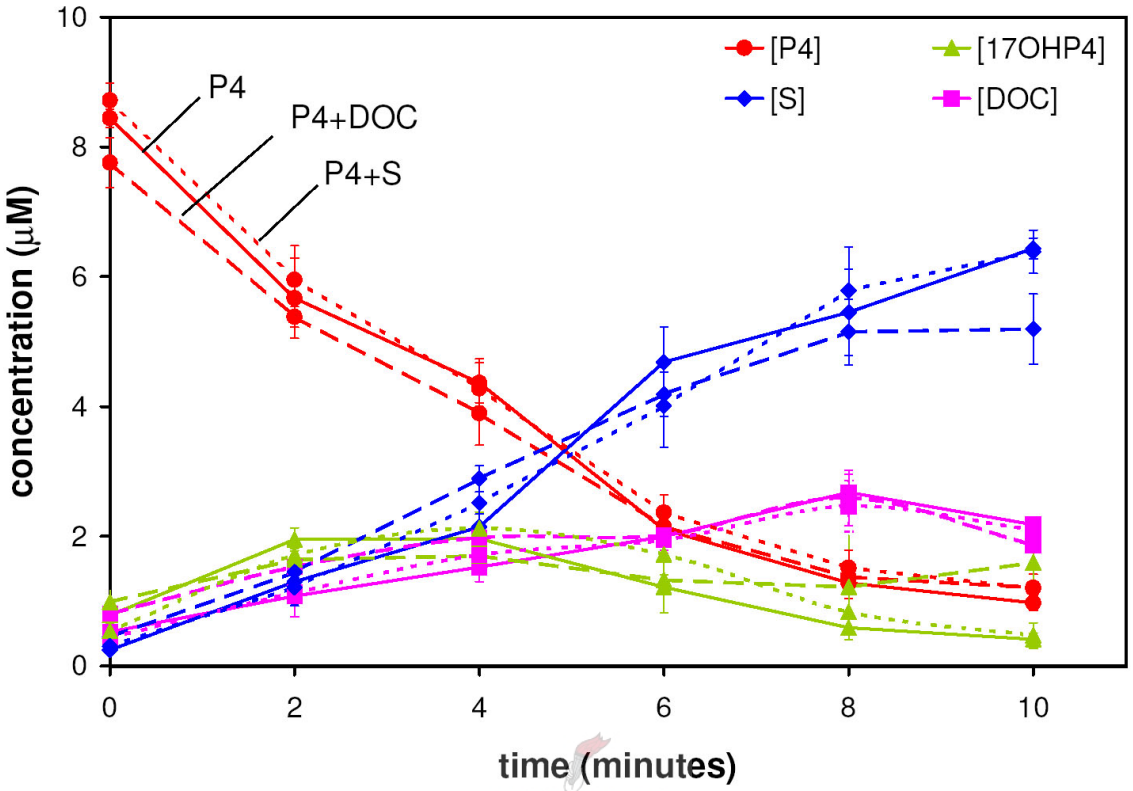

Figure 4.3: Adrenal microsome P4 conversion assays in the presence of no DOC or S; 10 μM DOC; and 10 μM S. There is little difference between the experiments for all points but the last. Time course spans 10 minutes and 6 data points. Note pseudo-steady-state at 2 to 4 minutes. All experiments were performed in triplicate and standard errors were worked out as described in [99]. Solid lines represent the control experiment, long-dashed lines represent the 10 μM DOC experiment and the short-dashed lines represent the 10 μM S experiment.

The concentration of DOC in each experiment is near equal for every time point including at 10 minutes where the DOC inexplicably decreases. This observation does not make sense unless there is another reaction occurring that is metabolizing the DOC to a compound not monitored for in the TLC. Samples run on HPLC showed no unaccounted metabolite (results not shown). No explanation is available for this observation hence 8 min was regarded as the end point.

Figure 4.4 compares the concentrations of the metabolites at 4 min. Statistical analysis of the samples using the software of GraphPad Prizm revealed no statistical difference ($p > 0.05$). This suggests that DOC and S do not affect steady-state flux and concentrations.

4.2.2 Steroid binding spectrophotomeric assays

Substrate binding microsome difference spectrum scans were performed to test for steroid binding. Experiments were performed as in Section A.2.3, page 72. The reference cell held 1 mL 1 mg/mL microsome suspension (final P450 concentration 0.64 μM) with ethanol plus inhibitor. The volume of steroid substrate and inhibitor was 10 μL (which equated to an approximate final concentration

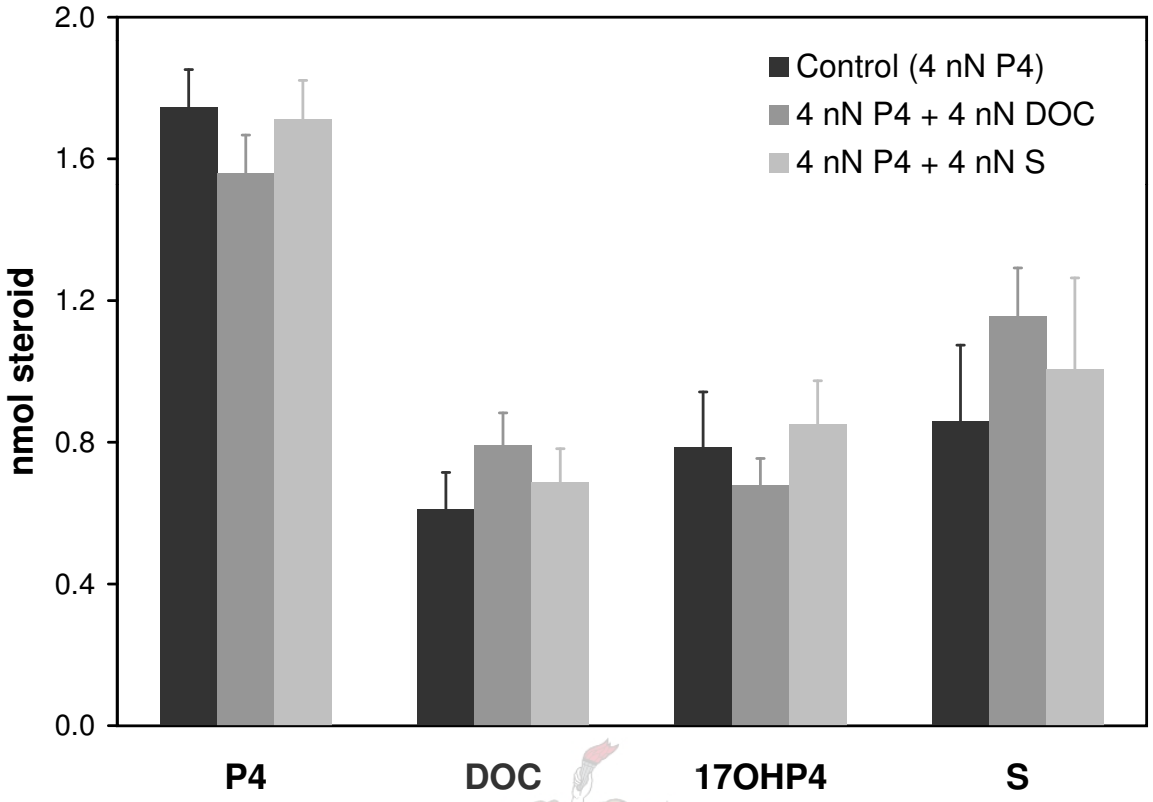

Figure 4.4: Comparison of pseudo-steady-state metabolite concentrations at 4 minutes. No statistical difference was observed between the control and the experiments. Statistical analysis shows no statistical difference ($p > 0.05$).

of $\approx 60\mu$M) and was enough to saturate all CYP present (data not shown). For the experiment the spectrophotometer was zeroed with the volume inhibitor added to both cuvettes. The steroid was then added to the experiment cuvette and the equivalent volume ethanol to the reference cuvette. The experiments performed are listed in Table 4.2 along with the volumes 2 mg/ml steroid stock solution.

The microsome substrate binding scan of P4 is shown in Figure 3.4. The scan for 17OHP4 was similar. There was no effect by ethanol nor was any measurable effect observed for DOC or S.

A summary of the results is given in Figure 4.5. Except in the case of S in combination with 17OHP4, inhibition was insignificant (less than 5%).

If at such high concentrations of inhibitor there are such small effects it is reasonable to assume that the enzymes are not inhibited by their products at the concentrations used in the tissue culture assays.

The physiological concentration of cortisol in human blood (bound and unbound to SHBG) is 3.8 nM [1]. With such a low physiological concentration product inhibition is unlikely to occur *in situ*.

For these reasons the inhibitory effect of DOC and S are judged to be inconsequential to the construction of the model due to their small influence at high concentrations.

Table 4.2: Microsome substrate binding difference scan experiment setup. First steroid mentioned is the steroid being tested for reduced binding, the second is the one tested for inhibiting the binding of the first.

	volume				
experiment	EtOH	P4	17OHP4	DOC	S
ethanol control	20 μL	—	—	—	—
P4 spectrum	10 μL	10 μL	—	—	—
P4 vs 17OHP4	—	10 μL	10 μL	—	—
P4 vs DOC spectrum	—	10 μL	—	10 μL	—
P4 vs S spectrum	—	10 μL	—	—	10 μL
17OHP4 spectrum	10 μL	—	10 μL	—	—
17OHP4 vs P4 spectrum	—	10 μL	10 μL	—	—
17OHP4 vs DOC spectrum	—	—	10 μL	10 μL	—
17OHP4 vs S spectrum	—	—	10 μL	—	10 μL

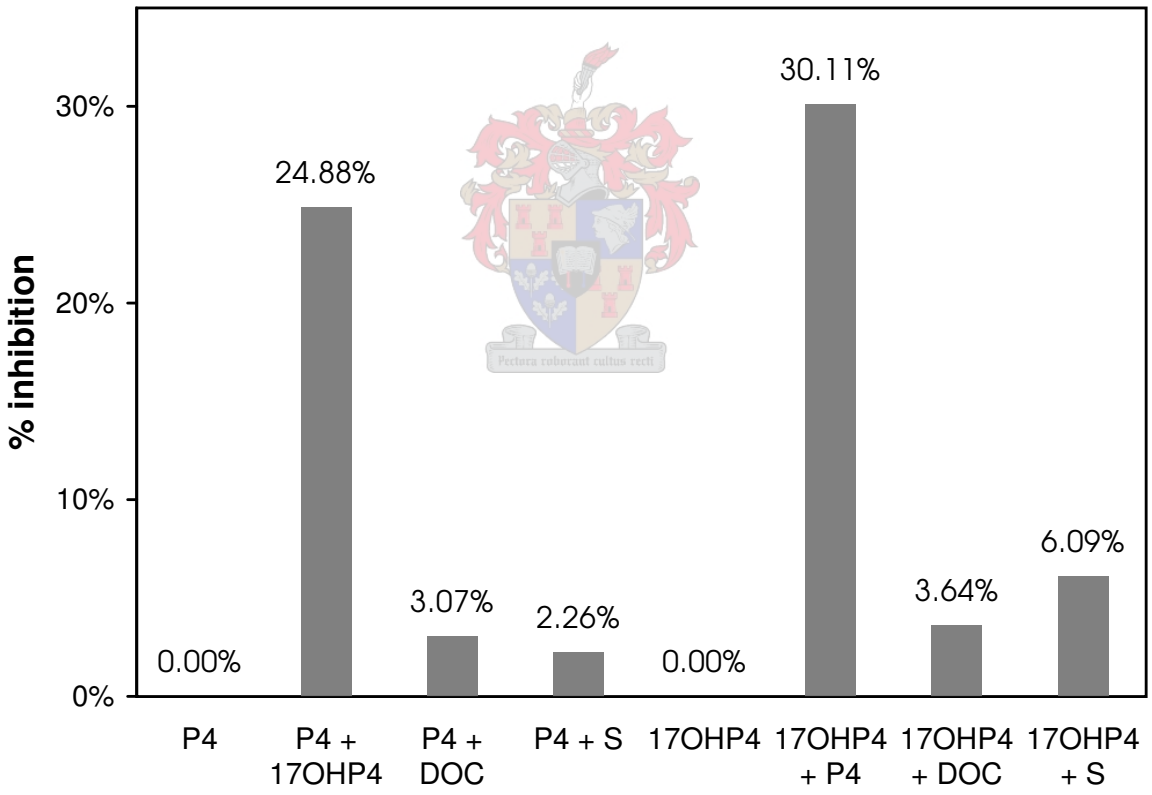

Figure 4.5: Bargraph summary of steroid binding inhibition. An ovine microsomal suspension and ethanol dissolved steroids were used to generate type 1 P450 spectral scans.

4.3 Parallel transfection data and model optimization

The Parallel transfection method [6] allows for the manipulation of the individual expressed CYP enzyme activities without having to purify the enzymes and reconstitute them in an artificial lipid environment. Working in the controlled environment of tissue culture removes the uncertainties of microsome experiments where enzyme contamination could yield experimental artifacts or metabolize products to unresolvable unknown metabolites.

A brief description of the Parallel Transfection method was given in Chapter 1. As Figure 1.2 shows, COS1 cells were grown up in petri dishes to 80% confluency as described in Section A.4. At 80% confluency the cells were split $1:6$ and plated onto the slices as described in Section A.4.6. The cells were transfected 24 hours after splitting. One set of dishes was transfected with a bovine CYP17 containing plasmid and the other set with a bovine CYP21 plasmid. The pCMV4 plasmid was used as a negative control. The transfected cells were left to grow for three days before the experiment was initiated.

For the experiment the medium was siphoned off and with sterile tweezers the individual slices were removed from the dishes and recombined with the other slices in a new dish. The experiment was carried out with a P4 concentration of 1 μM (yielding a total of 10 nmol steroid per 10 mL dish) as described in Section A.5. The assay continued for 12 hours where after there was not enough medium in the dishes to proceed further.

4.3.1 Results of Parallel transfection experiments

Figures 4.6 and 4.7 show the conversion profile from P4 to 17OHP4, DOC and S over 12 hours.

Increasing the amount of CYP17 results in an increase in the amount of 17OHP4. More S is produced in the 6 CYP17:2 CYP21 experiment relative to the amount of DOC produced in accordance with the hypothesis that a higher concentration CYP17 will result in a higher concentration of S.

Only the 2 CYP17: 6 CYP21 experiment reached a pseudo-steady state (see Figure 4.8). The 6 CYP17: 2 CYP21 experiment came close to reaching the pseudo-steady-state seen in microsomes.

Samples taken from the experimental medium were resolved by TLC as described in Section A.1.1. In addition to the mixed dishes there was a full CYP17 and CYP21 dish and untransfected control dishes. Samples from the untransfected dishes run on HPLC (see Section A.1.3) showed no steroidogenic activity (data not shown). The conversion profile of the full CYP17 and CYP21 dishes is shown in Figures 4.9 and 4.10.

4.3.2 Fitting the model to the data

The model fitting/optimizing utility of Gepasi [100] was used to fit the model to the experimental data in Figures 4.6 and 4.7. The model was programed with the K_m and K_i values for the enzymes in addition to the a value—the amount of enzyme (slices), eg.: 25 and 75 for a ratio of 2 CYP17: 6 CYP21. The V value was then fitted to the experimental profile. A fit was performed for each

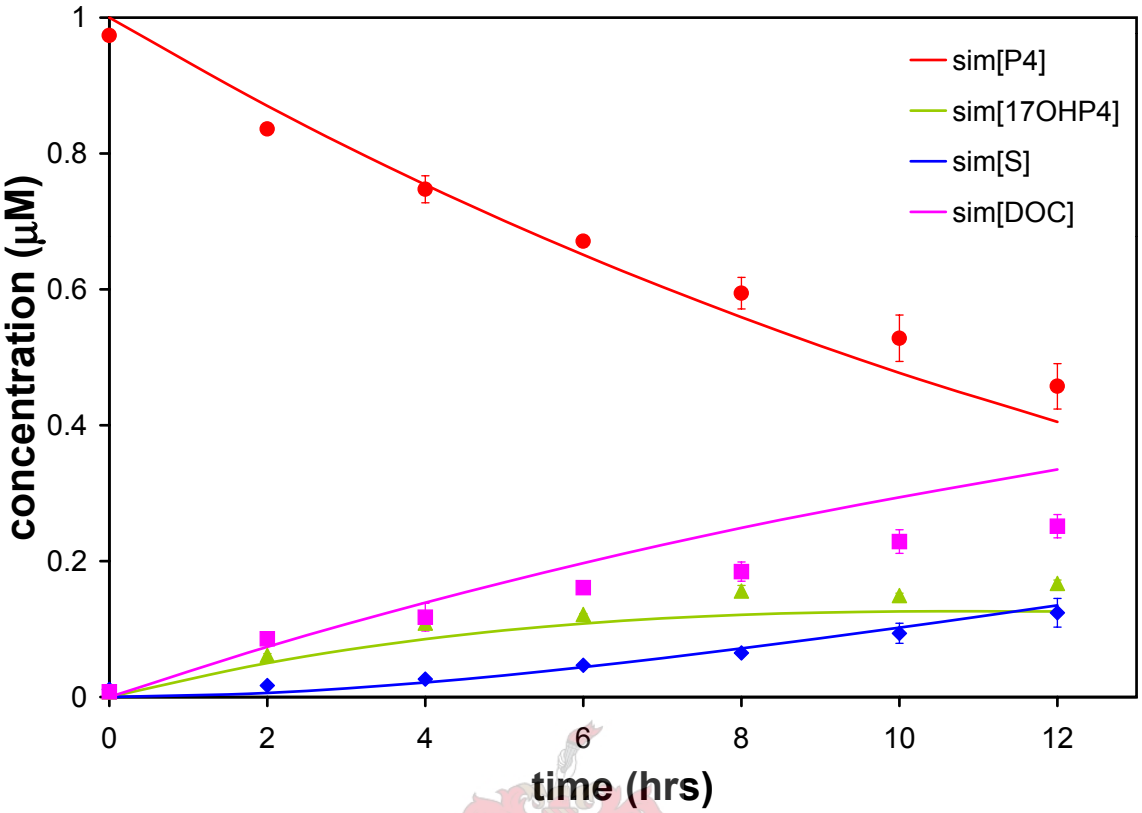

Figure 4.6: P4 metabolism in two CYP17 to six CYP21 assay compared to simulation. After 12 hours there was 55% conversion of P4 to products. The 17OHP4 appears to be in steady-state. Standard errors were worked out as described in [99] from triplicate data sets. Lines simulated data from model, points from experimental data. There is a 99.57% correlation between experimental and simulated results.

data set (n=6). The evolutionary programing optimization algorithm of Gepasi was used for the optimization. The generations were 1000 and the population set at 100. Sum of Squares was determined for each fit and ranged from 0.002 to 0.030 with a median value of 0.012. The results of the fit as well as the complete set of kinetic values per reaction are given in Table 4.3.

Simulations were performed based on 2 CYP17: 6CYP21 and 6 CYP17: 2 CYP21 ratios. Correlations were on average 0.993 and 0.997 respectively (see Figures 4.6 and 4.7) . Correlations were calculated using Microsoft Excel by comparing the experimental data set to simulation results per metabolite trace.

Table 4.3: Table of kinetic parameters for the model. Reactions are as defined in Section 4.1.2. K_m and K_i values are in μM. V values are in μmol/hr. Standard errors were calculated as shown in [99] from 6 data sets.

Reaction	K_m	K_i	V	se
1	2.0	N/A	0.0039	$\pm$0.000480
2	0.7	1.3	0.0024	$\pm$0.000182
3	1.3	0.7	0.0010	$\pm$0.000234

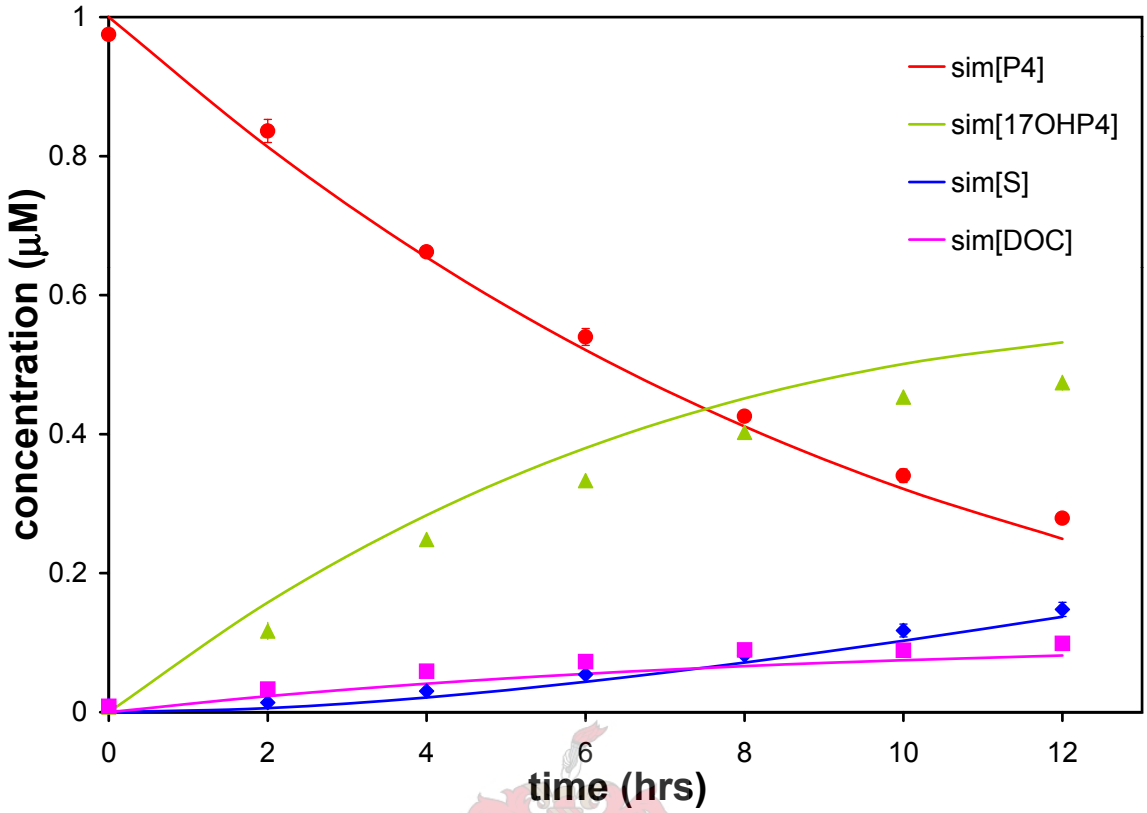

Figure 4.7: P4 metabolism in six CYP17 to two CYP21 assay compared to simulation. After 12 hours there was 72% conversion of P4 to products. 17OHP4 has not yet reached steady-state. Of note is the increase in S present compared to Figure 4.6. Standard errors were worked out as described in [99] from triplicate data set. Lines simulated data from model, points from experimental data. There is a 98.84% correlation between experimental and simulated results.

It can be argued that by comparing the simulation based on the fitted V values to the experimental data proves nothing. This is not so. The V values are derived from 2 different experiments

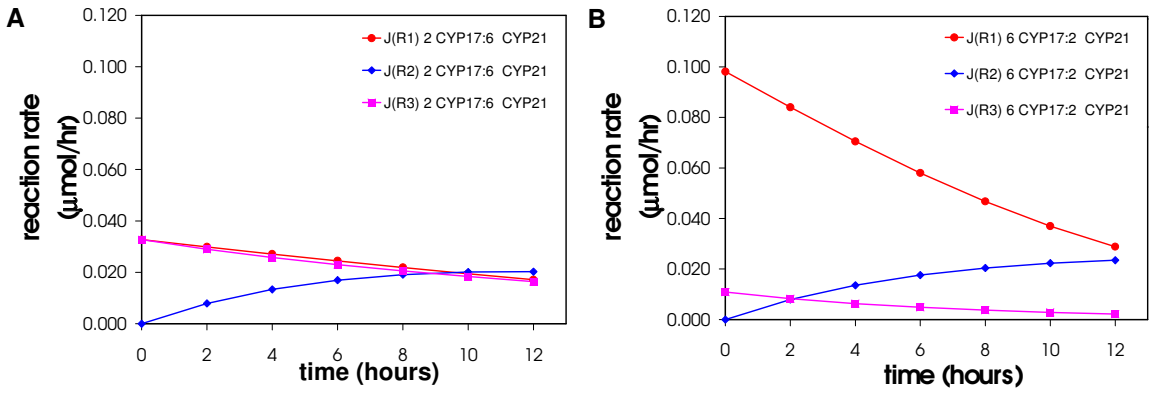

Figure 4.8: Reaction rates through the course of the experiments. **A** is the profile for the $2:6$ experiment and **B** the profile for the $6:2$ experiment. The point where reaction rates 1 and 2 bisect in **A** indicate the time where the pseudo-steady-state occurs. Note that reaction rate 2 does not change significantly in comparison to reaction rate 1.

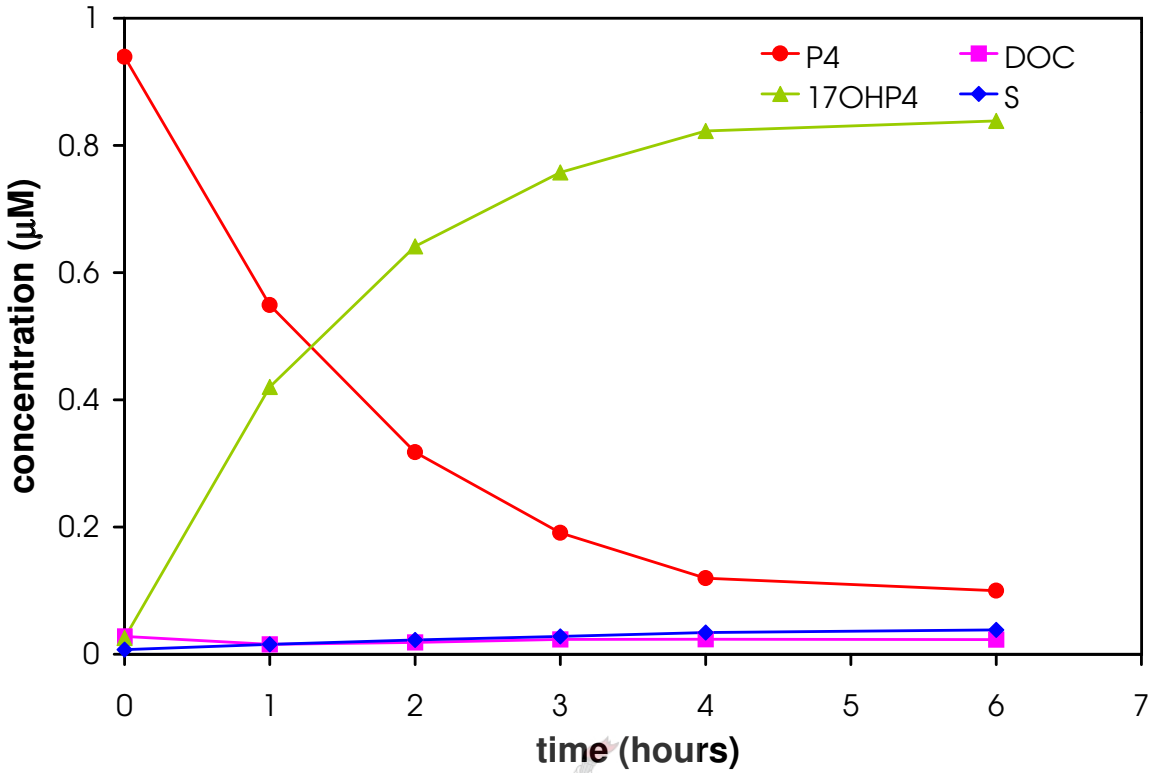

Figure 4.9: CYP17 control P4 conversion assay. In the CYP17 control the P4 was near fully converted to 17OHP4 after 6 hours. 0.333 mg/mL protein was present on the dish after removal of the cells from the dish and suspension in 1 mL PBS.

comprising 3 data sets each. The V values in Table 4.3 are medians of the 6 data sets. If the one experiment deviated from the other experiment in respect to the fitted V values then the correlation between experiment and simulation would be less. The high correlations of 99% indicate that the model fits both experiments accurately. It is reasonable to assume it would correlate accurately with other experiments performed with the parallel transfection technique and is a fair representation of the physiological CYP17/CYP21 branch point.

The model cannot be compared to the individual enzymes because the V values obtained from the experiments are from a system where there is competition for substrate and substrate binding sites. Due to this competition the V values will be inaccurate under-estimations of the true k_{cat} values for each enzyme expressed in COS1 cells.

This high correlation between the model and experiment is encouraging but further experimentation is needed to be confident in the model's ability to predict and explain characteristics of the COS1 and *in situ* system.

In the next chapter the model will be subjected to structural and control analysis where after the model will be manipulated and simulations run to test hypotheses drawn from the control analysis.

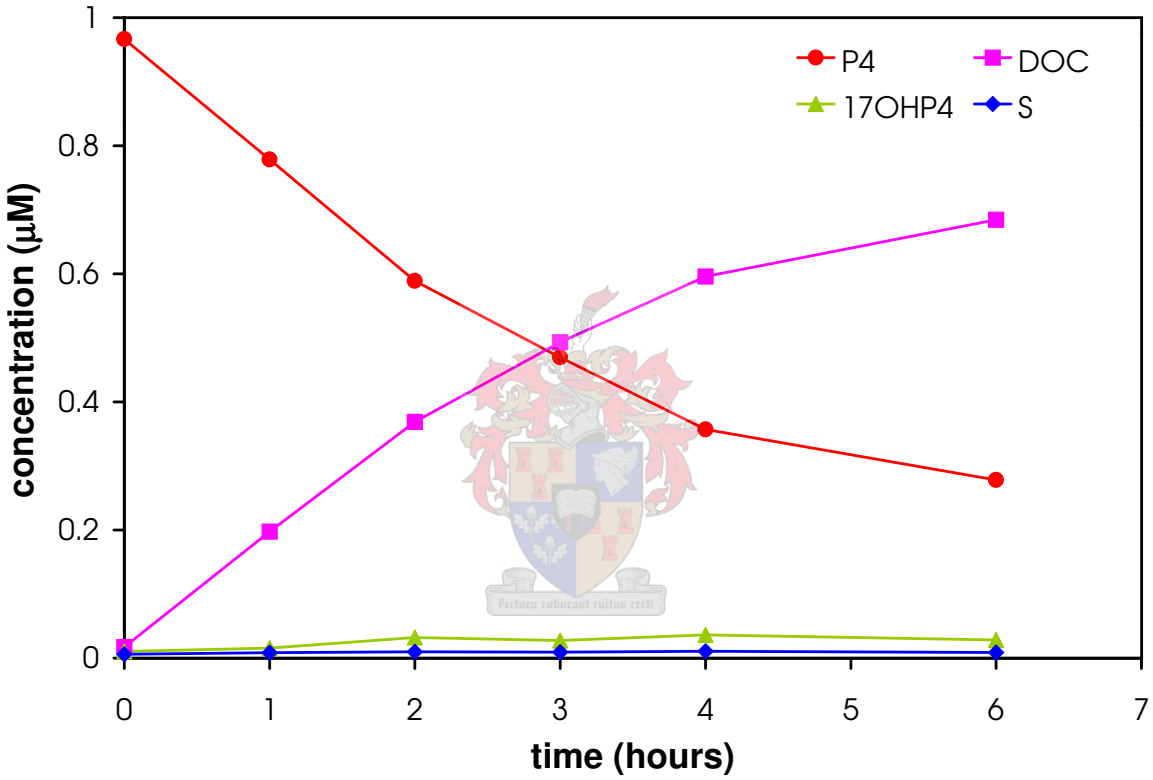

Figure 4.10: CYP21 control P4 conversion assay. In the CYP21 control 70% of the P4 was converted to DOC after 6 hours. 0.333 mg/mL protein was present on the dish after removal of the cells from the dish and suspension in 1 mL PBS.

Chapter 5

Control analysis of the CYP17/CYP21 branch point

The goal in this chapter is to apply control analysis to the CYP17/CYP21 branch point in an effort to determine which reactions have control over the flux and metabolite concentrations and to what degree they have this control. Two methodologies will be employed to accomplish this task. The first are structural analysis developed by Sauro *et al.* [101, 102] and control analysis [103, 104]. Using structural analysis the branch point will be expressed mathematically. The purpose of this is to derive $\mathcal{K}$ of the **E** term of the identity matrix [13]:

$$\mathrm{C^i E} = \begin{bmatrix} C^J \\ C^s \end{bmatrix} [\mathcal{K} \quad -\epsilon] = \mathbf{I} \tag{5.1}$$

$\mathrm{C^i}$ is the matrix of control coefficients. These coefficients are defined as:

$$C^y_{v_i} = \frac{(\partial \ln y / \partial \ln p)_{ss}}{(\partial \ln v_i / \partial \ln p)_{step \quad i}} \tag{5.2}$$

For C^J the variable y is the steady-state flux; for C^s the variable is the metabolite concentration. The enzyme activity of the particular step is v_i and p is the parameter associated with both y and v in the system [14]. $\mathcal{K}$ is the scaled version of the null-matrix expressing the steady-state fluxes in relation to the change in metabolite concentration [19]. ϵ is the matrix of elasticities. Elasticities are defined as:

$$\epsilon^v_s = \frac{\partial \ln v}{\partial \ln s} \tag{5.3}$$

They are a measure of the sensitivity of the enzyme (observed as a change in reaction rate) in response to changes in metabolite concentration.

$\mathcal{K}$ must be derived from the pathway structure, while the elasticity coefficients are either measured experimentally or, in a numerical model, calculated. Some elasticities will of course always be zero purely because the metabolite in question is neither a substrate, product, nor an effector

of the enzyme. Elasticities which in general are non-zero can become zero if for example an enzyme is always saturated with its substrate or always insensitive to its product. Such assumptions should only be made with great care. In this instance CYP reactions are well characterized and such assumptions are well supported by the literature.

Using the computer model presented in Chapter 4 the hypotheses constructed from the results of the control analysis will be tested and the effects of enzyme activity on each step demonstrated.

5.1 Control analysis of the CYP17/CYP21 branch point

The model scheme presented in Figure 4.1 does not reach a steady-state nor does it include a steroid precursor supply step nor metabolite demand step. For the purposes of control analysis a new model scheme is presented in Figure 5.1 that includes a supply and demand step.

In Figure 5.1 a supply block has been added that supplies S_1 (P4). This reaction 1 (R_1) is not the reaction catalyzed by 3βHSD on Figure 2.3 but instead represents the pathway from cholesterol to P4. The demand block is represented by reactions 4 (R_4) and 6 (R_6). These can be regarded as the reactions catalyzed by CYP11B1 in Figure 2.3.

For structural analysis, no detailed information regarding the kinetics is needed.

5.1.1 The stoichiometric matrix N

The use of matrices and their use in control analysis is explained by Hofmeyr [19, 105]. For the sake of brevity non-informative steps will be neglected from the text. The reader is advised to consult references [19, 101, 102, 105] for a full step-by-step explanation of the mathematics and [12] for an explanation of the theory behind control analysis.

The stoichiometric matrix is defined as:

$$\frac{d\mathbf{s}}{dt} = \mathbf{N}\mathbf{v}[\mathbf{s}, \mathbf{p}] \tag{5.4}$$

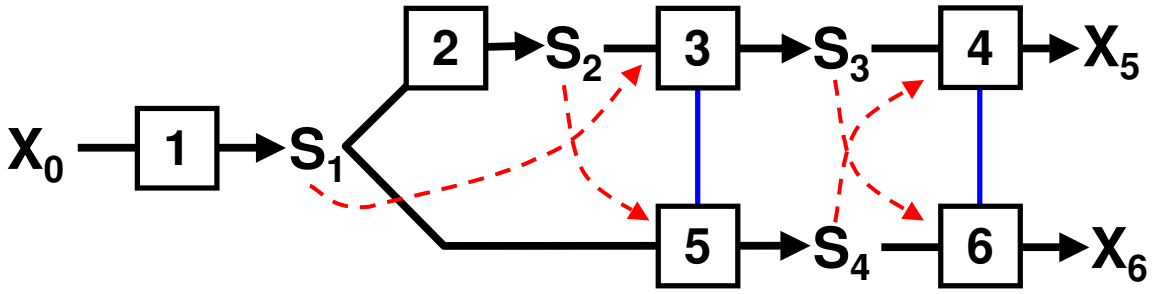

Figure 5.1: Steady-state reaction scheme with P4 supply and S/DOC demand. In the above reaction scheme X_0 represents P5; S_1, P4; S_2, 17OHP4; S_3, S; X_5, cortisol; S_4, DOC; and X_6, corticosterone. R_1 (Reaction 1) is a supply block; R_2 is catalyzed by CYP17, R_3 and R_5 by CYP21; and R_4 and R_6 by CYP11B1. Substrate inhibitions are indicated with dashed lines. The flux through the pathway can be divided up into three sections: J_a (J_1), J_b ($J_{2,3,4}$) and J_c ($J_{5,6}$) where $J_a = J_b + J_c$.

Where **N** is the stoichiometric matrix of dimensions $m \times n$ where n is the number of reactions and m the number of variable metabolites. **v** is the column vector of reaction rates; and **p** a p-dimensional column vector of parameters. X_0, X_5 and X_6 are fixed as constants: 1, 0 and 0 respectively.

Our model can be represented in matrix form as shown in Eqn 5.5.

	R_1	R_2	R_3	R_4	R_5	R_6	$\dot{s_1}$	$\dot{s_2}$	$\dot{s_3}$	$\dot{s_4}$
S_1	1	−1	0	0	−1	0	1	0	0	0
S_2	0	1	−1	0	0	0	0	1	0	0
S_3	0	0	1	−1	0	0	0	0	1	0
S_4	0	0	0	0	1	−1	0	0	0	1

(5.5)

The left matrix is the stoichiometry matrix **N** and it is augmented on the right with an identity matrix in which each column represents a time derivative. The matrix Eqn. 5.5 is an alternative means of displaying the differential equations shown by Eqn. 4.9 to 4.12. It can be seen from the matrix that s_2[1] is dependent on the rate of R_2 and -R_3 ($^{ds_2}/_{dt} = v_2 - v_3$).

The **N** matrix is reduced to give the reduced stoichiometric matrix $\mathbf{N_R}$, Eqn. 5.6 by means of Gaussian elimination to obtain the row echelon form. The term row echelon refers to the fact that the matrix has an upside-down staircase pattern with non-zero corners (ones in this case). Note that the columns number R_1, R_2, R_3 and R_5 each start a new stair. These are called the pivot columns and the ones are the pivots.

	R_1	R_2	R_3	R_4	R_5	R_6	$\dot{s_1}$	$\dot{s_2}$	$\dot{s_3}$	$\dot{s_4}$
S_1	1	0	0	−1	0	−1	1	1	1	1
S_2	0	1	0	−1	0	0	0	1	1	1
S_3	0	0	1	−1	0	0	0	0	1	1
S_4	0	0	0	0	1	−1	0	0	0	1

(5.6)

5.1.2 The $\mathcal{K}$-matrix

If the reduced stoichiometry matrix multiplied by the flux vector J is set to zero (i.e. the steady-state) the flux relationships can be derived. The simplest way of doing this is to choose the fluxes that refer to non-pivot columns as independent fluxes, in this case J_4 and J_6. This leads to the flux

[1] In control analysis terminology concentration is denoted as the symbol of the variable or parameter in lower case and italics in conjunction with the subscript number of the step. e_2 is therefore the concentration of enzyme number 2 (E_2).

relationships $\mathbf{J} = \mathbf{K}\mathbf{J_i}$ as shown in Eqn. 5.7.

$$\begin{bmatrix} J_1 \\ J_2 \\ J_3 \\ J_4 \\ J_5 \\ J_6 \end{bmatrix} = \begin{bmatrix} 1 & 1 \\ 1 & 0 \\ 1 & 0 \\ 1 & 0 \\ 0 & 1 \\ 0 & 1 \end{bmatrix} \cdot \begin{bmatrix} J_4 \\ J_6 \end{bmatrix} \tag{5.7}$$

The $\mathbf{K}$ matrix (Eqn. 5.7) is scaled to $\mathcal{K} = (\mathbf{D^J})^{-1}\mathbf{K}\mathbf{D^{J_i}}$ (Eqn. 5.8) that now expresses the flux relationships in terms of the independent (J_4 and J_6) and dependent fluxes (J_1). These fluxes were defined in Figure 5.1 as J_a, J_b and J_c.

$$\mathcal{K} = \begin{bmatrix} \frac{1}{J_4} & 0 & 0 & 0 & 0 & 0 \\ 0 & \frac{1}{J_6} & 0 & 0 & 0 & 0 \\ 0 & 0 & \frac{1}{J_1} & 0 & 0 & 0 \\ 0 & 0 & 0 & \frac{1}{J_2} & 0 & 0 \\ 0 & 0 & 0 & 0 & \frac{1}{J_3} & 0 \\ 0 & 0 & 0 & 0 & 0 & \frac{1}{J_5} \end{bmatrix} \cdot \begin{bmatrix} 1 & 0 \\ 0 & 1 \\ 1 & 1 \\ 1 & 0 \\ 1 & 0 \\ 0 & 1 \end{bmatrix} \cdot \begin{bmatrix} J_b & 0 \\ 0 & J_c \end{bmatrix} = \begin{bmatrix} 1 & 0 \\ 0 & 1 \\ \frac{J_b}{J_a} & \frac{J_c}{J_a} \\ 1 & 0 \\ 1 & 0 \\ 0 & 1 \end{bmatrix} \tag{5.8}$$

5.1.3 The local properties of E

With $\mathcal{K}$ the complete identity matrix can be written out as follows in Eqn. 5.9 below.

$$\mathbf{I} = \begin{bmatrix} C_{v_4}^{J_4} & C_{v_6}^{J_4} & C_{v_1}^{J_4} & C_{v_2}^{J_4} & C_{v_3}^{J_4} & C_{v_5}^{J_4} \\ C_{v_4}^{J_6} & C_{v_6}^{J_6} & C_{v_1}^{J_6} & C_{v_2}^{J_6} & C_{v_3}^{J_6} & C_{v_5}^{J_6} \\ C_{v_4}^{s_1} & C_{v_6}^{s_1} & C_{v_1}^{s_1} & C_{v_2}^{s_1} & C_{v_3}^{s_1} & C_{v_5}^{s_1} \\ C_{v_4}^{s_2} & C_{v_6}^{s_2} & C_{v_1}^{s_2} & C_{v_2}^{s_2} & C_{v_3}^{s_2} & C_{v_5}^{s_2} \\ C_{v_4}^{s_3} & C_{v_6}^{s_3} & C_{v_1}^{s_3} & C_{v_2}^{s_3} & C_{v_3}^{s_3} & C_{v_5}^{s_3} \\ C_{v_4}^{s_5} & C_{v_6}^{s_5} & C_{v_1}^{s_5} & C_{v_2}^{s_5} & C_{v_3}^{s_5} & C_{v_5}^{s_5} \end{bmatrix} \begin{bmatrix} 1 & 0 & -\epsilon_{s_1}^{v_4} & -\epsilon_{s_2}^{v_4} & -\epsilon_{s_3}^{v_4} & -\epsilon_{s_4}^{v_4} \\ 0 & 1 & -\epsilon_{s_1}^{v_6} & -\epsilon_{s_2}^{v_6} & -\epsilon_{s_3}^{v_6} & -\epsilon_{s_4}^{v_6} \\ \frac{J_b}{J_a} & \frac{J_b}{J_a} & -\epsilon_{s_1}^{v_1} & -\epsilon_{s_2}^{v_1} & -\epsilon_{s_3}^{v_1} & -\epsilon_{s_4}^{v_1} \\ 1 & 0 & -\epsilon_{s_1}^{v_2} & -\epsilon_{s_2}^{v_2} & -\epsilon_{s_3}^{v_2} & -\epsilon_{s_4}^{v_2} \\ 1 & 0 & -\epsilon_{s_1}^{v_3} & -\epsilon_{s_2}^{v_3} & -\epsilon_{s_3}^{v_3} & -\epsilon_{s_4}^{v_3} \\ 0 & 1 & -\epsilon_{s_1}^{v_5} & -\epsilon_{s_2}^{v_5} & -\epsilon_{s_3}^{v_5} & -\epsilon_{s_4}^{v_5} \end{bmatrix} \tag{5.9}$$

In accordance with the summation theorems [12], all flux control coefficients sum to unity ($\sum C_i^J = 1$) and all concentration control coefficients sum to zero ($\sum C_i^s = 0$). According to the connectivity theorem the products of the elasticities and flux control coefficients sums to 0 ($\sum C_i^J \epsilon_s^i = 0$) and the products of the elasticities and concentration control coefficients sums to negative one or zero ($\sum C_i^y \epsilon_s^i = -1 \quad \text{or} \quad 0$). $\sum C_i^y \epsilon_s^i$ sums to zero if the reference metabolite (y) is not the same as the perturbed metabolite (s); and sums to -1 if the two are equivalent [106]. Together the summation and connectivity theorems form a linear equation system that allows the control coefficients to be expressed in terms of the elasticies. This enables the researcher to solve for the control coefficients (system properties) by experimental measurement of the elasticies (local properties) [12, 19]. Eqn. 5.9 is the matrix formulation of the connectivity theorems.

Some of the local properties are known allowing the matrix $[\mathcal{K} \; -\epsilon]$ to be simplified in respect to $\mathbf{E}$ as shown in Eqn. 5.10. In Section 4.2 the enzymes CYP17 and CYP21 were shown to be insensitive to their products. Accordingly the model enzymes E_2 and $E_{3,5}$ are insensitive to down stream products s_2, s_3, s_4, x_5 and x_6; and s_3, s_4, x_5 and x_6 respectively. If we assume E_1, $E_{4,6}$ are also insensitive to their corresponding downstream metabolites and the reactions are far from equilibrium their elasticities will be zero as shown in Eqn. 5.10.

$$\begin{bmatrix} 1 & 0 & 0 & 0 & -\epsilon_{s_3}^{v_4} & -\epsilon_{s_4}^{v_4} \\ 0 & 1 & 0 & 0 & -\epsilon_{s_3}^{v_6} & -\epsilon_{s_4}^{v_6} \\ \frac{J_b}{J_a} & \frac{J_c}{J_a} & 0 & 0 & 0 & 0 \\ 1 & 0 & -\epsilon_{s_1}^{v_2} & -\epsilon_{s_2}^{v_2} & 0 & 0 \\ 1 & 0 & -\epsilon_{s_1}^{v_3} & -\epsilon_{s_2}^{v_3} & -\epsilon_{s_3}^{v_3} & -\epsilon_{s_4}^{v_3} \\ 0 & 1 & -\epsilon_{s_1}^{v_5} & -\epsilon_{s_2}^{v_5} & -\epsilon_{s_3}^{v_5} & -\epsilon_{s_4}^{v_5} \end{bmatrix} \tag{5.10}$$

All the elasticities in the third row are zero. This indicates that reaction block 1 has complete control over its flux (J_a), if the assumptions above are correct, and $E_1$is not subject to the downstream enzymes of the system [107]. We can thus tentatively conclude:

$$C_{\mathrm{R}_1}^{J_a} = 1 \quad \text{and} \quad C_{\mathrm{R}_i}^{J_a} = 0 \quad \text{where} \quad i = 2, 3, 4, 5, 6 \tag{5.11}$$

and

$$C_{\mathrm{R}_1}^{s_1} = -\sum C_{\mathrm{R}_i}^{s_1} \quad \text{where} \quad i = 2, 3, 4, 5, 6 \tag{5.12}$$

This does not imply that the supply block has any control over the distribution of flux between branch b and c. The partitioning of the fluxes J_b and J_c is determined by the response of either branch to s_1, i.e.:

$$C_{R_2}^{J_i} \cdot \epsilon_{s_1}^{v_2} \quad \text{where} \quad i = 2, 3, 4 \tag{5.13}$$

and

$$C_{R_5}^{J_i} \cdot \epsilon_{s_1}^{v_5} \quad \text{where} \quad i = 5, 6 \tag{5.14}$$

These responses would be measured by studying the branches in isolation (which is experimentally impossible due to $E_{3,5}$ having affinity for both S_1 and S_2).

These results lend some support to the theories put forward by Clark and Stocco [15] who report either StAR or CYP11A1 being the rate-limiting enzyme of adrenal steroidogenesis. The model E_1 is not equivalent to StAR or CYP11A1 but may be viewed as a composite of the enzymes from StAR (or CYP11A1 depending on where you consider steroidogenesis to begin) to 3βHSD. If the elasticities of 3βHSD and CYP11A1 are also zero in respect to their downstream metabolites, then the above reasoning will apply and the StAR-CYP11A1 block would be a true rate-limiting step. Whether the control is shared between StAR and CYP11A1 cannot be commented on.

To obtain the control coefficients one can solve the matrix Eqn. 5.9 by inserting the elasticity values into the matrix and solving for the control coefficients by inverting the $\mathbf{E}$ matrix ($\mathbf{C}(\mathbf{E})^{-1} = \mathbf{I}$).

As no elasticity values are available, another method is needed to solve for the control coefficients. This method is metabolic simulation based of the model in sections 4.3.2 and implemented in the computer environment of Gepasi [100].

5.2 Model simulations of the CYP17/CYP21 branch point

The allure of a computer model is that a years experiments can be carried out in one afternoon *in silico* but more importantly a model allows one to perform experiments that would not ordinarily be possible in order to generate new hypotheses and test existing ones. A model is a paradigm in which Kuhn's "normal science" can proceed [21].

The control analysis and previous research [15] suggest that the supply block is rate-limiting. Other evidence from various mutations of CYP17 and CYP21 (see Chapter 1) suggest that CYP17 and/or CYP21 effect the flux through steroidogenesis (i.e. the supply block is not rate-limiting).

These two hypotheses can be tested with the constructed model by determining the control coefficients for J_b and s_3.In the model S_3 corresponds to deoxycortisol. At steady-state s_3 will remain constant. If its value is high and the J_b is likewise high in respect to J_c then this would indicate a higher production of cortisol (X_5). If E_2 has a large proportion of the flux control then by increasing its activity there would be a corresponding increase in J_b and S_3.

This and other similar simulations aimed at determining the effect of each system component will be run using the model as defined in Figure 5.1. The CYP17 and CYP21 kinetics as defined in Table 4.3 were used for R_2 and $R_{3,5}$. The R_1, R_4 and R_6 were assigned kinetics in accordance with the assumption that the reactions are irreversible and insensitive to product. R_1 was assigned a constant flux of 0.0039 μmol/hr. R_4 and R_6 were assigned identical kinetics to that of R_3 and R_5 respectively, except for the value of V which was set at 0.0024 μmol/hr. These values were chosen so that the supply reaction would not have a lower flux than the reactions under investigation ($R_{2,3,5}$); and that the demand reactions would not have a higher flux than the reactions investigated. Beckert et al [108] report a K_m of 1.7 μM, derived from the unreliable Lineweaver-Burk plot [109][2] using data obtained from a mitochondrial suspension, for deoxycorticosterone to corticosterone reaction of CYP11B1; but no value for the deoxycortisol to cortisol reaction. This data was judged by the author to be inadequate for model inclusion as it still left the matter of the K_m, K_i and V values undetermined for $R_{4,6}$. $a = 100$ for all reactions.

From the simulation run with X_0 set to 1 μM it can be seen that P4, 17OHP4, DOC and S reach a steady-state from $\approx$ 400 hours (Figure 5.2). This result does not imply that the steroidogenic network or COS1 cell expression system will reach steady-state in 400 hours only that the model as laid out above does. s_2 (17OHP4) and s_3 (S) lie close together and the concentration increases occur in concert. s_1 (P4) and s_4 (DOC) also lie close together and follow the same pattern of increase. s_1 and s_4 reach steady-state later than s_2 and s_3. The fluxes are $J_a = 0.065$, $J_b = 0.055$

[2] All other kinetic values used were determined with the more reliable Hanes-Woolf Plot.

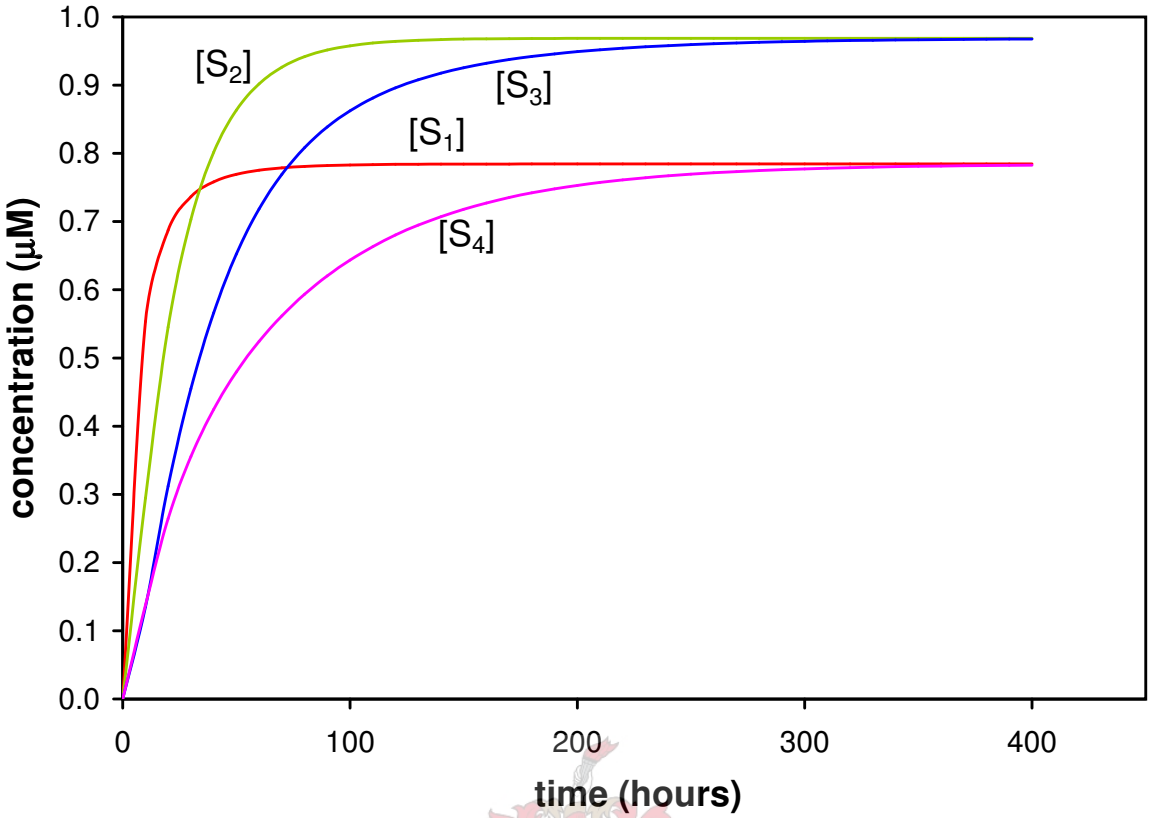

Figure 5.2: Steady-state time course plot of s_1, s_2, s_3 and s_4. All metabolite concentrations fall under 1 μM; x_0 is constant at 1 μM; and x_5 and x_6 constant at 0.

and $J_c = 0.010$ μmol/hour. At equal enzyme concentrations the CYP17 branch (J_b) of the pathway has a higher flux than that of the CYP21 branch (J_c).

The flux and concentration control coefficients in respect to E_2 (CYP17) and s_3 are shown in Table 5.1. E_2 and S_3 are examined because the flux through J_b determines the output of X_5 (cortisol) and s_3 is an indicator of the model concentration of S, the precursor of cortisol. These values support the hypothesis that the control over the flux and concentration rests in the supply of P4 to the branch point.

$C^{J_b}_{v_1}$ and $C^{s_3}_{v_1}$ have 88% and 90% of the flux and concentration control respectively. $C^{J_b}_{v_3}$ is negative because as E_3 converts S_2 to S_3 the inhibitory effect of S_2 on R_5 is lessened resulting in a decrease in J_b. $C^{J_b}_{v_5}$ is negative because R_5 produces S_4 that inhibits R_4 consequently decreasing J_b. $C^{s_3}_{v_2}$ is negative because S_2 inhibits R_5. A lower R_5 rate will mean a higher R_4 rate effectively increasing the rate of S_3 to X_5 turnover. For this reason $C^{s_3}_{v_4}$ is also negative. $C^{s_3}_{v_6}$ is negative because a high S_4 to X_6 conversion rate would mean there is less total S_4 in the system to inhibit R_4.

The natural question is what happens then if we alter the activities of each reaction? Will the control still rest with the supply of P4 if the demand reaction rates (4 and 6) are increased? What happens if we vary the enzyme activity of R_1, R_2 and $R_{3,5}$? These are the topics for the next sections.

Table 5.1: Control Coefficients in reference to [S] and flux through the glucocorticoid branch. Values were calculated for the steady-state model using Gepasi.

Flux control coefficients	Concentration control coefficients
$C^{J_b}_{v_1}$= 1.18	$C^{s_3}_{v_1}$= 2.82
$C^{J_b}_{v_2}$= 0.16	$C^{s_3}_{v_2}$=-0.15
$C^{J_b}_{v_3}$=-0.16	$C^{s_3}_{v_3}$= 0.14
$C^{J_b}_{v_4}$= 0.00	$C^{s_3}_{v_4}$=-2.38
$C^{J_b}_{v_5}$=-0.18	$C^{s_3}_{v_5}$= 0.17
$C^{J_b}_{v_6}$= 0.00	$C^{s_3}_{v_6}$=-0.60

5.2.1 Varying the activity of E_1

In this *in silico* experiment the value of a_1 was varied from 1 to 200 while all other a values were fixed at 100. The concentration steroid precursor was fixed at 1 μM. The result of the simulation is shown in Figure 5.3.

Increasing a_1 to 180 yields a ratio of s_3 (S) to s_4 (DOC) of $\approx 36:1$ with s_3 increasing exponen-

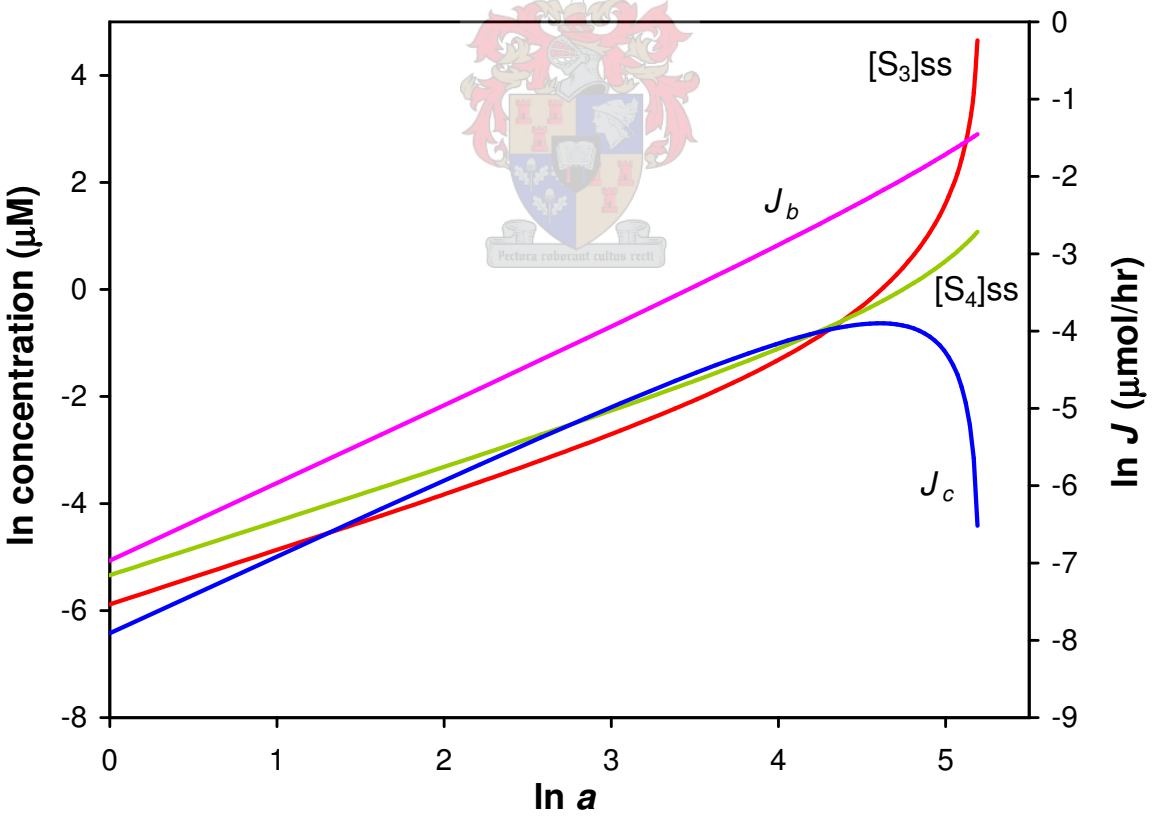

Figure 5.3: Steady-state plot with E_1 a varied from 1 to 200. x_0 is constant at 1 μM; and x_5 and x_6 constant at 0. The value of a for reaction 1 is varied from 1 to 200. All other values of a are maintained at 100. No steady-state was found at $a > 180$. There is a 36$\times$ difference between s_3 and s_4 at 180.

tially. At this value of a J_b is 158× greater than J_c. The increase in J_b is linear while the increase in J_c is only linear up to $a = 50$ where it peaks and decreases. This is hypothesized by the author to be due to the inhibitory action of S_2 (17OHP4) on R_5. As a result there is less flux through branch c and less S_4 and X_6.

5.2.2 Varying the activity of E_2

a_2 was varied from 1 to 200 while all other a values were fixed at 100. The concentration steroid precursor was fixed at 1 μM. The result of the simulation are shown in Figure 5.4.

The simulation shows that by varying the activity of E_2 a 2.51× difference between s_3 and s_4 is achieved (comparing steady-state concentrations). More S_3 is produced relative to S_4 at $a_2 = 82$. From this point s_4 declines near linearly due to the inhibitory action of S_2 (17OHP4). The s_3 also declines, at 7% of the gradient of the s_4 decline, due to the inhibitory action of S_3 on R_6. This will result in a higher reaction rate for R_4 and faster metabolism of S_3 to X_5.

J_b begins to exceed that of J_c from $a = 21$. At $a = 200$ J_b is 11× greater than that of J_c. If E_2 (CYP17) exercised full control over J_b then one would expect to see a much larger difference and the trace in Figure 5.4 of J_b to of been a near straight line. This is not seen. E_2 has only a portion of

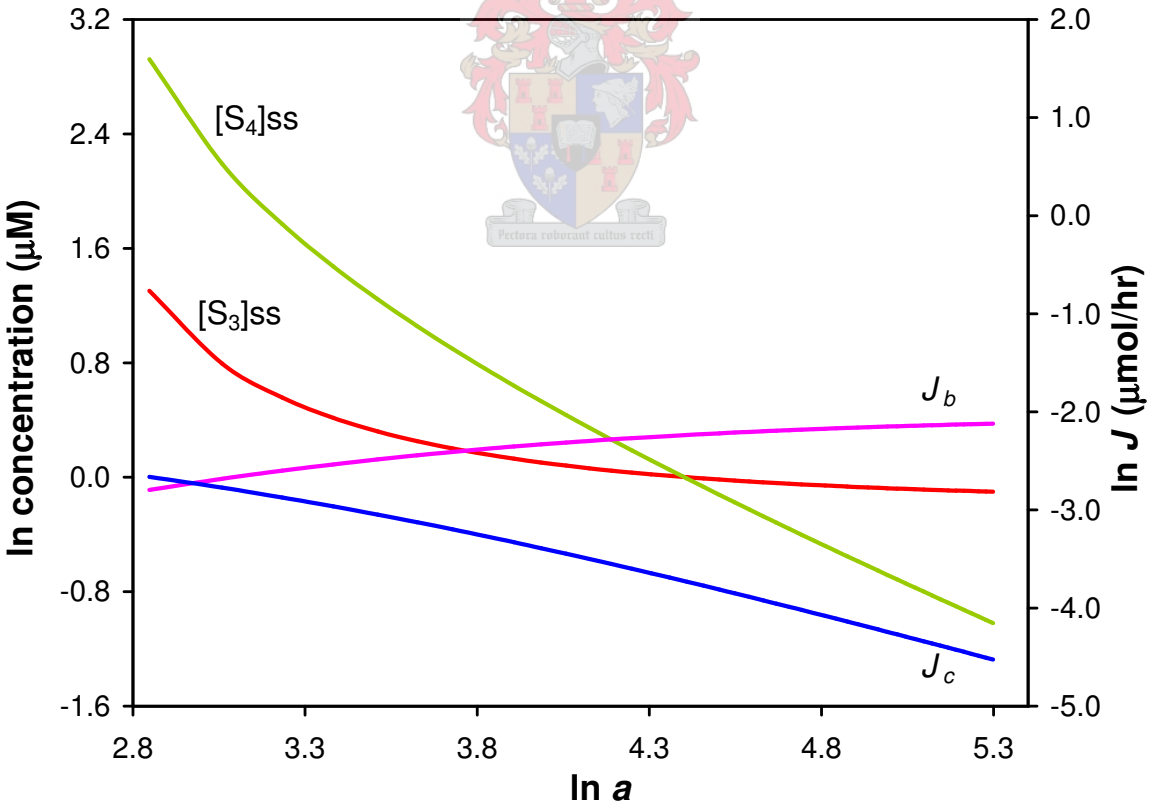

Figure 5.4: Steady-state plot with E_2 a varied from 1 to 200. x_0 is constant at 1 μM; and x_5 and x_6 constant at 0. The value of a for reaction 2 is varied from 1 to 200. All other values of a are maintained at 100. No steady-state was found at values of $a < 17$. There is a 251× difference between s_3 and s_4 at $a = 200$.

the control over the pathway (see Table 5.1).

5.2.3 Varying the activity of $E_{3,5}$

In this simulation a was varied from 1 to 200. The results of this simulation are shown in Figure 5.5. Because R_3 and R_5 are catalyzed by the same reaction, varying one's a value will result in the equivalent change in the a value of the other reaction in the model.

A 2.58× difference between s_4 and s_3 can be achieved by varying the activity of E_5 from $a_5 = 1$ to 200. At 200 s_4 is increasing linearly while s_3 increases only slightly due to the inhibitory action of S_4 on R_4.

J_b is 0.58× less than J_c at $a_5 = 200$. At twice the concentration of E_2, $E_{3,5}$ cannot shift the bulk of the flux from branch b to branch c. This is also seen from the reaction rate data presented in Figure 4.8. This data supplies experimental verification of this facet of the model. This effect may be due to the concentration of S_2 (17OHP4) rather than the concentration of E_2.

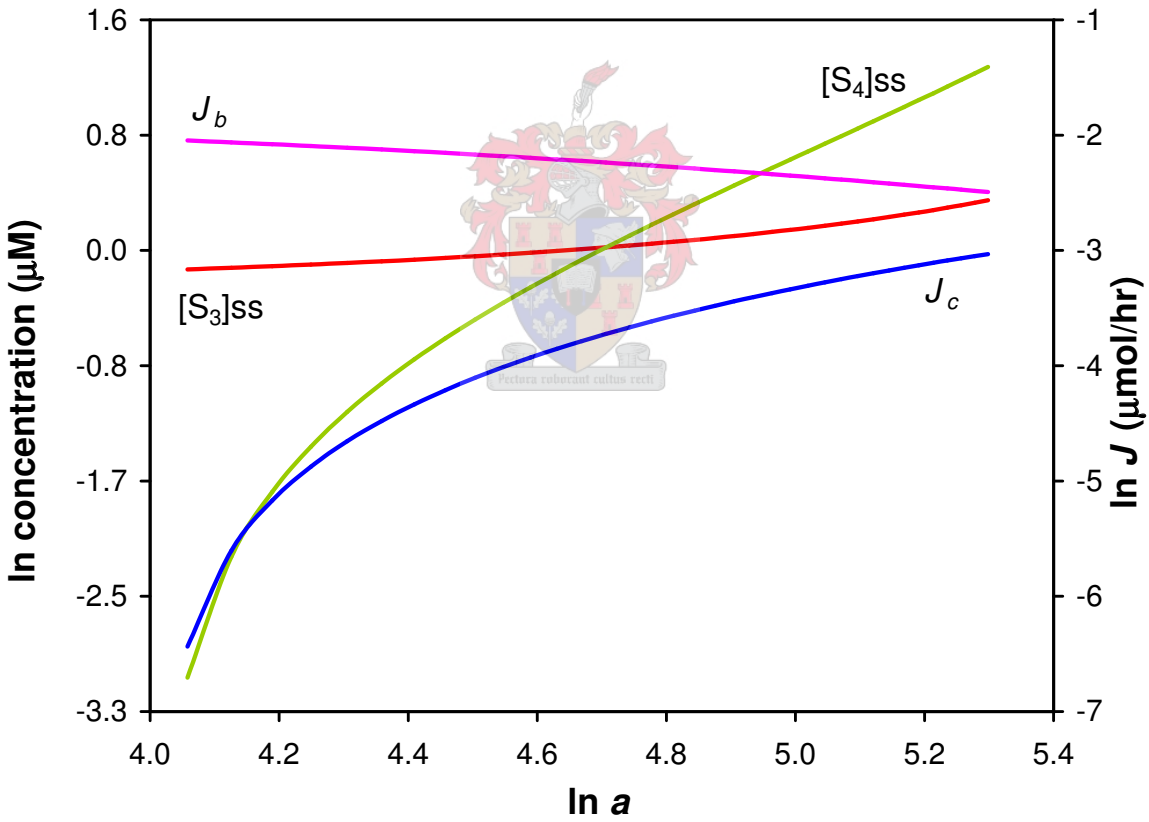

Figure 5.5: Steady-state plot with $E_{3,5}$ a varied from 1 to 200. x_0 is constant at 1 μM; and x_5 and x_6 constant at 0. The value of a for reaction 1 is varied from 1 to 200. All other values of a are maintained at 100. No steady-state was found at low values of a. There is a 258× difference between s_4 and s_3 at 200.

5.2.4 Varying the activity of $E_{4,6}$

The three last sections have shown that E_2 and $E_{3,5}$ have little impact on the flux through either pathway and that the supply block (reaction 1) has the largest effect on the flux and steady-state concentrations of S_3 and S_4. The question remains: what control does the demand for S_3 and S_4 have over the pathway.

The value of a for R_4 and R_6 was varied from 1 to 200. Because R_4 and R_6 are catalyzed by the same reaction, varying one's a value will result in the equivalent change in the a value of the other reaction in the model. No steady-state was found for $a < 47$. The results of this simulation are shown in Figure 5.6.

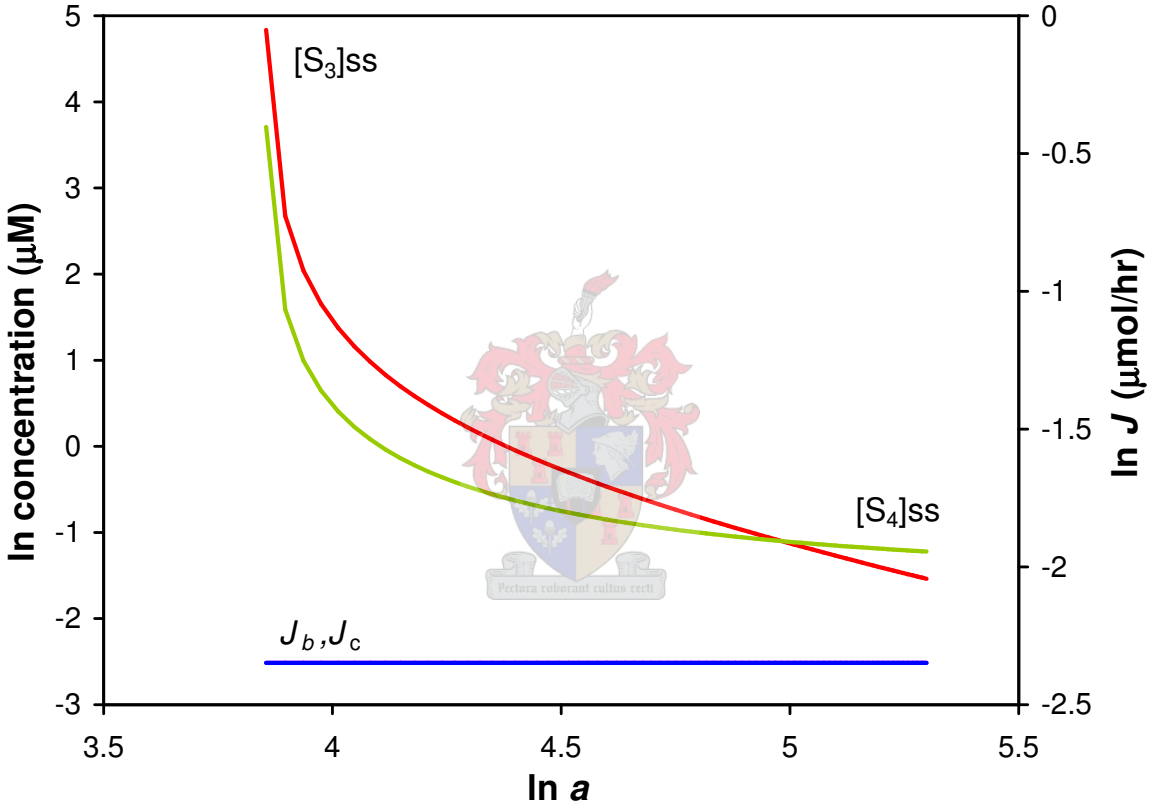

Figure 5.6: Steady-state plot with $E_{4,6}$ a varied from 1 to 200. x_0 is constant at 1 μM; and x_5 and x_6 constant at 0. The value of a for reaction 1 is varied from 1 to 200. All other values of a are maintained at 100. No steady-state was found at low values of a.

J_b and J_c do not change in respect to a change in demand and the change in ratio S_3 to S_4 is not large. The demand for steroid product within the pathway has no control over the flux through the pathway.

5.3 Summary of results

Assuming that the reactions depicted in Figure 5.1 are the only reactions to occur involving the shown metbolites, that all the the reactions are irreversible, and that the enzymes are in turn in-

sensitive to the metabolites downstream from them it can be shown using a purely mathematical approach, that the supply of steroid precursor has dominion over most of the control in the model pathway. R_1 controls its own flux and the downstream enzymes have to keep pace with it.

Using the model simulations it was shown that only by modulating the reaction rate of R_1 were the flux and steady-state concentrations of metabolites greatly perturbed. Varying the activity of E_2 and $E_{3,5}$ had effects on the flux and metabolite concentrations but not as dramatic as varying the activity of E_1. While some large changes in metabolite concentrations were observed for variations in a_2 and a_3 there was very little change in the flux. It is the flux that is important as in the stress response the goal is a larger turnover of steroid in the adrenal not higher adrenal steroid concentrations. Varying the activity of the demand reactions had very little effect on the ratio of s_3 to s_4.

Chapter 6

Conclusions

A model is an invention, not a discovery.
It may prove to be a valid description,
but is a far cry from being the essential truth.
Massoud et al. [21]

The central questions to be answered in this thesis were: what degree of control does CYP17 and CYP21 have over the CYP17/CYP21 branch point of mineralocorticoid and glucocorticoid synthesis; and which enzymes have the most control?

To answer this question a model describing the branch point was constructed. The model was analyzed mathematically using structural and control analysis. Using the model, thought experiments were performed *in silico* to ascertain the effect of the enzymes in the model pathway. From this data concentration and flux control coefficients were calculated.

6.1 The model

Using the data presented in Section 4.3 an empirical actual model (as defined in [21]) was constructed using Michaelis-Menten kinetics and K_m values from the literature [85, 91] that describe the activities of CYP17 and CYP21 in COS1 cell tissue culture using parallel transfection. The V values were derived by fitting the model to the experimental data using the evolutionary algorithm fitting module of Gepasi [100].

This model accurately (99% fit) describes the branch point as reconstituted in tissue culture (see Section 4.3.2).

With arbitrary modification of the initial model a conceptual model capable of reaching a steady-state *in silico* was constructed.

The model satisfies the intuitive test for model validity [21] in that:

1. The quantitative features of the overall performance appear to be explained by the combined properties of the conceptual units.

2. The qualitative features of the overall performance appear to be explained by the combined properties of the conceptual units.
3. The quantitative comparison of the model versus the experimental data is not grossly in error.
4. The model is capable of undergoing tests that may falsify it.
5. The model is heuristic in nature and permits application of the available techniques for its manipulation.
6. It is accessible to evaluation by a specified set of criteria satisfying the needs of a scientifically sound hypothesis.

6.2 Control analysis

Structural and control analysis suggests that the bulk of control over the steroidogenic pathway flux probably lies in the supply of P4 (see Section 5.1.3), but that the partitioning of flux between the branches to cortisol and corticosterone is the province of enzymes downstream from P4. The pace is set by the supply block. The three steroidogenic branches (Figure 1.1) divide the supply-block flux between them. Should one branch not be able to cope, the excess flux would be shunted down the alternative branches.

6.3 The importance of the enzymes in the steady-state model

The data obtained from computer simulations using the steady-state model show that both the model CYP17 and CYP21 exert an effect over the branch point and the flux through either branch (see Sections 5.2.2 and 5.2.3).

The data from the experiment varying the supply of P4 (see Section 5.2.1) shows that the supply of P4 to the branch point has a larger affect on the distribution of flux than varying either the model CYP17 or CYP21 as hypothesized from the results of control analysis.

Table 5.1 shows the control coefficients calculated by the Gepasi model. These results are explained in section 5.2.

6.4 How important are CYP17 and CYP21?

From the data presented in this thesis it must be concluded that the model CYP17 and CYP21 do not exercise as large an influence over the CYP17/CYP21 branch point as believed.

The data indicates that the supply of P4 to the branch point is the major determinant in the distribution of flux through the CYP17 branch of the pathway. This conclusion supports the hypothesis that the flux control over steroidogenesis lies in the supply of cholesterol/pregnenolone

[15]—if it can be assumed that the enzymes involved in cholesterol transport and conversion have similar kinetic properties as the other enzymes in the pathway.

It is the anatomy and mobilization of cholesterol in response to ACTH and/or angiotensin II that determine the ratio of steroid products released from the adrenal cortex. Only under extreme circumstances, where the activity of CYP17/CYP21 is severely reduced, does CYP17/CYP21 exert any control by creating a metabolic bottle-neck. This bottle-neck causes a spill over of steroid precursor being directed down alternative pathways causing physiological abnormalities.

6.5 Future Research

More data is needed to validate the model predictions. The experiments need to be repeated and more experiments performed in tissue culture and the V values recalculated with greater accuracy.

To test this hypothesis further the experimental system will need to be overhauled. A system will need to be constructed that can be more finely manipulated; to which more enzymes can be added and which can reach a steady-state.

The methodologies presented in this thesis have the possibility to provide mathematically quantifiable explanations of adrenal steroidogenesis observations. If it can be proved that this model applies equally to CYP and 3βHSD expressed in yeast as in COS1 cells then yeast would lend itself well to testing the hypothesis put forward in this thesis: that the control over steroidogenic flux lies in the supply of steroid precursor. This cross-species generalization would also strengthen the generality of the model and make it more applicable to the bovine adrenal, and eventually human physiology.

By constructing permanently transfected yeast strains, growing them up in culture to appropriate densities and then using them in experiments in non-growing medium where exact cell numbers are known (e.g. quantitated with a Coulter Counter) it would be possible to perform the needed experiments with greater accuracy and control. By saturating the experimental medium with cholesterol or pregnenolone it would be possible to simulate a constant supply of substrate needed for steady-state experimentation.

Such a system with 3βHSD in it would more accurately represent the topology of the steroidogenic pathway. In Figure 2.3 it can be seen that P5 is converted to both P4 and 17OHP5. The 17OHP5 is converted to 17OHP4 by 3βHSD. This source of 17OHP4 is not accounted for in the current model system and may significantly alter the control coefficient values shown in Table 5.1.

The V values obtained from the mixed experiments are underestimates of the true V values. Accurate V values are required for the reaction of P5 to P4, P5 to 17OHP5, 17OHP5 to 17OHP4, P4 to 17OHP4, P4 to DOC, 17OHP4 to S, DOC to corticosterone and S to cortisol. The employment of yeast will yield V values of conversion per time interval per yeast cell, a much finer measurement than conversion per time interval per slice of tissue culture dish.

The outlook for research in steroidogenesis employing the methodologies of control analy-

sis, metabolic modeling, and parallel transfection promises to yield many new avenues of research (e.g. synergy and antagonism between CYP and *N*-acetyltransferase enzymes in xenobiotic metabolism [75]) and test many current hypotheses—most notably, the ones expressed in this thesis.

6.6 Summary

A model was constructed using Michaelis-Menten kinetics; and adrenal microsomes and the parallel transfection technique was used to perform experiments to complete and test the model. From the data supplied the model described would appear to be an accurate expression of steroid metabolism in transfected COS1 cells. This model suggests that the supply of steroid precursor determines the downstream response and controls the flux through the pathways as reconstituted in tissue culture. The model predicts that 88% of the flux control of the CYP17 branch; and 90% of the concentration control of S lies in the activity of the supply-block of P4. The higher CYP17 branch flux relative to the CYP21 branch in response to an increase in [P4] is due to the inhibitory action of 17OHP4 on the P4⟶DOC reaction.

Bibliography

[1] Ganong, W.F. (1997) *Review of Medical Physiology*. Appleton and Lange 18th edition.

[2] Miller, S.A. and Harvey, J.P. (1996) *Zoology*. Wm. C. Brown Publishers.

[3] Mellon, S.H. (1994) Neurosteroids: biochemistry, modes of action, and clinical relevance. *J. Clin. Endocrinol. Metab. 78*, 1003–1008.

[4] Ross, M.H., Romrell, L.J. and Kaye, G.I (1995) *Histology: a text and atlas*. Williams and Wilkins 3rd edition.

[5] Pedersen, R.C. and Brownie, A.C. (1986) The mechanism of action of adrenocorticotrophic hormone on cholesterol metabolism in the adrenal cortex. *Biochemical Actions of Hormones 13*, 129–166.

[6] Schäfer, W.E. (1999) *A control analysis study of adrenal microsomal progesterone metabolism.* M.Sc. thesis, University of Stellenbosch.

[7] White, P.C. and Speiser, P.W. (2000) Congenital adrenal hyperplasia due to 21-hydroxylase deficiency. *Endocrine Reviews 21*, 245–291.

[8] Engelbrecht, Y. (2000) *A study of hypoandrenocorticism in the angora goat.* PhD thesis, University of Stellenbosch.

[9] Slabbert, J.T. (2003) *Identification of two CYP17 alleles in the south african angora goat.* M. Sc. thesis, University of Stellenbosch.

[10] Auchus, R.J and Miller, W.L (1999) Molecular modeling of human P450c17 (17α-hydroxylase/17,20-lyase): insights into reaction mechanisms and effects of mutations. *Mol. Endocrinology 13*, 1169–1182.

[11] Sakai, Y., Yanase, T., Hara, T., Takayanagi, R., Haji, M. and Nawata, H. (1994) In-vitro evidence for the regulation of 17,20-lyase activity by cytochrome b5 in adrenocortical adenomas from patients with cushing's syndrome. *Clin. Emdo. 40*, 205–209.

[12] Fell, D. (1997) *Understanding the control of metabolism.* Portland Press, London.

[13] Hofmeyr, J.-H.S and Cornish-Bowden, A. (1996) Co-response analysis: a new experimental strategy for metabolic control analysis. *J. theor. Biol 182*, 371–380.

[14] Hofmeyr, J.-H.S and Rohwer, J.M. (1998) A revised nomenclature and symbolism for metabolic control analysis. `http://www.sun.ac.za/biochem/mcanom7.pdf`.

[15] Stocco, D.M. and Clark, B.J. (1996) Regulation of the acute production of steroids in steroidogenic cells. *Endocrine Reviews 17*, 221–243.

[16] Teusink, B., Passarge, J., Reijenga, C.A., Esgalhado, E., van der Weijden, C.C., Schepper, M., Walsh, M.C., Bakker, B.M., van Dam, K., Westerhoff, H.V. and Snoep, J.L. (2002) Can yeast glycolysis be understood in terms of *in vitro* kinetics of the constituent enzymes? Testing biochemistry. *Eur. J. Biochm. 267*, 1–18.

[17] Rohwer, J.M and Botha, F.C. (2001) Analysis of sucrose accumulation in the sugar cane culm on the basis of in vitro kinetic data. *Biochem. J 358*, 437–445.

[18] Schäfer, W.E., Rohwer, J.M. and Botha, F.C. (2004) A kinetic study of sugarcane sucrose synthase. *Eur. J. Biochm. 271*, 3971-3977.

[19] Hofmeyr, J.-H.S. (2001) Metabolic control analysis in a nutshell. In Yi, T.-M., Hucka, M., Morohashi, M. and Kitano, H., editors, *Proceedings of the* 2nd *International Conference on Systems Biology* pages 291–300. Omnipress, Wisconsin (2001). `http://www.icsb2001.org/Papers/19_icsb2001_distiller.pdf`

[20] Hofmeyr, J.-H. S. and Cornish-Bowden, A. (2000) Regulating the cellular economy of supply and demand. *FEBS. Lett. 476*, 46–51.

[21] Massoud, T.F., Hademenos, G.J., Young, W.L., Gao, E., Pile-Spellman, J. and Vinuela, F. (1998) Principles and philosophy of modeling in biomedical research *FASEB J. 12*, 275–285.

[22] Brock, B.J. and Waterman, M.R. (1999) Biochemical differences between rat and human cytochrome P450c17 support the different steroidogenic needs of these two species. *Biochemistry 38*, 1598–1606.

[23] Wu, F-.S., Gibbs, T.T. and Farb, D.H. (1991) Pregnenolone sulfate: a positive allosteric modulator at the *N*-methyl-D-aspartate receptor. *Mol. Pharm. 40*, 333–336.

[24] Rupprecht, R. and Holsboer, F. (1999) Neuroactive steroids: mechanisms of action and neuropsychopharmacological perspectives. *Trends Neurosci. 22*, 410–416.

[25] Zwain, I.H. and Yes, S.S.C. (1999) Dehydroepiandrosterone: Biosynthesis and metabolism in the brain. *Endo 140*, 880–887.

[26] Saez, J.M (1994) Leydig cells: Endocrine, paracrine, and autocrine regulation. *Endrocrine Reviews 15*(5), 574–626.

[27] Lee-Robichaud, P., Wright, J.N., Akhtar, M.E. and Akhtar, M. (1995) Modulation of the activity of human 17α-hydroxylase-17,20-lyase (CYP17) by cytochome b5: endocrinological and mechanistic implications. *Biochem. J. 308*, 901–908.

[28] Yuan, B.-B, Tchao, R., Voigt, J.M. and Colby, H.D. (2001) Maturational changes in CYP2D16 expression and xenobiotic metabolism in adrenal glands from male and female guinea pigs. *Drug Metabolism and Disposition 29*, 194–199.

[29] Yamazaki, Y., Ohno, T., Sakaki, T., Akiyoshi-Shibata, M., Yabusaki, Y., Imai, T. and Kominami, S. (1998) Kinetic analysis of successive reactions catalyzed by bovine cytochrome $P450_{17\alpha,lyase}$. *Biochemistry 37*, 2800–2806.

[30] Soucy, P. and Luu-The, V. (2000) Conversion of pregnenolone to DHEA by human 17α-hydroxylase/17,20-lyase (P450c17): Evidence that DHEA is produced from the released intermediate, 17α-hydroxypregnenolone. *Eur. J. Biochem. 267*, 3243–3247.

[31] Bourama, B., Hanoux, V., Mittre, H., Fral, C., Benham, A. and Leymarie, P. (2001) Expression of the rabbit cytochrome P450 aromatase encoding gene uses alternative tissue-specific promoters. *Eur. J. Biochem. 268*, 4506–4512.

[32] Garret, R.H. and Grisham, C.M (1995) *Biochemistry*. Saunders College Publishing.

[33] Slominski, A., Gomez-Sanchez, C.E., Foecking, M.F. and Wortsman, J. (1999) Metabolism of progesterone to DOC, corticosterone and 18OHDOC in cultured melanoma cells. *FEBS Lett. 455*, 364–366.

[34] Parker K.L. and Schimmer B.P. (1994) The role of nuclear receptors in steroid hormone production. *Semin Cancer Biol 5*, 317–325.

[35] Wijesuriya, S.D., Zhang, G., Dardis, A. and Miller, W.L. (1999) Transcriptional regulatory elements of the human gene for cytochrome P450c21 (steroid 21-hydroxylase) lie within intron 35 of the linked *C4B* gene. *J. Biol. Chem. 274*, 38097–38106.

[36] Geller, D.H., Auchus, R.J. and Miller, W.L. (1999) P450c17 mutations R347H and R358Q selectivity disrupt 17,20-lyase activity by disrupting interactions with P450 oxidoreductase and cytochrome b_5. *Mol. Endocrinology 13*, 167–175.

[37] Izem, L and Morton, R.E (2001) Cholesterol ester transfer protein biosynthesis and cellular cholesterol homeostasis are tightly interconnected. *J. Biol. Chem. 276*, 26534–26541.

[38] Clark, B.J., Wells, J., King, S.R. and Stocco, D.M. (1994) The purification, cloning and expression of a novel luteinizing hormone-induced mitochondrial protein in MA-10 mouse leydig tumor cells. *J. Biol. Chem. 269*, 28314–28322.

[39] Bowen, R (2003) Pathophysiology of the endocrine system: Overview of adrenal histology. *http://arbl.cvmbs.colostate.edu/hbooks/pathphys/endocrine/adrenal/histo_overview.html*.

[40] Coulter, C.L. and Jaffe, R.B. (1998) Functional maturation of the primate fetal adrenal *in vivo*: 3. specific zonal localization and developmental regulation of CYP21A2 (P450c21) and CYP11B1/CYP11B2 (P450c11/aldosterone synthase) lead to integrated cocenpt of zonal and temporal steroid biosynthesis. *Endo 139*(12), 5144–5150.

[41] Miller, W.L., Auchus, R.J. and Geller, D.H. (1997) The regulation of 17,20 lyase activity. *Steroids 62*, 133–142.

[42] Calnan B.J., Szychowski S., Chan F.K., Cado D. and Winoto A. (1995) A role for the orphan steroid receptor Nur77 in apoptosis accompanying antigen-induced negative selection. *Immunity 3*, 273–282.

[43] Reyland, M.E. (1993) Protein kinase c is a tonic negative regultor of steroidogenesis and steroid hydroxylase gene expression in Y1 adrenal cells and functions independantly of protein kinase A. *Mol. Endocrinology 7*, 1021–1030.

[44] Lehoux, J.G., Fleury, A and Ducharme, L. (1998) The acute and chronic effects of adrenocorticotropin on the levels of messenger ribonucleic acid and protein of sterodogenic enzymes in the rat adrenal *in vivo*. *Endo 139*(9), 3913–3922.

[45] Kalthoff, K (1996) *Analysis of Biological Development*. McGraw-Hill, Inc.

[46] Xu, T., Bowman, E.P., Glass, D.B. and Lambeth, J.D. (1991) Stimulation of adrenal mitochondrial cholesterol side-chain cleavage by GTP, steroidogenesis activator polypeptide (SAP), and sterol carrier protein$_2$. *JBC 266*, 6801–6807.

[47] Mertz, L. M. and Pedersen, R.C. (1989) The kinetics of steroidogenesis activator polypeptide in the rat adrenal cortex. *JBC 264*, 15274–15279.

[48] Jäätelä, M., Ilvesmäki, V., Voutilainen, R., Stenman, U.H. and Saksela, E. (1991) Tumor necrosis factor as a potent inhibitor of adrenocorticotropin-induced cortisol production and steroidogenic P450 enzyme gene expression in culturued human fetal adrenal cells. *Endo 128*(1), 623–629.

[49] Conley, A.J., Graham-Lorence, S.E., Kagimoto, M., Lorence, M.C., Murry, B.A., Oka, K., Sanders, D. and Mason, J.I. (1992) Nucleotide sequence of a cDNA encoding porcine testis 17α-hydroxylase cytochrome P450. *Biochim. Biophys. Acta 1130*, 75–77.

[50] Lee-Robichaud, P., Kaderbhai, M.A., Kaderbhai, N., Wright, J.N. and Akhtar, M. (1997) Interaction of human CYP17 (p-450$_{17\alpha}$, 17α-hydroxylase-17,20-lyase) with cytochrome b$_5$: im-

portance of the orientation of the hydrophobic domain of cytochrome b_5. *Biochem. J. 321*, 857–863.

[51] Auchus, R.J., Lee, T.C. and Miller, W.L. (1998) Cytochrome b_5 augments the 17,20-lyase activity of human P450c17 without direct electron transfer. *J. Biol. Chem. 273*, 3158–3165.

[52] Zhang, L.H., Rodriguez, H., Ohno, S. and Miller, W.L. (1995) Serine phosphorylation of human P450c17 increases 17,20-lyase actvity: implications for adrenarche and the polycystic ovary syndrome. *Proc. Natl. Acad. Sci. 92*, 10619–10623.

[53] Lombard, N., Swart, A.C., van der Merwe, M.J. and Swart, P. (2002) Sheep adrenal cytochrome b_5: active as a monomer or a tetramer *in vivo*? *Endocrine Research 28*, 485–495.

[54] Swart, P., Engelbrecht, Y., Bellstedt, D.U., de Villiers, C.A. and Dreesbeimdieke, C. (1995) The effect of cytochrome b_5 on progesterone metabolism in the ovine adrenal. *Endocrine Research 21*, 297–306.

[55] LeRoux, A., Mota Viera, L. and Kahn, A. (2001) Transcriptional and traslational mechanisms of cytochrome b_5 reductase isoenzyme generation in humans. *Biochem. J 355*, 529–535.

[56] Soucy, P. and Luu-The, V. (2001) Assessment of the ablity of type 2 cytochrome b_5 to modulate 17,20-lyase activity of human P450c17. *J. Steroid Biochem. Mol. Biol. 80*, 71–75.

[57] Hiroi, T., Kishimoto, W., Chow, T., Imaoka, S., Igarashi, T. and Funae, Y. (2001) Progesterone oxidation by cytochrome P450 2D isoforms in the brain. *Endo 142*, 3901–3908.

[58] Bhagwat, S.V., Biswas, G., Anandatheerthavarada, H.K., Addya, S., Pandak, W. and Avadhani, N.G. (1999) Dual targeting property of the N-terminal signal sequence of P4501a1. *J. Biol. Chem. 274*(34), 24014–24022.

[59] Gonzalez, F.J. (1989) The molecular biology of cytochrome P450s. *Pharmacological Reviews 40*, 243–288.

[60] Nelson, D.R. (2004) Cytochrome P450 Homepage `http://drnelson.utmem.edu/CytochromeP450.html`.

[61] Straub, P., Lloyd, M., Johnson, E.F. and Kemper, B. (1994) Differential effects of mutations in substrate recognition site 1 of cytochrome P450 2C2 on lauric acid and progesterone hydroxylation. *Biochemistry 33*, 8029–8034.

[62] Degtyarenko, K.N. and Archakov, A.I. (1993) Molecular evolution of P450 superfamily and P450-containing monooxygenase systems. *FEBS Lett. 332*, 1–7.

[63] Guiterrez, A., Lian, L.Y., Wolf, C.R., Scrutton, N.S. and Roberts, G.C.K. (2001) Stopped-flow kinetic studies of flavin reduction in human cytochrome P450 reductase and is component domains. *Biochemistry 40*, 1964–1975.

[64] Omura, T. and Sato, R. (1962) A new cytochrome in liver microsomes. *J. Biol. Chem. 237*, 1375-1376.

[65] Omura, T. and Sato, R. (1964) The carbon monoxide-binding pigment of liver microsomes. I. evidence for its hemoprotein nature. *J. Biol. Chem. 239*, 2370-2378.

[66] Nebert, D.W., Nelson, D.R., Coon, M.J., Estabrook, M.J., Feyereisen, R., Fujii-Kuriyama, Y., Gonzalez, F.J., Guengerich, F.P., Gunsalus, I.C., Johnson, E.F., Loper, J.C., Sato, R., Waterman, M.R. and Waxman, D.J. (1991) The P450 superfamily: update on new sequences, gene mapping, and recommended nomenclature. *DNA & Cell Biol. 10*, 1–14.

[67] Cupp-Vickery, J., Anderson, R. and Hatziris, Z. (2000) Crystal structure of ligand complexes of P450erf exhibiting homotropic cooperativity. *Proc. Natl. Acad. Sci. 97*, 3050–3055.

[68] Cosme, J and Johnson, E.J. (2000) Engineering microsomal cytochrome P450 2C5 to be a soluble, monomeric enzyme. mutations that alter aggregation, phospholipid dependence of catalysis, and membrane binding. *J. Biol. Chem 275*, 2545–2553.

[69] Williams, P.A., Cosme, J., Srindhar, V., Johnson, E.F.. and McRee, D.E. (2000) The crystal structure of a mammalian microsomal cytochrome P450 monooxygenase: structural adaptations for membrane binding and functional diversity. *Mol. Cell. 5*, 121–132.

[70] Scott, E.E., He, Y.A., Wester, M.R., White, M.A., Chin, C.C., Halpert, J.R., Johnson, E.F. and Stout, C.D. (2003) An open conformation of mammalian cytochrome P450 2B4 at 1.6 Å resolution. *Proc. Natl. Acad. Sci. USA 100,* 13196-13201.

[71] Wester, M.R., Johnson, E.F., Marques-Soares, C., Dansette, P.M, Mansuy, D. and Stout, C.D. (2003) Structure of a substrate complex of mammalian cytochrome P450 2C5 at 2.3 Å resolution: evidence for multiple substrate binding modes. *Biochemistry 42*, 6370–6379.

[72] Johnson, E.J., Wester, M.R. and Stout, C.D. (2002) The structure of microsomal cytochrome P450 2C5: a steroid and drug metabolizing enzyme. *Endo. Res. 28*, 435–441.

[73] White, R.E. and Coon, M.J. (1980) Oxygen activation by cytochrome p-450. *Annu. Rev. Biochem 49*, 315–356.

[74] Hlavica, P. and Lewis, D.F.V. (2001) Allosteric phenomena in cytochrome P450-catalyzed monooxygenations. *Eur. J. Biochem. 268*, 4817–4832.

[75] Yanagawa, Y., Sawada, M., Deguchi, T., Gonzalez, F.J. and Kamataki, T. (1994) Stable expression of human CYP1A2 and *N*-acetyltransferase in chinese hamster CHl cells: Mutageneic activation of 2-amino-3-methylimidazol[4,5-f]quinoline and 2-amino-3,8-dimethylimidazol[4,5-f]quinoxaline. *Cancer. Res. 54*, 3422–3427.

[76] Munro, A.W., Noble, M.A., Robledo, L., Daff, S.N. and Chapman, S.K. (2001) Determination of the redox properties of human NADPH-cytochrome P450 reductase. *Biochemistry 40*, 1956–1963.

[77] Wang, M., Roberts, D.L, Pashke, R., Shea, T.M., Masters, B.S.S. and Kim, J.-J. P. (1997) Three-dimensional structure of NADPH-cytochrome P450 reductase: Prototype for FMN- and FAD-containing enzymes. *Proc. Natl. Acad. Sci. USA 94*, 8411–8416.

[78] Kominami, S., Owaki, A., Iwanaga, T., Tagashira-Ikushiro, H. and Yamazaki, T. (2001) The rate-determining step in P450 c21-catalyzing reactions in a membrane-reconstituted system. *J. Biol. Chem. 276*, 10753–10758.

[79] Coon, M.J. (2002) Enzyme ingenuity in biological oxidations: A trail leading to cytochrome P450. *J. Biol. Chem. 277*, 28351-28363.

[80] Miyatake, A., Tsubaki, M., Hori, H. and Ichikawa, Y. (1994) Purification and comparative characterization of cytochrome p-450scc (CYP XIA1) from sheep adrenocortical mitochondria. *Biochim. Biophys. Acta 1215*, 176–182.

[81] Sato, R. and T., Omura (1978) *Cytochrome P-450*. Kodansha Ltd., Tokyo.

[82] Hoornsby, P.J., Yang, L., Raju, S.G., Maghsoulou, S.S., Lala, D.S. and Nallaseth, F.S. (1992) Demethylation of specific sites in the 5′-flanking region of the *CYP17* genes when bovine adrenocortical cells are placed in culture. *DNA & Cell Biology 11*, 385–395.

[83] Nakajin, S. and Hall, P.F. (1981) Microsomal cytochrome p-450 from neonatal pig testis. *J. Biol. Chem. 256*, 3871–3876.

[84] Tagashira, H., Kominami, S. and Takemori, S. (1995) Kinetic studies of cytochrome $P450_{17\alpha,lyase}$ dependant androstenedione formation from progesterone. *Biochemistry 34*, 10939–10945.

[85] Swart, P., Estabrook, R.W., Mason, I.J. and Waterman, M.R. (1989) Catalytic activity of human and bovine adrenal cytochromes p-$450_{17\alpha,lyase}$ expressed in COS 1 cells. *Biochemical Soceity Transactions 17*, 1025–1026.

[86] Swart, P., Swart, A.C., Waterman, M.R., Estabrook, R.W. and Mason, J.I. (1993) Progesterone 16α-hydroxylase activity is catalyzed by human cytochrome P450 17α-hydroxylase. *J. Clin Endocrinol and Metab. 77*, 98–102.

[87] Yangibashi, K. and Hall, P.F. (1986) Role of electron transport in the regulation of the lyase activity of c_{21} side-chain cleavage p-450 from porcine adrenal and testicular microsomes. *J. Biol. Chem. 261*, 8429–8433.

[88] Wijesuriya, S.D., Zhang, G., Dardis, A. and Miller, W.L. (1999) Transcriptional regulatory elements of the human gene for cytochrome P450c21 (steroid 21-hydroxylase) lie within intron 35 of the linked *C4B* gene. *J. Biol. Chem. 274*(53), 38097–38106.

[89] Crawford, R.J., Hammond, V.E., Connell, J.M. and Coghlan, J.P. (1992) The structure and activity of two cytochrome $P450_{c21}$ proteins encoded in ovine adrenal cortex. *J. Biol. Chem. 267*, 16212–16218.

[90] Hsu, L.C., Hsu, N.C., Guzova, J.A., Guzov, V.M., Chang, S.F. and Chung, B.C. (1996) The common I172N mutation causes conformational change of cytochrome P450c21 revealed by systematic mutation, kinetic, and structural studies. *J. Biol. Chem. 271*, 3306–3310.

[91] Lorence, M.C., Trant, J.M., Mason, J.I., Bhasker, C.R., Fujii-Kuriyama, Y., Estabrook, R.W. and Waterman, M.R. (1989) Expression of a full-length cDNA encoding bovine adrenal cytochrome P450c21. *Arch Biochem Biophys 273*, 79–88.

[92] Nokoshkov, A., Lajic, S., Holst, M., Wedell, A. and Luthman, H. (1997) Synergistic effect of partially inactivating mutations in steroid 21-hydroxylase deficiency. *J. Clin. Endocrinol. Metab. 82*, 194–199.

[93] Tsubaki, M., Matsumoto, N., Tomita, S., Ichikawa, Y. and Hori, H. (1998) 20β-hydroxy-c21-steroid 20β-oxidase activity of cytochrome P450c21 purified from bovine adrenocrtical microsomes. *Biochemica et Biophysica Acta 1390*, 197–206.

[94] Hu, M.C. and Chung, B.C. (1990) Expression of human 21-hydroxylase (P450c21) in bacterial and mammalian celle: a system to characterize normal and mutant enzymes. *Mol. Endocrinology 4*, 893–898.

[95] New, M.I. (1998) Steroids in prepubertal period: Inborn errors of steroidogenesis. *Steroids 63*, 238–242.

[96] Sakaki, T., Shibata, M., Yabusaki, Y., Murakami, H. and Ohkawa, H. (1990) Expression of bovine cytochrome P450c21 and its fused enzymes with yeast NADPH-cytochrome P450 reductase in *Saccharomyces cerevisiae*. *DNA Cell Biol. 9*, 603–614.

[97] Wu, D.A., Hu, M.C. and Chung, B.C. (1991) Expression and functional study of wild-type and mutant human cytochrome P450c21 in *Saccharomyces cerevisiae*. *DNA Cell Bio. 3*, 201–209.

[98] Wu, D.A. and Chung, B.C. (1991) Mutations of P450c21 (steroid 21-hydroxylase) at CYS^{428}, VAL^{281}, SER^{268} result in complete, partial, or no loss of enzymatic activity, respecitively. *J. Clin. Invest. 88*, 519–523.

[99] Wardlaw, A. C. (1995) *Practical statistics for experimental biologists.* John Wiley & Sons.

[100] Mendes, P. (2004) *Gepasi*. `http://www.gepasi.org`.

[101] Sauro, H. M., Small, J. R. and Fell, D. A. (1987) Metabolic control and its analysis : Extensions to the theory and matrix method. *Eur. J. Biochem. 165*, 215–221.

[102] Reder, C. (1988) Metabolic control theory: a structural approach. *J. Theor. Biol. 135*, 175–201.

[103] Kacser, H. and Burns, J. A. (1973) The control of flux. *Symp. Soc. Exp. Biol. 32*, 65–104.

[104] Heinrich, R., Rapoport, S. M. and Rapoport, T. A. (1977) Metabolic regulation and mathematical models. *Progr. Biophys. Molec. Biol. 32*, 1–82.

[105] Hofmeyr, J.-H.S (2000) *Stoichiometric matrix analysis.* Unpublished lecture notes.

[106] Kell, D.B. (2004) *The Metabolic Control Analysis Web.* `http://dbk.ch.umist.ac.uk/mca_home.htm`.

[107] Hofmeyr, J.-H. S. (1995) Metabolic regulation: a control analytic perspective. *J. Bioenerg. Biomembranes 27*, 479–490.

[108] Beckert, V., Dettmer, R. and Bernhardt R. (1994) Mutations of tyrosine 82 in bovine adrenodoxin that affect binding to cytochromes P45011A1 and P45011B1 but not electron transfer. *J Biol Chem. 269*, 2568–2573.

[109] A. Cornish-Bowden (2004) *Fundamentals of Enzyme Kinetics* (3rd edn.) Portland Press, London.

[110] Yang, M.-X. and Cederbaum, A.I. (1994) Fractionation of liver microsomes with polyethylene glycol and purification of NADH-cytochrome b_5 oxidoreductase and cytochrome b_5. *Arch. Biochem. Biophys. 315*, 438–444.

[111] Ausubel, F. M., Brent, R., Kingston, R. E., Moore, D. D., Seidman, J. G., Smith, J. A. and K., Struhl, editors (1998) *Current Protocols in Molecular Biology*. John Wiley and Sons Inc.

Appendix A

Methods and Materials

A.1 Steroid Analysis

A.1.1 Steroid separation by TLC

Merck chemicals supplied thin Layer Chromatography (TLC) Plates (Cat#: 1.05554). Steroid preparations of P4, 17OHP4, DOC, and S (2 mg/mL 100% ethanol) were spotted onto the TLC plate and developed twice consecutively in two different solvent mixes. The TLC plate was first developed in a mixture of 99% chloroform ($CHCl_3$) and 1% ethyl acetate (EtAct), dried under hot air and subsequently developed in a mixture of 99% methylene chloride (CH_2Cl_2) and 1% methanol (MeOH). A typical elution profile obtained is given in Figure A.1.

Experimental samples were spotted onto a plate in 0.8 to 1 cm wide lanes along with standards. The lanes were carved out with a 1 mL plastic pipet tip . Care was taken not to bend the plate as this would facilitate ”smiling”.The steroids were resolved to a minimum inter-spot distance of 2 cm. The spots were excised for examination without the threat of cross contamination of steroid spots and samples.

A.1.2 Radioactive quantification of steroid metabolites from TLC plate separation

The steroid spots were cut from the TLC plate and placed in a scintillation vial with 8 ml scintillation fluid (Beckman, Ready Flo Scintillation fluid, cat# 586603). 1 cm of TLC plate was excised on either side of the spot to get as much of the radioactive steroid as possible so as to quantitatively compare radioactivity between TLC segments and ignore the different lateral and vertical diffusion of the spots. The samples were counted with a Beckman LS 3801 scintillation counter. Samples were counted for 10 minutes.

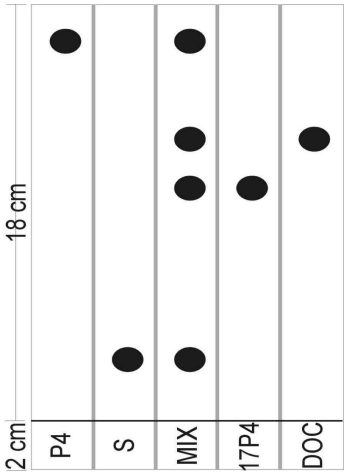

Figure A.1: Typical TLC separation profile of steroids. Steroids separated: P4, S, 17OHP4, DOC.

A.1.3 HPLC analysis of steroids

Steroids were separated by HPLC on a Novapak® C18 reverse phase column with 65:35 MeOH:H_2O and 100% MeOH solvents. The elution gradient used is given in Table A.1.

Table A.1: HPLC elution gradient. Solvent A was 65:35 MeOH:H_2O and Solvent B 100% MeOH. Total run time was 35 minutes. Radioactive detector was engaged from 5 minutes to 25 minutes. The gradient was linear.

time (min)	% solvent A	% solvent B
0.1	100%	0%
10.0	100%	0%
20.0	0%	100%
30.0	0%	100%
35.0	100%	0%

Radioactive detection was by means of a Flo-one β-radioactive flow detector from Radiomatic fitted with a 500 μL detection cell using Beckman Ready Flo III scintillation fluid (Cat# 534497-6). The radioactive detector was calibrated to filter out background noise.

Retention times of the steroids are given in Table A.2.

A.2 Microsome isolation and enzyme assay

A.2.1 Polyethylene glycol precipitation of adrenal microsomes

Polyethylene glycol precipitation of adrenal microsomes based on a protocol from Yan & Cederbaum [110].

Sheep adrenals were collected at Maitland Abattoir from freshly slaughtered sheep. The

Table A.2: Retention times of steroids analyzed by HPLC. The gradient and solutions described in Section A.1.3 were used.

Steroid	Retention time (min)
S	9.87
17OHP4	14.3
DOC	16.6
P4	22.9

adrenals were stored in chilled (4°C) 1.15% KCl and kept on ice and later washed in the afore mentioned solution before the capsule was removed. At all times the adrenals were kept chilled on ice or in ice-water (4°C).

Refer to Fig A.2 for a diagramatic explanation of the protocol that follows.

The washed and prepared adrenals were placed in a buffer of 10 mM TRIS, 1.0 mM EDTA, 0.25 M sucrose, pH 7.4. 50 grams of adrenal was homogenized in the latter buffer in a Waring blender and Thomas teflon pestle tissue homogenizer attached to a Black & Decker Drill. The buffer to adrenal volume was 1:3 $^{\mathrm{m}}/_{\mathrm{m}}$. The homogenate was then centrifuged at 500×g for 10 minutes at 4°C using a Beckman J-21B centrifuge and JA20 rotor. The resulting pellet was discarded.

The supernatant was centrifuged at 11 000×g for 16 minutes at 4°C and the pellet discarded.

50% polyethelene glycol solution was added to the supernatant from the previous centrifuge step to a final polyethelene glycol concentration of 8.5%[1]. The solution was stirred at 4°C for 10 minutes. Thereafter the solution was centrifuged at 13 000×g for 20 minutes at 4°C to yield the adrenal microsome pellet.

The pellet was resuspended in 10 mM TRIS, 150 mM KCl, 1.0 mM EDTA, pH 7.4 and again 50% polyethelene glycol was added to a final concentration of 8.5%. The solution was stirred at 4°C for 10 minutes and then centrifuged at 13 000×g for 20 minutes at 4°C. This process of resuspension and centrifugation was repeated until the supernatant was clear. The clean pellet was then resuspended in 100 mM Phosphate buffer, 20% glycerol, 100 μM DTT at pH 7.2. The microsomes were assayed for P450 concentration, aliquotted out and stored at -80°C for later use.

A.2.2 P450 concentration assay

A volume of microsome suspension was diluted 10 times in 100 mM sodium phosphate buffer at pH 7.2 to a final volume of 2 mL. This volume was bubbled with carbon monoxide gas for 2 minutes at 1 bubble per second. 400 μL of this suspension was added to each of two quartz cuvettes to which an additional 15 μL of 10 mM NADH was added. The tubes were inverted to mix the contents and then placed in the spectrophotometer (Cary 100 Conc Double-beam UV-VIS

[1] $V_{50\%\,^{m}/_{V}\,PEG} = 0.186 \times V_{supernatant}$

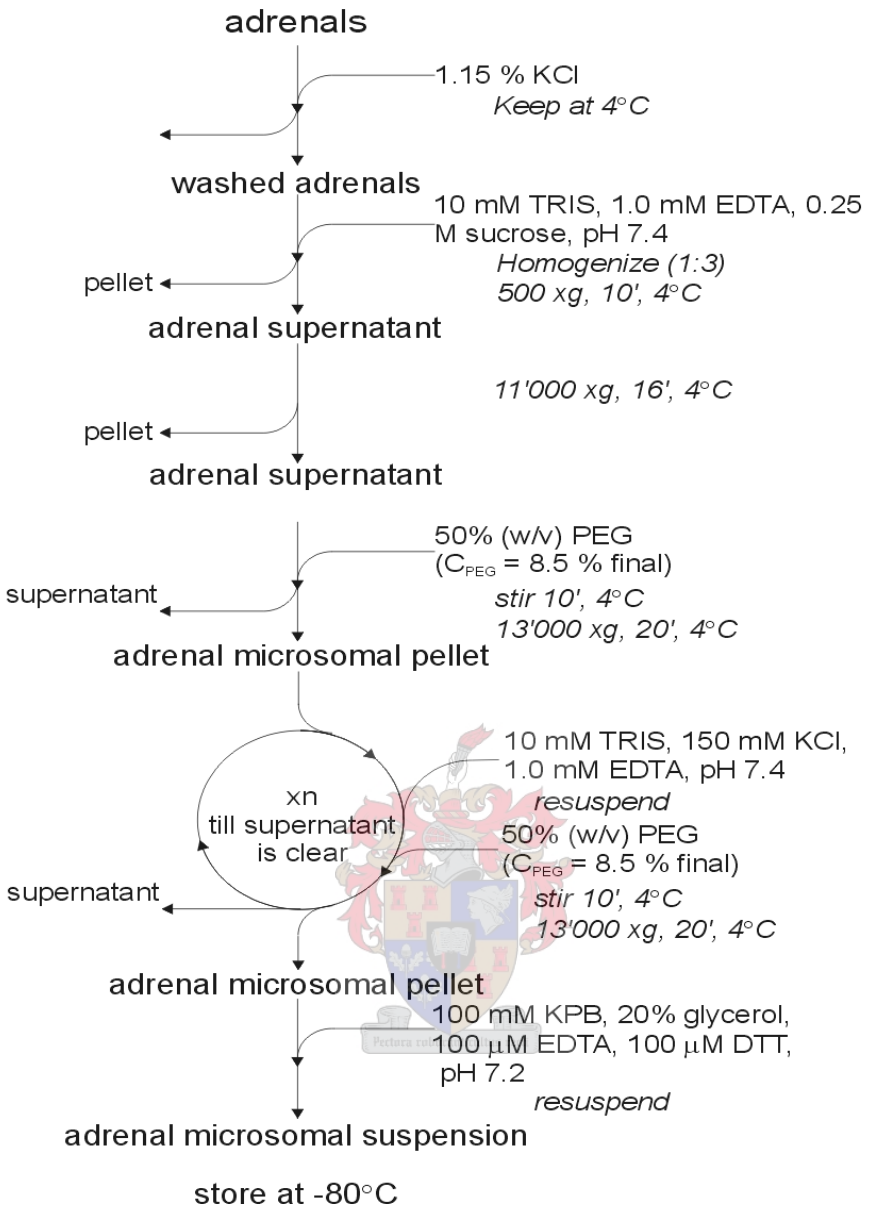

Figure A.2: Flow diagram outlining polyethelen glycol precipitation of adrenal microsomes.

spectrophotometer). The machine was zeroed and a scan was carried out between 400 and 500 nm. The experiment cuvette was removed and 3 to 5 grains of sodium dithionate added. The tube was inverted to mix the contents. The reference cell was also inverted to counteract settling. Another scan was performed between 400 and 500 nm to yield the characteristic CO induced difference spectrum of reduced P450 in Fig 3.1 after ten minutes. The concentration was calculated (Abs $= \varepsilon$Lc) using an extinction coefficient of 92 mM^{-1}.cm^{-1} and the amplitude difference between 450 and 490 nm.

A.2.3 Steroid substrate binding scans

Microsomal suspension was diluted to 10 mg/mL in microsomal resuspension buffer (see A.2.1). Quartz cuvettes were used for analysis. 1 mL suspension was added to each of the two cuvettes. The spectrophotometer (Cary 100 Conc Double-beam UV-VIS spectrophotometer) was zeroed over a range of 350 to 500 nm with a volume of pure ethanol (the equivalent volume of steroid-ethanol solution used for the scans).

In performing the scans steroid was added to the experiment cuvette and the equivalent volume of pure ethanol to the reference cuvette and a scan performed from 350 to 500 nm. This yielded the scan given in Fig 3.4. The ethanol volume did not surpass 2% of the total volume.

2 mL test samples were prepared in test tubes before scanning with relevant reagents. For the experiment 1 mL of each was added to each cuvette where after the test steroid was added.

The difference between the 390 and 420 nm points was taken as the peak amplitude. These amplitudes were compared between samples.

A.2.4 Microsomal protein concentration

Protein concentrations were determined with the BCA kit by Pierce (Cat# 23225) as per the manufacturers instructions. A BSA standard (Roche bovine serum albulmin fraction V, Cat# 735078) was prepared in the microsomal resuspension buffer. The samples were prepared in triplicate in a microtiter plate and read with a microtiter plate reader at 420 nm.

A.2.5 Microsomal steroid conversion assay

Steroid standards were made up in 100% ethanol to a concentration of 2 mg/ml. The standards were stored in dark bottles at -20°C.

Reactions were carried out in 20 mL glass test tubes at 37°C in a shaking water bath. The final reaction volume was 400 μL. Prior to beginning the experiment 5 mL CH_2Cl_2 was poured into 10 mL screw-cap sample tubes. 450 μL of H_2O was pipetted onto the CH_2Cl_2. These tubes were then chilled over night at 4°C.

P4 was blotted on to cellulose disks ($\varnothing = 3\mathrm{mm}$). Enough cold P4 was blotted onto the disk to bring the final reaction concentration to 10 μM; in addition 100 000 counts per minute of radioactive P4 were blotted onto the disk. The disks were left to dry where after a volume of buffer (1% BSA, 50 mM NaCl, 50 mM Tris, pH 7.4) was added dependent on the volume of other reagents and microsomes. 4.4 μL of 100 mM $MgCl_2$ and 4.2 μL of a 100 mM isocitrate solution was then added to the buffer and steroid. 6.44 μL isocitrate dehydrogenase (10.3 mg/mL protein, 6 units/mg protein) was added to the reaction mixture and then incubated at 37°C for 10 minutes. The tubes were gently shaken (150 rpm) in a water bath to facilitate mixing and gaseous exchange.

After 10 minutes a volume microsomal suspension was added dependent on the μM P450 required. The mixture was then incubated for a further five minutes at 37°C.

50 μL of the sample was drawn off and injected into the cold CH_2Cl_2/H_2O mixture as a time zero where after 44 μL 10 mM NADPH was added to initiate the reaction. 50 μL samples were drawn off at regular intervals and added to the chilled CH_2Cl_2/H_2O mixture and thoroughly mixed to stop the reaction.

A.2.6 Preparation of steroid assay samples

The CH_2Cl_2/H_2O extracts were centrifuged at maximum speed in a bench top centrifuge. The water was then aspirated off. A spatula tip of anhydrous Na_2SO_4 was added to each test tube. The samples were then centrifuged again as before and the supernatant decanted into disposable glass test tubes. The CH_2Cl_2 was evaporated under nitrogen gas. The dried samples were then ready for analysis by TLC. For HPLC analysis no Na_2SO_4 was added.

A.3 Transformation of *E. coli* JM109 cells with pCMVc17αbov and pCMVc21y401

A.3.1 Preparation of competent cells

E. coli JM109 cells were revived from freezer stocks in 100 mL LB medium (1% bactopeptone, 0.5% yeast extract, 1% NaCl) overnight at 37°C. 1 mL of this overnight culture was used to inoculate a preheated 100 mL LB medium at 37°C. This culture was grown ($\pm 2\frac{1}{2}$ hours) to an OD of 0.375 (measured at a wavelength of 590 nm).

Freezer stocks were prepared from this overnight culture to a final glycerol concentration of 40% and stored at -80°C. The rest of the culture was centrifuged at 1 480×g for seven minutes at 4°C after incubating on ice for seven minutes. After centrifugation the supernatant was discarded and the pellet left to drip dry after which it was centrifuged as before and the remaining medium sucked off with a sterile pipette.

10 mL of chilled (4°C) 10 mM $MgSO_4$ was added to the cell pellet to resuspend it. The cells were then centrifuged for 5 minutes at 4°C at 760×g. The supernatant was discarded and the pellet was left to drip dry where after 10 mL chilled 75 mM $CaCl_2$ was added to the pellet and the cells resuspended.

The resuspended cells were incubated on ice (4°C) for 30 minutes and then centrifuged at 760×g, 4°C for five minutes. The supernatant was discarded and the gooey pellet resuspended in 2 mL 75 mM $CaCl_2$ per original 50 mL of culture volume.

The competent cells were then stored at (4°C) until used for transformation or frozen at -80°C in 40% glycerol.

A.3.2 Transformation of competent *E. coli* JM109

200 μL of competent cells were pipetted into a chilled sterile 14 mL Falcon® Polypropylene Round-Bottom Tube. 50 ng of pCMVc17αBov, pCDc17αBov and pCMVc21y401 DNA was added to each separate transformation experimental tube. The pUC18 plasmid was used as a positive control. Competent cells and 5 μL sterile mQ H_2O were used as a negative control. The tubes were gently agitated to facilitate mixing. The mixture was incubated for 30 minutes at 4°C.

Immediately after the incubation on ice the tubes were incubated at 42°C for exactly 90 seconds without any agitation. The cells were then promptly removed and put on ice for one to two minutes in which time 800 μL of SOC medium (2% bactotryptone; 0.5% yeast extract; 10 mM NaCl, $MgCl_2$ $MgSO_4$; 2.5 mM KCl; 20 mM dextrose, pH 7) was added. The tubes were then incubated at 37°C for 45 minutes.

After the incubation at 37°C, 100 μL of each tube was plated out on LB agar (LB medium with 5% bactoagar) with ampicillan (0.1 mg/mL). The plates were left at room temperature right side up till the liquid had been absorbed. After absorbtion the plates were inverted and incubated at 37°C for 12 to 16 hours where upon the plates were examined for colonies. The plates and colonies were then stored at 4°C for later use.

A.3.3 Bacterial culture and plasmid DNA preparation by MiniPrep

The Wizard Kit (Cat# A7100) by Promega was used as per instruction.

A.3.4 Bacterial culture and plasmid DNA preparation by MidiPrep

Large scale plasmid DNA was prepared with the Nucleobond Plasmid Preparation Kit (Cat# 740573). Bacterial cells and cell lysate were centrifuged in 50 mL polypropylene tubes. Mixing at the lysis step was done by gentle rolling. The column was eluted over a 10 mL polypropylene tube and then centrifuged after addition of the iso-propanol. The pellet was then redissolved in ethanol and pipetted into 1.5 mL eppendorf tube and centrifuged as per the supplied protocol to clean the pDNA pellet.

Large scale plasmid preparation was also performed using the alkaline-lysis protocol in Current Protocols [111] but the products not used.

A.3.5 Plasmid DNA analysis

Plasmid was analyzed by restriction enzyme digestions and electrophoresis through TAE (40 mM·Tris acetate, 2 mM EDTA pH 7) agarose gels.

The pCMVc17α and pCMVc21y401 were digested with Xba and EcoR1 as per the RE manufacturers instructions.

Near completion, the electrophoresis was stopped and the gel stained with ethidium bromide for 30 minutes. The gel was again electrophoresed after being rinsed of the excess ethidium bromide. At completion the pDNA bands were visualized under ultra violet light and the gel photographed.

EcoR1 lyses the pCMVc17 plasmid twice, excising the fragment seen in the 3 pCMVc17 digest lanes. The three pCMVc21y401 digests show that pCMVc21y401 does not have a Xba site that generates a fragment of large enough size to be seen on the gel.

The digests and plasmids were run on a 1% molecular grade agarose gel in cold TAE buffer with λ Marker III. Along with the isolated plasmids, standard plasmids were loaded in to adjacent lanes. The results are shown in Figure A.3. From the restriction fragment length analysis it can be seen that the pCMVc21y401 plasmids correspond to each other; as do the pCMVc17 plasmids. The pCDc17α plasmid is not shown as it was never used for any experiments.

A.4 Maintenance and transfection of COS1 cells

A.4.1 Tissue culture stock solutions and media

All media and solutions were filtered with a 0.22 micron filter if they could not be autoclaved.

DMEM high glucose was purchased from Gibco BRL as 13.36 g bottles and made up in mQ H_2O with 3.7 g sodium bicarbonate per liter. The PenStrep was purchased from Gibco BRL as 100 mL 5000 U.mL^{-1} mixtures. FCS was purchased as 100 mL bottles from Gibco BRL. 10 mL of the PenStrep and 100 mL of the FCS were added to the filtered DMEM medium after testing for contamination. Trypsin-EDTA media was bought as a 10$\times$ stock solution and diluted to the working solution with mQ H_2O which was then filter sterilized, tested and frozen at -20°C.

Freezing medium was prepared as 10 mL aliquots consisting of 4 mL DMEM, 1 mL DMSO and 5 mL FCS. This medium was then filter sterilized and stored at -20°C . DMSO was purchased from Highveld Biologicals (Cat# 224).

10 mL of 1 M Hepes was added to 500 mL DMEM (without FCS) for the preparation of Hepes-medium for transfection purposes. The 1 M Hepes buffer was prepared with Sigma Hepes salt in H_2O with the pH adjusted to 7.4 and filter sterilized. The solution was aliquoted in 10 mL portions and stored at -20°C . 5 mL Pen-Strep was added and the medium tested and stored at 4°C. The DEAE-dextran was purchased from Sigma and made up to a concentration of 10 mg/mL in 0.1 M Tris base pH 7.5 and filter sterilized. The solution was then stored at 4°C for a maximum of three months. The chloroquine was made up as 52 mg in 10 mL H_2O, filter sterilized and aliquoted in 1 ml portions and frozen at -20°C.

COS1 cells were grown at 37°C, 5% CO_2 and 90% humidity without exception. COS1 freezer stocks were maintained in liquid nitrogen in the freezing medium until needed and thawed.

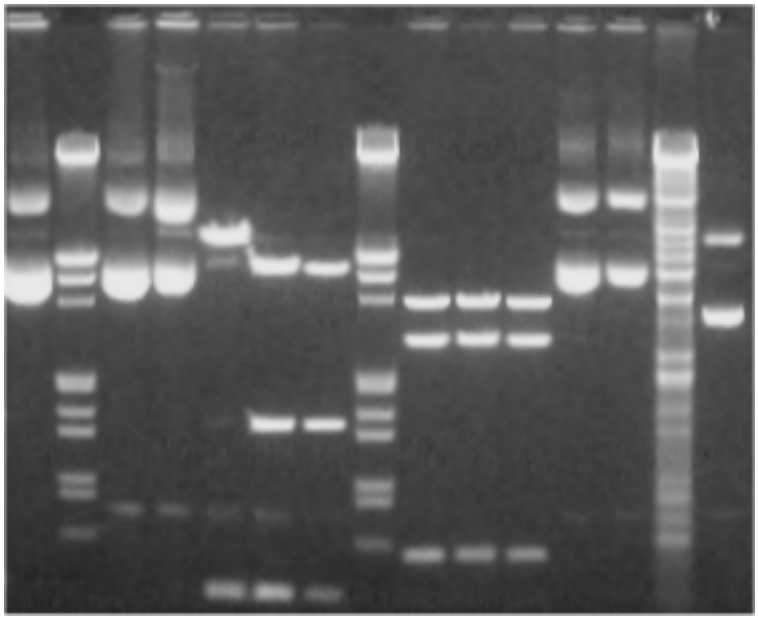

Figure A.3: Plasmid restriction fragment length analysis. Lanes are as follows from left to right: uncut pCMVc17; Marker III; uncut pCMVc17 standard; uncut pCMVc17 isolated; EcoR1 digested pCMVc17 isolate; EcoR1 and Xba digested pCMVc17 standard; EcoR1 and Xba digested pCMVc17 isolate; Marker III; EcoR1 digested pCMVc21y401 isolate; EcoR1 and Xba digested pCMVc21y401 isolated; EcoR1 and Xba digested standard; uncut pCMVc21y401 standard; uncut pCMVc21y401 isolate; failed λ marker preparation; uncut pCMV4.

A.4.2 Thawing and plating cells

The required number of freezer vials were taken from the liquid nitrogen and thawed at 37°C. The cells were resuspended in 1 mL culture media. The resuspended cells were added to 30 mL culture media in 50 mL falcon tube. The cells were dispersed by repeated drawing up and expelling of the medium with a sterile 10 mL glass pipette. The cells were then plated out in a 100 mm Corning tissue culture dish with 10 mL DMEM medium.

A.4.3 Splitting cells

The cells were left to grow to confluency (3 days). At this stage the cells were split one dish to three.

In splitting the cells the culture medium was siphoned off with a sterile Pasteur pipette. The dishes were washed with 1 mL 37°C Trypsin-EDTA and then siphoned again. 1 mL Trypsin-EDTA was added to the dishes and left to incubate under the tissue culture hood for three minutes. The cells were washed from the dish and dispersed by gently drawing up the Trypsin-EDTA medium with a 1 mL Gilson pipette with sterile filter tips and blasting the media on to the plate to dislodge the cells. This was repeated till all the cells were free. The cell suspension was then drawn up and

added to 30 mL growing medium.

The cells were then plated out into three dishes as described above.

A.4.4 Transfecting cells

The cells were grown to 70% confluency and split one to six 24 hours before transfection.

The media was removed from the dish and the dish washed with Hepes Media (4 mL to a 100 mm dish and 2 mL to a 50 mm dish). The Hepes media was then removed. Transfection media was then added to the plates with the respective plasmid of choice. The transfection medium was composed of Hepes Medium with DEAE-dextran (25 μL 10 mg/mL per mL medium). After the addition of the DEAE-dextran the plasmid was added to the transfection media to a final concentration of 5 μg pDNA/mL. 2 mL of transfection media was added to the 100 mm dishes (and 1.2 mL to the 50 mm dishes). The cells were left to incubate for one hour in the transfection medium.

After one hour the transfection media was drawn off and 10 mL chloroquine media was added (5 mL for a 50 mm dish). This media was composed of DMEM media with 100 μL of 5.2 mg/mL chloroquine stock solution per 100 mL of medium. The cells were incubated in this media for five hours where after the chloroquine media was drawn off and 10 mL DMEM media added.

Transfected cells were left to grow for 72 hours before the experiment was initiated.

A.4.5 Freezing cells

When the cells were confluent the media was drawn off and the dish washed with Trypsin-EDTA. The cells were dislodged and resuspended as described in Section A.4.3. The 50 mL Falcon tubes were then centrifuged at 1 200 rpm for five minutes.

The supernatant was drawn off and the cell pellet resuspended in 3 mL freezing media per dish of culture. The freezing media/cell suspension was then aliquotted out into a 2 mL cryo-vial in 1 mL portions.

The cells, in freezing media, were stored for 48 hours in a styrofoam casing at -80°C before being moved to the liquid nitrogen for long term storage.

A.4.6 Parallel tissue culture and manipulation of "pie" slices

The "pie" slices were prepared from Corning 100 mm tissue culture dishes (Cat# 25020) by the Stellenbosch Physics Workshop (Figure A.4). The new radius of the slices were 40 mm old dish radius: 42.5 mm and one slice represented 11% of the surface area of a full dish ($\approx {}^{1}/_{8}$th of a full dish). Quarter slices were prepared but found inadequate for experimentation. The slices were packed eight slices per dish and sterilized by gamma irradiation. The slices could only be used once.

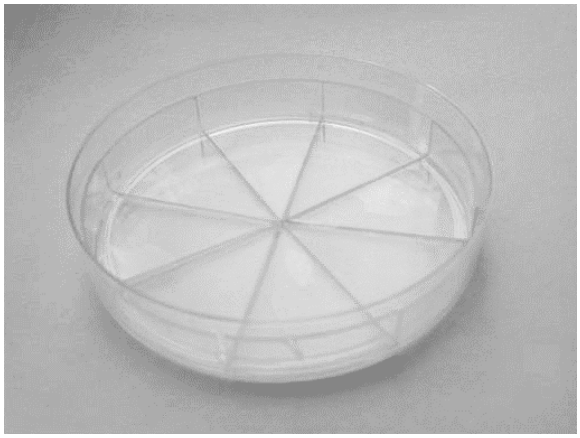

Figure A.4: Picture of dish used for parallel transfections. Photo by Dirk Bellstedt.

On the day of use fresh 2% agar was prepared (20 mL is adequate for six dishes) and autoclaved with a magnetic stirrer bar. After autoclaving, the agar was kept fluid on a combination hot plate/magnetic stirrer. The agar was applied slice by slice with an autoclaved Pasteur pipette and ethanol sterilized rubber teat. Enough agar was applied to the plate to line the base of one slice at a time. With flame sterilized curved tweazers the slices were pressed into the fluid agar.

The agar was left to set in the sterile hood before the suspended cells were added.

For transfection, 4 mL of transfection medium was used.

A.5 Tissue culture assays

A.5.1 Beginning the assay

72 hours after transfection the assay was initiated. 190 000 cpm of tritiated steroid was used per mL. The final concentration of non-tritiated steroid was 1 μM. The steroids were mixed into DMEM medium in an autoclaved schott bottle marked to the level of the volume media needed. The steroids were mixed by gentle inverting to avoid shaking the medium and causing it to foam. 10 mL[2] of medium was added to each experimental plate where the pie slices were involved. The slices were manipulated with sterile curved tweazers and placed into a new culture dish.

A 500 μL time zero sample was take from each dish at the beginning of the experiment. Additional 500 μL samples were drawn off with sterile filter tips are regular intervals.

Samples were collected in 10 mL screw cap glass tubes with 5 mL CH_2Cl_2. No water was added to the sample vial as described for the microsomal steroid conversion assay.

Samples were processed as in Section A.2.6. The tubes were left to warm up before processing.

[2]This volume was found to be too low and 20 mL is suggested for future use.

A.5.2 Determination of protein concentration per dish/slice

After the experiment the medium was drawn off and the dishes washed with PBS (137 mM NaCl, 2.7 mM KCl, 4.3 mM Na_2HPO_4, 1.4 mM KH_2PO_4, pH 7.3). The cells were removed from the washed dishes/slices by scraping with a stiff piece of plastic. The cells were resuspended in 10 mL PBS and then centrifuged at 1 200 rpm for five minutes. The pellet was then resuspended in 1 mL PBS and frozen until the protein concentration was to be determined.

The cells were homogenized with a glass mortar and pestle homogenizer. The homogenization process was helped by the freezing/thawing process.

The protein was quantitated as in Section A.2.4. BSA standards were prepared in PBS.